Wind-induced Shear and Torsion on Low- and Medium-Rise

Earthquake Resistant Steel Braced Frame Buildings

Thai Son Nguyen

A Thesis

in

The Department

of

Building, Civil and Environmental Engineering

Presented in Partial Fulfilment of the Requirements

for the Degree of Master of Applied Science (Building Engineering) at

Concordia University

Montreal, Quebec, Canada

August 2017

© Thai Son Nguyen, 2017

ABSTRACT

Wind-induced Shear and Torsion on Low- and Medium-Rise Earthquake Resistant Steel Braced Frame Buildings

Thai Son Nguyen

There are locations in Canada where buildings are equally affected by wind and earthquake loads. In these areas, designers may rise questions about the governing lateral load. It is known that buildings are designed to respond in the elastic range under wind load and in the inelastic range when subjected to earthquake load. Besides, there are other elements that influence the building responses under lateral loading, such as: building configuration, height, selected ductility level, structural irregularity types and geotechnical characteristics.

This thesis addresses the effect of wind-induced shear and torsion on 22 low-rise and medium-rise steel buildings located on Site Class C and Site Class B. These buildings were designed as earthquake resistant systems according to the 2015 edition of National Building Code of Canada (NBCC 2015) and Steel Design standard specifications (CSA S16-2014). The study examines the impacts from building configurations by considering different width-to-length ratios and heights on two sets of buildings: i) width-to-length ratio 1:4 and ii) width-to-length ratio 1:2. The 1st set comprises five buildings with heights ranging from 14.8 m (4-storey low-rise building) to 43.6 m (12-storey medium-rise building). The 2nd set comprises only medium-rise buildings with 8, 10, and 12 storeys. In addition, two types of ductility levels were selected for the lateral force resisting systems

(LFRS): limited-ductility (LD-CBF) and moderately-ductile concentrically braced frames (MD-CBF). Two types of geotechnical characteristics were considered: Site Class C (firm soil) and Site Class B (rock). All designed buildings are structural regular. The effects from torsion, notional lateral load, and P-Δ effect was also studied.

On the process of computing wind load, several ambiguities have been found in the NBCC 2015 wind load provisions. Consequently, recommendations were made to resolve these issues. In addition, these recommendations were implemented in several low-rise and medium-rise buildings before comparing with the results obtained when the ASCE/SEI 7-10 standard and the wind tunnel test were used. It was found that for low-rise buildings, the American standard and Canadian code yielded similar shear but quite different torsional coefficients. On the other hand, for medium-rise buildings, clear agreement was found, for both shear and torsion coefficients.

The comparisons between earthquake and wind loadings show that depending on building heights, horizontal dimensions, location and ductility level, the dominant loads are different. In taller, larger and more ductile buildings in Montreal, for direction normal to the larger face, wind loads may exceed the earthquake loads in the lower floor levels. In all other cases, earthquake load controls the design. For Montreal buildings taller than 8 storeys, selecting LD-CBF is recommended for the LFRS in order to balance the earthquake/wind design criteria. Caution should be given to buildings taller than 10 storeys when verifying the building deflection under the dynamic effect of wind load.

ACKNOWLEDGMENTS

TABLE OF CONTENTS

LIST OF FIGURES

LIST OF TABLES

NOMENCLATURE

B	building width
B_x	ratio to determine structure torsional sensitivity
C_f, C_r	member compressive force and factored compressive resistance
C_e	exposure factor
C_t	topographic factor
C_g	gust effect factor
C_p	external pressure coefficient
C_u, C'_u	probable compressive resistance and probable post-buckling compressive resistance
C_V, C_T	shear and torsional coefficients
D	building width parallel to the wind direction
D_{nx}	Plan dimension of the building at level x perpendicular to the direction of earthquake loading being considered
E	elastic modulus of steel
e_X, e_Y	eccentricities in E-W and N-S directions
f_n	building fundamental frequency
F	gust energy ratio
F_u	specified minimum tensile strength
F_y	specified minimum yield stress, yield point or yield strength
g_p	peak factor

H, h_n	building height
h_i	storey height
I	moment of inertia
I_E, I_W	earthquake and wind importance factors
K_d	wind directionality factor (ASCE/SEI 7-10)
K_i	structure stiffness
K_z	velocity pressure exposure coefficient (ASCE/SEI 7-10)
K_{zt}	topographic factor (ASCE/SEI 7-10)
L	building length
M_f, M_r	member flexural force and factored flexural resistance
M_V	factor to account for higher mode effect on base shear
N_x	notional load
p	specified external pressure acting statically and in a directional normal to the surface
P_x	gravity loads supported by the structure
P_{WX}, P_{LX}	wind pressures in windward and leeward direction
q	reference velocity pressure
q_H	mean dynamic wind pressure at roof level
Q_G	gravity-induced lateral demand on the LFRS at the critical level of the yielding system
Q_y	the resistance of the yielding mechanism required to resist the minimum earthquake loads

R_d	ductility-related force modification factor
R_o	overstrength-related force modification
s	size reduction factor
$S(T)$	design spectral response acceleration
T_u	probable tensile resistance
T_a	fundamental lateral period of vibration of the building
T_f, T_r	member tensile force and factored tensile resistance
U_{1x}, U_{1y}	factor to account for moment gradient and second-order effects of axial force acting on the deformed member
U_2	amplification factor to account for second-order effects of gravity loads acting on the laterally displaced storey
V, V_e, V_d	earthquake force
v	wind velocity
W	building weight
α	ratio to determine structural irregularity Type 9
β	damping ratio
Δ	member deflection
$\delta_{max}, \delta_{ave}$	maximum and average lateral deflections of the building
θ_x	stability coefficient

Chapter 1

INTRODUCTION

1.1. GENERAL

In active earthquake zones, building structures are designed to withstand earthquake loading, while behaving in the inelastic range. Meanwhile, these buildings should respond elastically under the wind load. It is important to understand which one of the two types of lateral load governs the design and which building characteristics are more sensitive to wind loading comparing to earthquake loading.

1.2. EARTHQUAKE LOADS

Earthquakes release large amount of energy and may produce considerable damages. For instance, in 1975, an earthquake with a 7.3 magnitude destroyed 90% of the cities in Sichuan, China (**Figure 1.1**). The level of damage was substantial because fire brought up during ground shaking. The damage and reconstruction raised to billions of dollars. In 2010, an earthquake with 8.8 magnitude occurred in Chile and more than 500 deaths were reported. The most severe mega-thrust earthquake occurred in March 2011 in Japan. Because the earthquake was always followed by tsunami, there were more than 20,000 deaths and over 2,500 people were reported missing. The total economic loss was found to be more than $300 billion.

The earthquake forces are caused by the movement of the storey mass. While the lower part of the building moves with the motion of the ground, the upper part resist against the movements due to its weight. The upper part follows the lower part in the displaced position and the movement cycle is repeated as long as the shear wave is induced into the building. In general, the heavier the building is, the more damage it experiences during an earthquake. Thus, when the building is stiff, its period is shorter and the base shear increases. Usually, steel buildings are more flexible than concrete buildings, which leads to higher fundamental period and lateral deflection.

In earthquake design, some predetermined structural members are allowed to yield during an earthquake, while the remaining members behave in the elastic range. This approach used in earthquake design is known as the capacity design.

Figure 1.1: City damaged by earthquake in Beichuan Quiand County, Sichuan, China (http://archive.boston.com/bigpicture/2008/05/earthquake_damage_in_beichuan.html).

1.3. WIND LOADS

Wind is the motion of the air, which can be horizontal or vertical. In the area near the surface of the earth, wind motion is three-dimensional with the horizontal actions stronger than the vertical ones. However, wind actions depend on the distance from ground surface. High turbulence may rise in a region up to roughly 500 m aboveground. Hence, wind speed increases gradually until it reaches a stable value, called gradient wind speed. Above this level, wind movement is more stable and less turbulence is formed comparing to boundary layer wind region.

Wind can be a hazardous element in the case of windstorms or hurricanes and it can cause thousands of deaths along with great economic loss and even deaths. Comparing to other natural disasters, such as earthquakes and floods, hurricane winds may produce significant economic loss. Thus, according to Taranarth (2004) between 1986 and 1993, in the United States, hurricane winds were the cause of $41 billion loss, greatly ahead of $6.18 billion from all other hazards combined. In Canada, between February 9 and 14 (2010), losses of $800 million have been resulted from windstorms. In fact, 57% natural-caused losses in the United States are due to wind.

Conversely to earthquake loads, wind acts in the form of external forces applied on building facades. For wind design, the lateral load resisting system needs to respond elastically and the building sway should be within the code limit.

1.4. OBJECTIVES AND SCOPE

This study focuses on the response of multi-storey steel structures located in Montreal on Site Class C and Site Class B when subjected to earthquake load and to wind load. The

lateral load resisting system (LFRS) selected for the studied buildings is the concentrically braced frame (CBF) with multi-storey X-braces. Both the Equivalent Static Force Procedure and the Dynamic Analysis Procedure by means of modal response spectrum method (NBCC 2015) are used for the earthquake design.

In terms of wind load, the current thesis focuses on Montreal region and two exposure terrains: open and urban. The procedures used for wind computation are from the NBCC 2015 and the ASCEI/SEI 7-10 standard provisions.

The objectives of this thesis are:

- To compute and compare earthquake and wind loads applied on low-rise and medium-rise CBF buildings regarding both strength and serviceability requirements by following the current building code (NBCC 2015) provisions.

- To provide a recommendation to improve the wind loading provisions given in NBCC 2015 based on studies involving the ASCE/SEI 7-10 standard provisions and wind tunnel test results reported in previous studies.

- To give design cautions for steel braced frame buildings when both earthquake and wind loads are considered.

1.5. METHODOLOGY

The methodology used in this thesis is shown in the flowchart given in **Figure 1.2**. Firstly, 22 steel office buildings were selected for investigation. These buildings contain CBFs with limited and moderate ductility located in Montreal on Site Class C and Site Class B. Secondly, these buildings were designed to respond earthquake load in inelastic range. Thirdly, on the process of designing wind load, some issues have been encountered. In

NBCC 2015 provisions. In this study, recommendations are made for wind load based on comparisons with ASCE/SEI 7-10 provisions and wind tunnel tests. Lastly, wind and earthquake loads are compared regarding strength and serviceability requirements. After that, recommendations are made for selecting braced frames for Montreal's buildings that comply with cost-efficiency criteria.
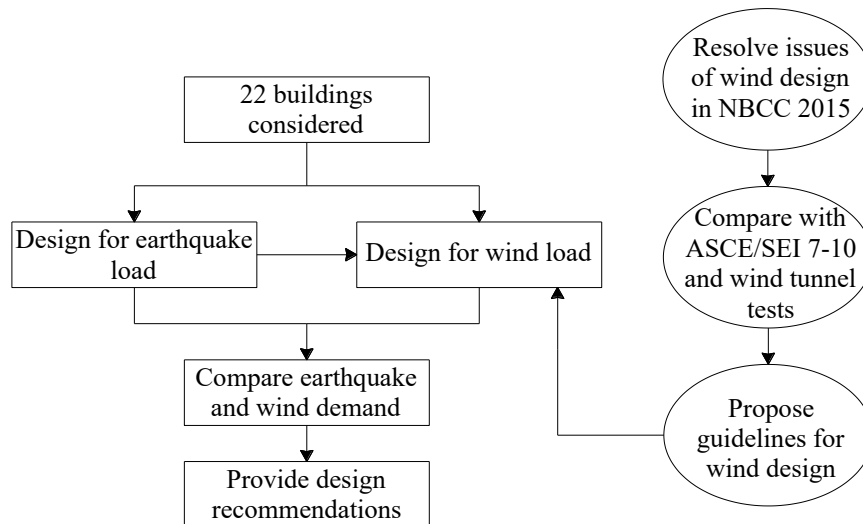
Figure 1.2: Methodology flowchart.

1.6. THESIS STRUCTURE

This thesis consists of 6 chapters.

- Chapter 1 gives an overview about damages caused by earthquakes and windstorms, as well as the objectives and scope of the current thesis. The methodology and outline of this thesis are also provided.

- Chapter 2 covers a detailed literature review referring to earthquake and wind loading provisions given in NBCC 2015. For wind loading, the issues found in NBCC 2015 provisions are addressed. The ASCE/SEI 7-10 provisions are also

discussed along with the introductions of past studies that provide the wind tunnel test's results.

- Chapter 3 presents the earthquake design for two sets of multi-storey office buildings located in Montreal. The first set refers to office buildings with a plan having the width-to-length ratio 1:4, labelled plan "A" and the second set to office buildings with a width-to-length ratio 1:2, labelled plan "B". The 1st set is divided into two groups of buildings, G1.C and G1.B, that refers to Site Class C and Site Class B, respectively. The G1.C group contains five LD-CBF buildings: 4-, 6-, 8-, 10- and 12-storey buildings and five MD-CBF buildings with the same heights. The G1.B group contains three LD-CBF and three MD-CBF buildings of 8, 10 and 12 storeys. The 2nd set contains six MD-CBF buildings. Among them, three MD-CBF buildings: 8-, 10- and 12-storey, belonging to G2.C group, are located on Site Class C and 3 MD-CBF buildings with the same heights are located on Site Class B (group G2.B). In total, there are 22 buildings. The detailed design is presented for the 12-storey LD-CBF office building located in Montreal, on Site Class C. It is noted that notional loads, torsional and P-Δ effects were considered in the designs.

- Chapter 4 addresses the issues regarding wind load provisions given in NBCC 2015 for both low- and medium-rise buildings. Using the wind design procedure provided in the ASCE/SEI 7-10 standard and wind tunnel test results released in four previous studies, improved guidelines referring to wind design according to NBCC 2015 are provided. This chapter also includes the definition for medium-rise buildings.

- Chapter 5 shows the wind design based on the recommendation made (Chapter 4) for the set of 22 buildings designed to resist earthquake load (Chapter 3), which were considered in open terrain.

- Chapter 6 exhibits the comparisons between the maximum base shear/ storey shear developed in the CBF buildings due to earthquake load and that obtained under wind load. Also, the serviceability conditions due to each type of loads are verified. Finally, the governing type of load is pointed out for each building.

- Lastly, Chapter 7 concludes the results of the current thesis and gives some recommendations for future work.

Chapter 2

LITERATURE REVIEW

2.1. EARTHQUAKE DESIGN PROVISIONS ACCORDING TO NBCC 2015 AND CSA S16-2014 STANDARD

2.1.1. Equivalent Static Force Procedure

According to NBCC 2015, the design for earthquake actions is carried out in accordance with either the Equivalent Static Force Procedure or the Linear Dynamic Analysis by the Modal Response Spectrum method. The former can be used for structures that meet any of the following conditions: $I_E F_a S_a(0.2)$ less than 0.35; regular structures less than 60 m in height having T_a less than 2 s in each of two orthogonal directions; and structures with structural irregularity other than Type 7 with height lesser than 20 m and T_a less than 0.5 s in each of two orthogonal directions. According to the Equivalent Static Force Procedure, the minimum lateral earthquake force, V, is given in Equation (2-1). However, V shall not be less than the value given in Equation (2-2).

$$V = S(T_a)M_V I_E W/(R_d R_o) \tag{2-1}$$

$$V_{min} = S(2.0)M_V I_E W/(R_d R_o) \tag{2-2}$$

where $S(T_a)$ is the design spectral response acceleration; M_V is the factor to account for higher mode effect on base shear; I_E is the earthquake importance factor of the building; W is the dead load including 25% of the snow load and 60% of the storage load for areas

used for storage; R_d, R_o are the ductility-related and overstrength-related force modification factor, respectively.

The fundamental period, T_a, proposed for steel braced frames in the current NBCC is:

$$T_a = 0.025h_n \tag{2-3}$$

where h_n is the building height in meters.

When a dynamic analysis is used, it is accepted to consider fundamental period greater than T_a but not exceeding $2T_a$.

The shear force distribution over the building height is:

$$F_x = (V - F_t)W_x h_x / \left(\sum_{i=1}^{n} W_i h_i \right) \tag{2-4}$$

where F_t is a portion of V that is concentrated at the top of the building and is equal to: $0.07T_a V$ but it cannot exceed $0.25V$ for buildings with lateral period greater than 0.7 s and it is zero if the fundamental lateral period is less than 0.7 s; W_x is the seismic weight of the floor at level x; and h_x is the height of story x.

Then, the shear force is distributed among the LFRS according to each braced frame stiffness and location. Torsional effects due to earthquake actions are generated from the inherent eccentricity and the accidental eccentricity. The inherent eccentricity is given by the difference between the center of mass and the center of rigidity, which are controlled by the configuration of the building and the placement of the LFRS. The accidental eccentricity, e_a, is considered 10% of the building dimension perpendicular to the direction of lateral force application and takes into account the uncertainty of earthquake load. With torsion considered, the distribution of shear force in a LFRS at floor x is:

$$V_x = V \frac{K_i}{\sum K_i} + \frac{T}{d} \frac{K_i d_i^2}{\sum K_i d_i^2}$$ (2-5)

where K_i is the stiffness of the braced frame; T is the torsion caused by earthquake load; d is the distance of the braced frame under consideration to the center of rigidity.

To verify if a building is irregular due to torsional sensitivity, the value of B, which is the maximum of B_x, should be greater than 1.7. This criterion is applied in both orthogonal directions and B is computed as shown below.

$$B_x = \delta_{max}/\delta_{ave}$$ (2-6)

Herein, δ_{max} and δ_{ave} are the maximum and average storey displacement at the extreme points of the structure in the direction of the earthquake acting at distances $\pm 0.10 D_{nx}$ from the center of mass at each floor.

2.1.2. Dynamic Analysis Procedure

In terms of Dynamic Analysis Procedure, the types of analysis are: Linear Dynamic Analysis and Non-linear Dynamic Analysis. The former can be carried out by either the Modal Response Spectrum Method, where the spectral acceleration values, $S(T)$, are used or the Numerical Integration Linear Time History Method. The latter analysis is performed in the nonlinear range (Filiatrault et. al., 2013).

In this thesis, the Modal Response Spectrum Method is chosen. In NBCC 2015, the ordinates of the uniform hazard spectrum are given for periods of 0.2 s, 0.5 s, 1.0 s, 2.0 s, 5.0 s and 10 s for each location in Canada. The analysis is performed separately in both orthogonal directions: e.g. West-East (E-W) and North-South (N-S). In the case that the

elastic spectrum was input in the analysis ($R_d \times R_o = 1$), the resulted base shear is labeled the elastic base shear, V_e.

For buildings located on Site Class other than Class F with the ductility-related force modification factor of the LFRS, $R_d \geq 1.5$, the elastic base shear, V_e, obtained from a Linear Dynamic Analysis may be multiplied by the largest of the following factors to obtain the design elastic base shear, V_{ed}:

$$\begin{cases} \dfrac{2S(0.2)}{3S(T_a)} \leq 1 \\ S(0.5)/S(T_a) \leq 1 \end{cases} \qquad (2\text{-}7)$$

To obtain the design base shear, V_d the V_{ed} is multiplied with I_E/R_dR_0. After that, for regular structures, the design base shear, V_d, needs not to be less than 80% of the base shear, V, determined by the Equivalent Static Force Procedure. If the structure is irregular, V_d shall be taken as the larger of that results from dynamic analysis and 100% of V.

2.1.3. Structural Irregularities

Previous records on earthquake hazard have shown that buildings with irregularities, such as irregular geometry or stiffness discontinuity, can be significantly damaged under earthquake loads. A list of structural irregularities is given in NBCC 2015.

Hence, nine types of structural irregularities, namely: 1) vertical stiffness irregularity, 2) mass irregularity, 3) vertical geometric irregularity, 4) in-plan discontinuity irregularity, 5) out-of-plane offsets of the vertical elements of the LFRS, 6) discontinuity in capacity weak storey, 7) torsional sensitivity, 8) non-orthogonal system irregularity and 9) gravity-induced lateral demand irregularity on the LFRS, are defined in NBCC 2015.

2.1.4. Stability Effects

The P-Δ effects amplify the lateral displacements of structures subjected to lateral loads. If the structure is deformed laterally in the nonlinear range, the P-Δ effects may cause the building collapse. To calculate the stability coefficient, θ, at each storey, the following equation is used:

$$\theta_x = \frac{\sum C_{fx} R_d \Delta_{fx}}{\sum V_{fx} h_{sx}} \tag{2-8}$$

where C_{fx} is the cumulated gravity load computed at floor level x; Δ_x is the interstorey drift at floor level x; V_{fx} is the storey shear force at the same floor x; and h_{sx} is the storey height of the floor x.

If the stability coefficient, θ_x, is greater than 0.1, the P-Δ effects are taken into account by multiplying the earthquake loads at each level by the factor, U_2:

$$U_2 = 1 + \theta_x \tag{2-9}$$

On the other hand, when θ_x is less than 0.1, the P-Δ effect can be neglected. However, if the factor U_2 is greater than 1.4, the structure is instable and the stiffness shoul be increased. Additionally, the notional lateral load should be considered in design. Its value at each floor, is computed as:

$$N_x = 0.005 C_{fx} \tag{2-10}$$

where C_{fx} is the total gravity load at level x component from $(D + 0.5L + 0.25S)$, which is associated to the earthquake load combination $(D + 0.5L + 0.25S + 1.0E)$.

2.1.5. Storey Drifts

Lateral deflection under earthquake load should be within the code limit, which is $2.5\%h_s$ for ordinary buildings (h_s is the storey height). The deflections determined from dynamic analysis, using a nonlinear acceleration spectrum for example, need to be multiplied by R_dR_0/I_E to attain realistic values of anticipated maximum deflections (Mitchell et. al., 2003). According to the importance category of the building, the maximum interstorey drift values are given in the table below.

Table 2.1: Interstorey drift limits.

Importance category	Maximum interstorey deflection
Post-disaster buildings	$0.01h_s$
High importance category	$0.02h_s$
Other buildings	$0.025h_s$

2.1.6. Concentrically Braced Frame System

Concentrically Braced Frames (CBF) are among the most popular LFRS in North America because they provide high stiffness and strength. In addition, the process of constructing CBF is cost-effective and time-saving. There are a variety of brace types for CBFs, such as Chevron bracing, multi-storey X bracing, tension-only bracing and others. According to NBCC, CBFs can be designed with limited (LD-CBF) or moderately ductility (MD-CBF). In moderate to high risk seismic zone ($I_EF_aS_a(0.2) \geq 0.35$), it is recommended to limit the height of LD-CBF with tension-compression braces to 60 m and that of MD-CBF to 40 m. Tension-compression braces of CBF are designed to yield in tension and buckle in compression. At the same time, the CBF beams and columns are designed to withstand the

effects from the yielding and buckling of the braces in addition to the associated gravity load.

2.1.7. Capacity Design According to CSA S16-2014

In light of ductile design, inelasticity is concentrated in members designed to yield/buckle during an earthquake. All adjacent members need to be able to sustain the yielding/buckling of ductile members while behaving in the elastic range.

In general, yielding members are sized such that they are the weakest link among all members and the elastic members are designed to sustain the capacity of yielded members. The NBCC 2015 stipulates different types of LFRS with different level of ductility, which are controlled by the ductility-related force modification factor, R_d. The yielding/buckling mechanism of these LFRS are predefined through experimental tests, which does not significantly affect the overall integrity of the structure.

In a steel braced frame, the probable tensile resistance, T_u, probable compressive resistance, C_u, and the probable post-buckling compressive resistance, C'_u, of the braces upon yielding are computed, as following:

$$T_u = A_g R_y F_y \tag{2-11}$$

$$C_u = \min \begin{cases} \dfrac{1.2 A_g R_y F_y}{\left(1 + \lambda_y^{2n}\right)^{1/n}} \\ A_g R_y F_y \end{cases} \tag{2-12}$$

$$C'_u = \min \begin{cases} \dfrac{A_g R_y F_y}{\left(1 + \lambda_y^{2n}\right)^{1/n}} \\ 0.2 A_g R_y F_y \end{cases} \tag{2-13}$$

14

According to CSA S16-2014, R_y is equal to 1.1 for all W-shape steel members. However, the value of $R_y F_y$ cannot be lesser than $460\ MPa$ for hollow structural sections (HSS).

2.2. WIND LOADING PROVISIONS ACCORDING TO NBCC 2015 AND ASCE/SEI 7-10 STANDARD

2.2.1. Wind Load Provisions – NBCC 2015

Based on its configuration and fundamental frequencies, three procedures are stipulated in NBCC 2015 for computing wind load on a building, namely: Static Procedure, Dynamic Procedure and Experimental Procedure (**Figure 2.1**). Only the Static Procedure and the Dynamic Procedure are considered in the current thesis.
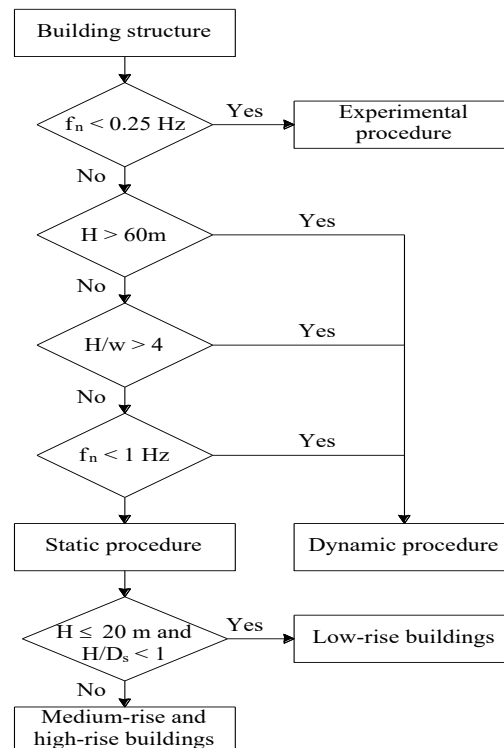
Figure 2.1: Flowchart for wind loading procedures on buildings – according to NBCC 2015.

2.2.1.1. Static Procedure

The static procedure is applied to buildings that are lower than 60 m height, having the ratio of height over the effective width of the building equal or less than 4 and natural frequency greater than 1.0 Hz. In NBCC 2015, the full wind external pressure is given by

$$p = I_W q C_e C_t C_g C_p \tag{2-14}$$

where I_W is the importance factor for wind load, q is the reference velocity pressure; C_e, C_t, C_g are the exposure, topographic and gust effect factor; and C_p is the external pressure coefficient.

After the wind pressures are acquired, they are multiplied by the corresponding projected/tributary areas to attain the external wind forces acting on the building walls. The wind loads are computed for each floor before being summed up to obtain the base shear. The process is carried out in both North-South (N-S) and East-West (E-W) directions. Under wind loading, torsion is formed by the unbalance of wind pressures on building wall faces, as specified in the partial loading cases.

2.2.1.2. Dynamic Procedure

For buildings that are higher than 60 m or the height to width ratios is higher than 4 or the lowest natural frequency is lower than 1, the dynamic procedure should be applied. The dynamic procedure is similar to the static procedure, including the partial loading cases, except that the exposure factor, C_e and the gust factor, C_g are evaluated differently (NBCC 2015). The calculation of C_g is given below.

$$C_g = 1 + g_p \sqrt{\frac{K}{C_{eH}} \left(B + \frac{sF}{\beta}\right)} \qquad (2\text{-}15)$$

$$s = \frac{\pi}{3} \left[\frac{1}{1 + \frac{8f_n H}{3V_H}}\right] \left[\frac{1}{1 + \frac{10 f_n w}{V_H}}\right] \qquad (2\text{-}16)$$

$$F = \frac{(1220 f_n / V_H)^2}{[1 + (1220 f_n / V_H)^2]^{4/3}} \qquad (2\text{-}17)$$

Herein, C_g is the gust factor; g_p is the peak factor; K is a factor related to the surface roughness coefficient of the terrain; C_{eH} is the exposure factor evaluated at the top of the building; B is the background turbulence factor; s is the size reduction factor; F is the gust energy ratio at the natural frequency of the structure; β is the critical damping ratio in the along-wind direction; f_n is the fundamental frequency; H is the height of the building; V_H is the mean wind the speed at the top of the structure; w is the effective width of windward face of the building.

As shown in Equations (2-16) and (2-17), the fundamental frequency of the building should be known before applying the dynamic procedure. The lowest natural frequency of the building is computed by the following equation:

$$f_n = \frac{1}{2\pi} \sqrt{\frac{\sum_{i=1}^{N} F_i \frac{x_i}{x_N}}{x_N \sum_{i=1}^{N} M_i \left(\frac{x_i}{x_N}\right)^2}} \qquad (2\text{-}18)$$

where N is the number of stories; F_i, M_i are the lateral load and floor mass at level i^{th}; x_i and x_N are the horizontal deflections of floor at level i and N, respectively.

17

2.2.1.3. Partial Loading Cases

2.2.1.3.1. Medium-Rise Buildings

To investigate the critical impacts of wind load on medium-rise buildings defined in this study as those whose height is between 20 m and 60 m and have the ratio of height to the smaller plan dimension between 1 and 4, along with the conventional full loading case (Case A), three additional partial loading cases have been introduced in NBCC 2015 (Cases B, C, D) as shown in **Figure 2.2**. In general, the wind pressure is distributed differently in each case. The differences in the magnitude of the pressure and the corresponding tributary area create different wind-induced effects in these cases.

Wind-induced shear effects are evaluated by considering load Cases A and C. The conventional loading method is followed in Case A when 100% of wind forces are loaded separately in each principal axis. Clearly, this case produces the maximum base shears. Wind blowing diagonally to the walls can be illustrated equivalently by simultaneously reduced forces. Indeed, 75% of full load is applied simultaneously on both wall faces to create Case C. Although the load magnitude is reduced in this case, simultaneous effect from wind in both directions can yield higher stresses in some structural members. The magnitude and tributary area of wind loading are well-defined in these two cases, which makes the procedure easy-to-follow. However, several issues have been encountered in the process of determining torsions in load Cases B and D.

Case A: Full wind pressure applied in both diretions separately

Case C: 75% of full wind pressure applied in both diretions simultaneously

Case B: Case A wind pressure applied only on parts of wall faces

Case D: 50% of case C wind load removed from part of projected area
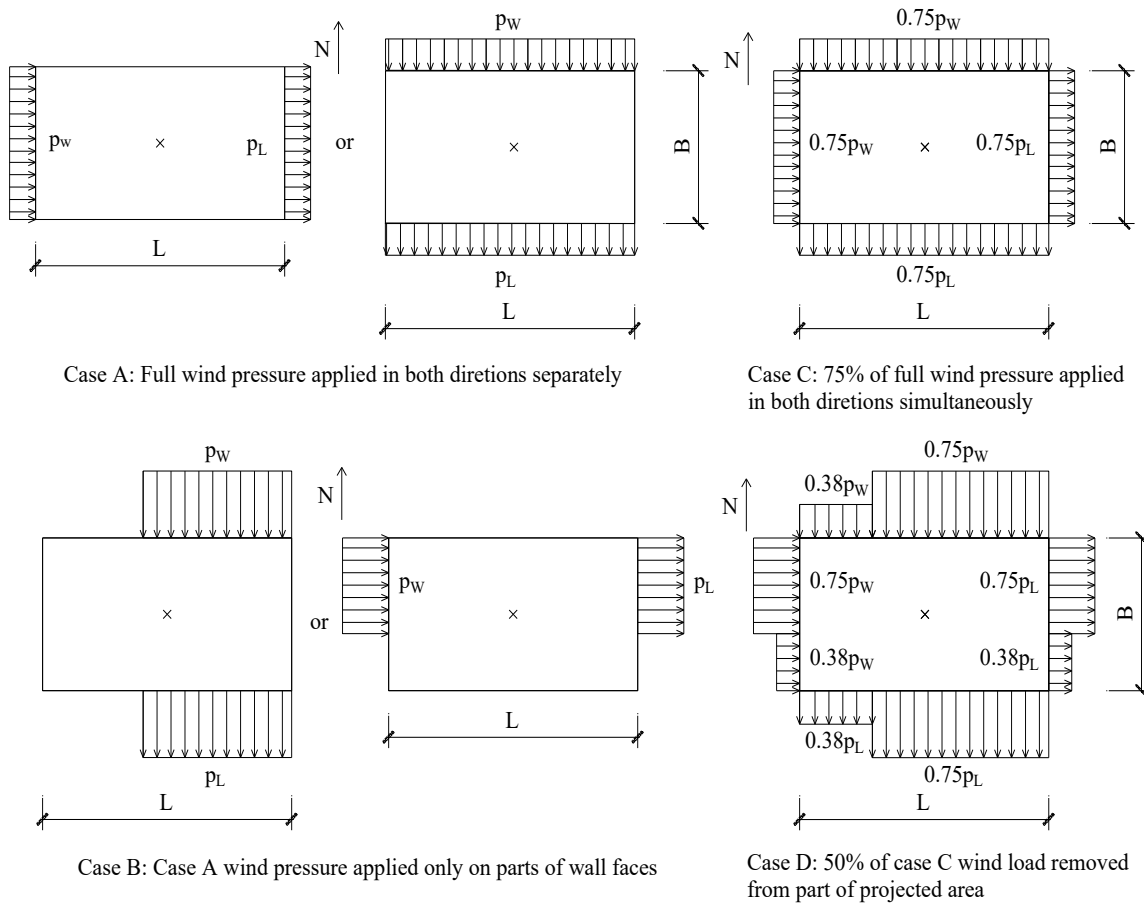
Figure 2.2: Load cases for medium-rise buildings adapted from NBCC 2015.

In the torsional load cases, the uniformly distributed wind forces acting on the building are partly reduced (in both magnitude and tributary area) in one or both principal directions. The tributary area of the wind pressure acting on a particular story wall face is a product of the height of the story under consideration and the horizontal distribution length of the wind load. However, the latter is not provided explicitly in Case B and Case D. In particular, the wind projected area is mentioned as "reduced from part of projected area". The term "part" and the tributary areas in both cases need to be clarified as it rises questions among code users, which may lead to different tributary areas, and therefore, potential false wind-induced torsions.

Although these issues have been known for a while, not much research has been carried out to address them systematically in order to modify the Canadian wind load specifications accordingly. An effort to resolve this issue will be provided in Chapter 4 of this thesis.

Other wind codes and standards address torsional loads differently. For instance, the American standard ASCE/SEI 7-10 specifies that, for low-rise buildings, besides applying higher wind loads on wall corners, 25% of the full design wind pressure is reduced by half on the wall face to account for torsional effects. For medium-rise/high-rise buildings, eccentricities and torsion moments are defined explicitly by formulas with wind loads applying to full tributary areas in all load cases. In Eurocode 1 (EN 1991-1-4:2005), the torsional effects are taken into account by changing the uniformly distributed wind load in windward direction represented by rectangular loading to inclined triangular loading while keeping the same load on the leeward wall face. It also regulates that in some cases, wind loads on locations that create beneficial impacts should be completely removed, but this regulation is not very clear for the users. The Australian/New Zealand building code (AS/NZS 1170.2:2011) fully neglects the wind-induced torsion for low-rise and medium-rise buildings whereas for high-rise buildings ($> 70\ m$), an eccentricity of 20% of the shorter horizontal dimension is considered to account for torsion.

2.2.1.3.2. Low-Rise Buildings

As illustrated in **Figure 2.3**, two load cases are provided in NBCC 2015 for low-rise buildings, namely Case A and Case B, which simulate the wind loads applying perpendicular and parallel to the ridge of a building, respectively. In general, wind loads for low-rise buildings are computed in a similar manner as for medium-rise buildings.

However, wind pressures are not distributed uniformly over the wall or roof face. In general, wind pressures are greater in wall corners, which in turn generates torsions in both load cases. However, Stathopoulos et al. (2013) has shown that these provisions may not be adequate for torsion in low-rise buildings. As specified in Case B, when acting parallel to the building's ridge, wind forces also create impacts to both sides of the building including opposite sides of the roof. When considering buildings with flat roofs, these effects can be neglected because the across-wind forces on opposite wall faces eliminate each other. As a result, the two load cases merge into a single case.
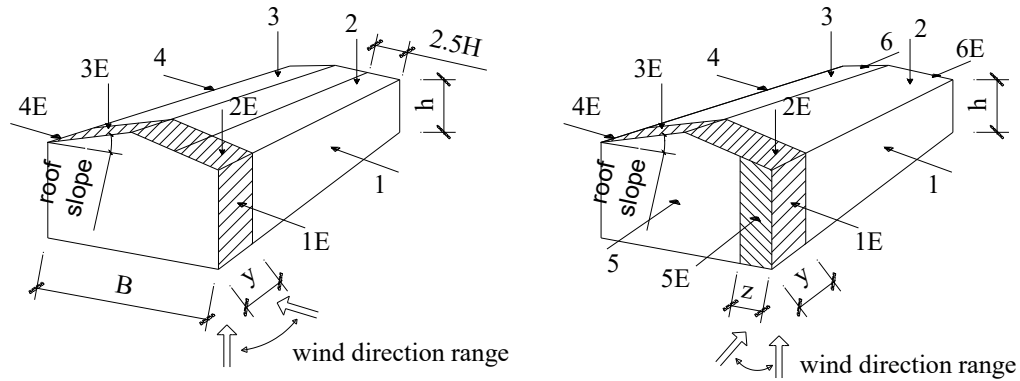
Load case A: winds generally perpendicular to ridge   Load case B: winds generally parallel to ridge

Roof slope	Building surfaces - Case A							
	1	1E	2	2E	3	3E	4	4E
0° to 5°	0.75	1.15	-1.3	-2.0	-0.7	-1.0	-0.55	-0.8

Roof slope	Building surfaces - Case B											
	1	1E	2	2E	3	3E	4	4E	5	5E	6	6E
0° to 90°	-0.85	-0.9	-1.3	-2.0	-0.7	-1.0	-0.85	-0.9	0.75	1.15	-0.55	-0.8

End-zone width y should be the greater of 6m or 2z, where z is the gable wall end zone defined for Load Case B below. Alternatively, for buildings with frames; the end zone y may be the distance between the end and the first interior frame

End-zone width z is the lesser of 10% of the least horizontal dimension or 40% of height, H, but not less than 4% of the least horizontal dimension or 1m

Figure 2.3: Load cases for low-rise buildings according to NBCC 2015.

2.2.2. Wind Load Provisions - ASCE/SEI 7-10

Two different procedures, namely Directional and Envelope Procedures, are available in ASCE/SEI 7-10 standard for wind loading. The Directional Procedure can be applied to buildings of all heights, while the Envelope Procedure is specified only for low-rise buildings. The wind pressure, following Directional and Envelope Procedure, are as follows:

$$p = qGC_p - q_i(GC_{pi}) \ (Directional) \qquad\qquad (2\text{-}19)$$

$$p = q_h[(GC_{pf}) - (GC_{pi})] \ (Envelope) \qquad\qquad (2\text{-}20)$$

where q is the velocity pressure evaluated at height z above the ground for windward walls, and at height h for leeward walls; q_h and q_i are the velocity pressure evaluated at mean roof height h; G is the gust factor; C_p is the external pressure coefficient; (GC_{pi}) is the peak internal pressure coefficient and (GC_{pf}) is the peak external pressure coefficient. In this thesis, it is assumed that all buildings under consideration are enclosed. Consequently, the internal pressure effects have been neglected, since they cancel each other on opposite walls.

The ASCE/SEI 7-10 standard specifies four partial loading cases for the Directional Procedure, and four cases for the Envelope Procedure (including two torsional load cases), as shown in **Figure 2.4** and **Figure 2.5**, respectively. Clearly, Cases 1 and 3 of the Directional Procedure are similar to NBCC 2015, but a difference can easily be witnessed in the torsional load cases (Cases 2 and 4). In these cases, the same approach as Cases B and D (NBCC 2015) is used, except that a torsion M_T is defined explicitly and the wind

pressure is distributed uniformly over the full tributary area of the building wall face. This matter will be discussed more in Chapter 4. Torsion is defined as following:

$$\begin{cases} M_T = 0.75(P_{WX} + P_{LX})B_X e_X \ (Case\ 2) \\ M_T = 0.75(P_{WY} + P_{LY})B_Y e_Y \ (Case\ 2) \end{cases}$$ (2-21)

$$M_T = 0.563(P_{WX} + P_{LX})B_X e_X + 0.563(P_{WY} + P_{LY})B_Y e_Y \ (Case\ 4)$$ (2-22)

In terms of low-rise buildings, two additional torsional load cases are specified in the Envelope Procedure besides two conventional load cases. In these cases, only 25% of the full wind pressures are applied to half of the building wall, while the rest remain unchanged comparing to conventional case, which in turn creates a greater amount of torsion comparing to the Canadian provisions.

All ASCE/SEI 7-10 values have been multiplied by 1.53^2 due to the difference between the 3-second and 1-hour wind speed used in NBCC 2015 and ASCE/SEI 7-10, respectively. In particular, the wind speed in NBCC 2015, measured over a period of 1 hour, is 1.53 times smaller than that of ASCE/SEI 7-10, which is calculated over a period of 3 seconds (Durst, 1960).
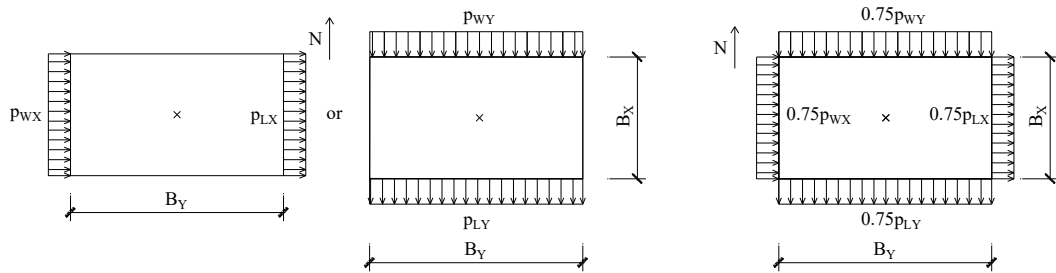
Case 1: Full design wind pressure acting on the projected area perpendicular to each principal axis of the structure, considered separately along each principal axis.

Case 3: Wind loading as defined in Case 1, but considered to act simultaneously at 75% of the specified value.

$M_T=0.75(P_{WX}+P_{LX})B_X e_X$
$e_X=\pm0.15B_X$

$M_T=0.75(P_{WY}+P_{LY})B_Y e_Y$
$e_Y=\pm0.15B_Y$

$M_T=0.563(P_{WX}+P_{LX})B_X e_X+0.563(P_{WY}+P_{LY})B_Y e_Y$
$e_X=\pm0.15B_X$ $\qquad e_Y=\pm0.15B_Y$
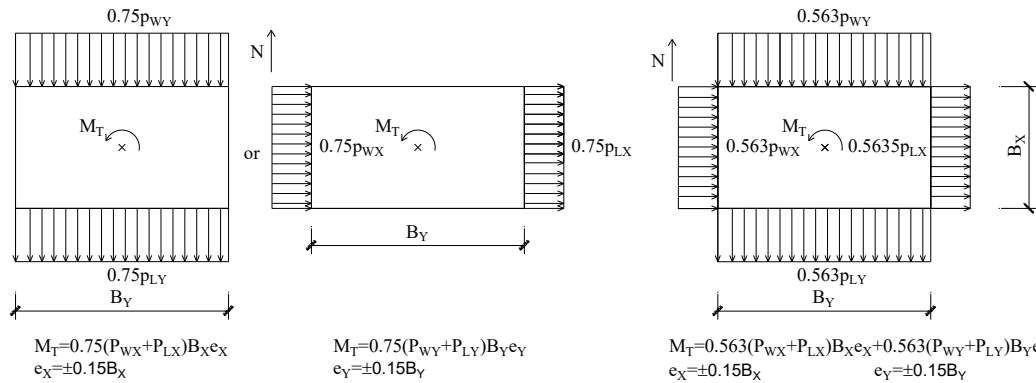
Case 2: Three quarters of the design wind pressure acting on the projected area perpendicular to each principal axis of the structure in conjunction with a torsional moment as shown, considered separately for each principal axis.

Case 4: Wind loading as defined in Case 2, but considered to act simultaneously at 75% of the specified value.

Figure 2.4: Partial loading case for the Directional Procedure after ASCE/SEI 7-10.

Figure 2.5: Partial loading cases for the Envelope Procedure after ASCE/SEI 7-10.
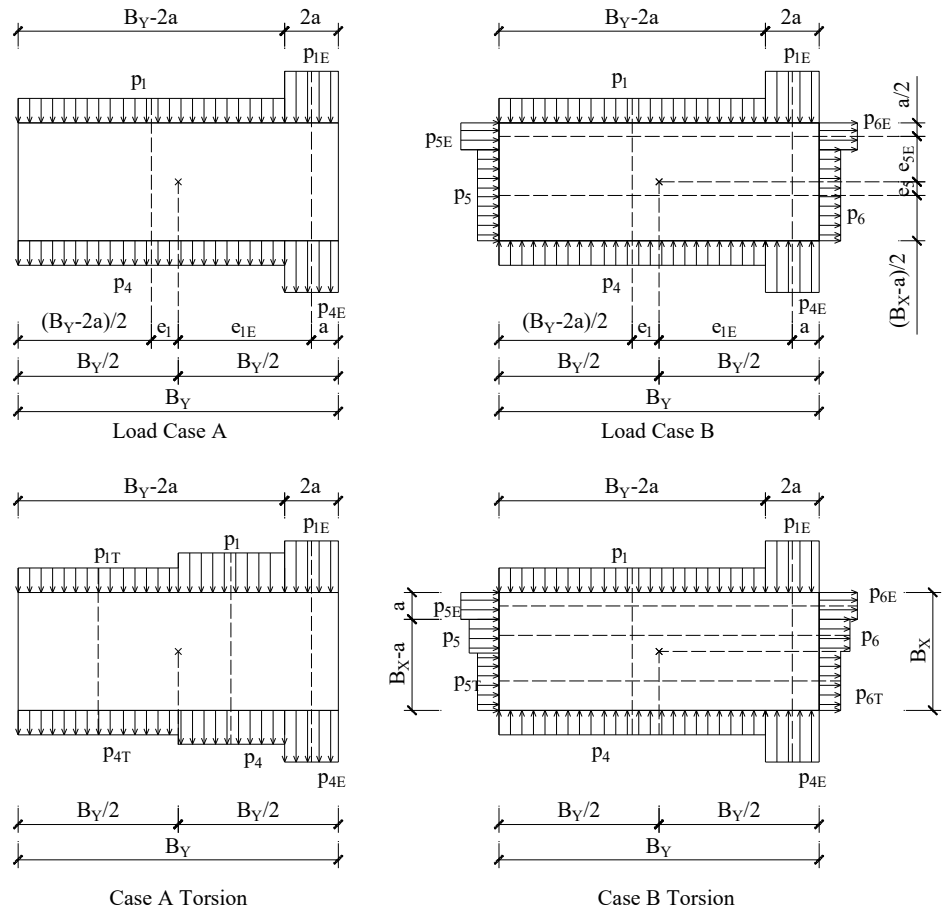
a: 10% of least horizontal dimension or 0.4h, whichever is smaller, but not less than either 4% of least horizontal dimension or 3ft (0.9m)

2.2.3. Review of Previous Studies

In this thesis, the results from wind tunnel tests are taken from four past studies for comparing purpose. The results will be discussed in detail in Chapter 4. This section only gives an overview about these studies in terms of experimental setups. Also, the definitions of the normalized coefficients corresponding to each study are provided.

2.2.3.1. The Study of Tamura et al. (2003)

Two buildings were chosen from the study of Tamura et al. (2003). These buildings were examined using the wind tunnel tests. The horizontal dimensions of the two buildings are $L \times B \times H = 42.5\ m \times 30\ m \times 12.5\ m$ (low-rise building) and $L \times B \times H = 50\ m \times 25\ m \times 50\ m$ (medium-rise building). The building models were made in a geometrical scale of 1/250. The low-rise building was tested on both urban and open terrains, while the medium-rise building was tested on urban terrain only. The power law index of mean wind speed was 1/4 for urban terrains and 1/6 for open terrain. The wind speed applied on building models ranged from 10.9 to 14.1 m/s. The time scales were set from 1/109 to 1/178.

Wind was directed perpendicular toward the wall face. In this study, 154 and 110 samples were tested from a time interval of 0.00128s over 10-minute long tests in both terrains for low-rise buildings. The maximum wind forces and base torsional moments, obtained by the integrated fluctuating pressures, were normalized as follows:

$$C_V = \frac{V}{q_H LH} \tag{2-23}$$

$$C_T = \frac{T}{q_H LHR} \tag{2-24}$$

$$R = \frac{(L^2 + B^2)^{1/2}}{2} \tag{2-25}$$

2.2.3.2. The Study of Keast et al. (2011)

The experimental data was of a medium-rise rectangular building: $L \times B \times H = 40\ m \times 20\ m \times 60\ m$. The geometrical scale of the study was 1/400, simulated in open terrain. The experimental buildings configurations were 6 degree-of-freedom for a 10-hour

full-scale equivalent time. Wind was blown on the buildings from different angles. The angle increment was 15°. Further, the natural frequency of the buildings was set at a level so that resonance can be avoided.

The maximum wind forces and base torsional moments, obtained by the integrated fluctuating pressures, were normalized as follows:

$$R = \frac{(L^2 + B^2)^{1/2}}{2} \tag{2-26}$$

$$C_T = \frac{T}{q_H L^2 H} \tag{2-27}$$

2.2.3.3. The Study of Isyumov and Case (2000)

The study of Isyumov and Case (2000) was carried out to analyze the wind-induced torsional loads and responses on buildings. The experimental results from the low-rise building from this study were used for the current thesis. The building configuration is $L \times B \times H = 29.26\,m \times 9.75\,m \times 4.88\,m$, resulted from a model with the geometrical scale of 1/100. The building was classified low-rise building with gable roof with a slope of 4/12. The experiment simulated the wind in urban terrain, with the power index of mean wind speed equal to 0.16. The wind was directed normal toward the building in both directions. Only the torsional coefficient of the model was presented in this study. The torsional coefficient was defined as:

$$C_T = \frac{T}{q_H B L H} \tag{2-28}$$

2.2.3.4. The Study of Stathopoulos et al. (2013)

The wind tunnel tests from the study of Stathopoulos et al. (2013) were carried out in the boundary layer wind tunnel of Concordia University $(12.2\ m \times 1.80\ m)$ on 3 flat-roof buildings configurations with the same horizontal dimensions, but different building heights. The buildings were selected for the current study as follows: $L{\times}B{\times}H = 61\ m{\times}38\ m{\times}20\ m$, $L{\times}B{\times}H = 61\ m{\times}38\ m{\times}30\ m$ and $L{\times}B{\times}H = 61\ m{\times}38\ m{\times}40\ m$. The geometric scale was 1/400. The models were tested under the wind velocity of 13.6 m/s and the power law index of the mean wind speed of 0.15. For a conservative approach, the wind was simulated over an open terrain exposure. Restrictors were used in the tubing for frequency corrections. Also, the sampling rate was 300 Hz over a 27- second period on each channel.

The shears and torsions were computed by the product of the measured pressures at pressure taps and their effective areas. Then, they are expressed in the non-dimensional forms of shear and torsional coefficients:

$$C_V = \frac{V}{q_H B^2} \tag{2-29}$$

$$C_T = \frac{T}{q_H B^2 L} \tag{2-30}$$

The coefficients from these four studies are used in this thesis to verify the wind load provisions given in NBCC 2015 in Chapter 4.

Chapter 3

EARTHQUAKE DESIGN

In this study, two sets of multi-storey CBF office buildings ranging from 4 storeys (14.8 m height) to 12 storeys (43.6 m height), located in Montreal, Quebec, are considered. The 1st set employs the building with plan "A" and the 2nd set employs the building with plan "B". The building with plan "A" has the width-to-length ratio 1:4 and the buildings with plan "B" has the width-to-length ratio 1:2. The 1st set is divided into two groups of buildings G1.C and G1.B implying Site Class C and Site Class B, respectively. The G1.C group contains five LD-CBF buildings with 4, 6, 8, 10 and 12 storeys and five MD-CBF with the same height ranges. The G1.B group contains three LD-CBF and three MD-CBF buildings with 8, 10 and 12 storeys. The 2nd set contains three MD-CBF buildings of 8-storey, 10-storey and 12-storey, located on Site Class C (G2.C group) and three MD-CBF buildings with same heights on Site Class B (group G2.B). All studied buildings are listed in **Table 3.1**.

Firstly, all 22 buildings are designed for gravity load and earthquake load. The maximum earthquake-induced shear forces in the studied CBF systems include shear caused by notional lateral loads, torsional and the P-Δ effects. The shear force is computed in both orthogonal directions (e.g. E-W and N-S). Due to design similarities, only the design of a 12-storey building is explicitly given in this chapter. The design of all other buildings is summarized in Tables of Appendix A.

Table 3.1: Selected buildings.

Buildings with Plan "A"				Buildings with Plan "B"	
Group G1.C (Site Class C)		Group G1.B (Site Class B)		Group G2.C (Site Class C)	Group G2.B (Site Class B)
LD-CBF (R_d=2)	MD-CBF (R_d=3)	LD-CBF (R_d=2)	MD-CBF (R_d=3)	MD-CBF (R_d=3)	MD-CBF (R_d=3)
12-storey	12-storey	12-storey	12-storey	12-storey	12-storey
10-storey	10-storey	10-storey	10-storey	10-storey	10-storey
8-storey	8-storey	8-storey	8-storey	8-storey	8-storey
6-storey	6-storey				
4-storey	4-storey				

3.1. BUILDING DESCRIPTION

There are two building plans used in this study: plan "A" (where $B = 38\ m$ and $L \approx 4B = 150.5\ m$) and plan "B" (where $B = 38\ m$ and $L \approx 2B = 75.5\ m$). It is noted that the maximum length of the building versus its width was selected to comply with the upper limit for the in-plan slenderness, which is 4.0 according to Eurocode 8 (e.g. for plan "A" the ration $L/B \approx 4$). These building dimensions include the hanging of 250 mm on each side of the floor, while the typical span is 7.5 m in both orthogonal directions. The building height raises from 14.8 m to 43.6 m. The ground floor height is 4.0 m and that of typical floor is 3.6 m. For building with plan "A" there are 8 CBFs placed in each orthogonal direction. The location of each CBF was selected to provide symmetry. All studied buildings are offices, located in Montreal, Quebec, Canada on both Site Class C and Site Class B, and have two types of ductility factors: $R_d = 3$ (MD-CBF) and $R_d = 2$ (LD-CBF). The building plans and elevations are given in **Figure 3.1**.

The design of the 12-storey LD-CBF building with plan "A", located in Montreal on Site Class C, is presented in Section 3.2.
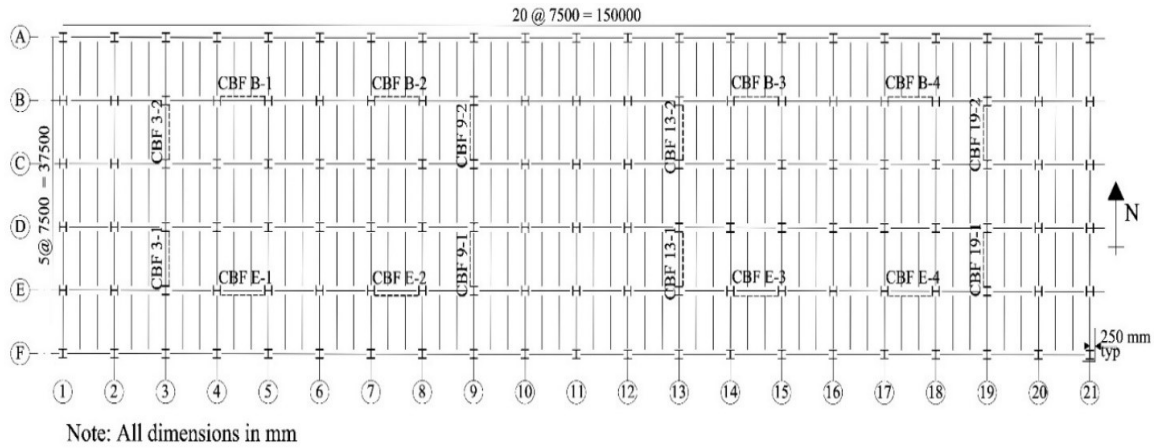
a. Plan "A"
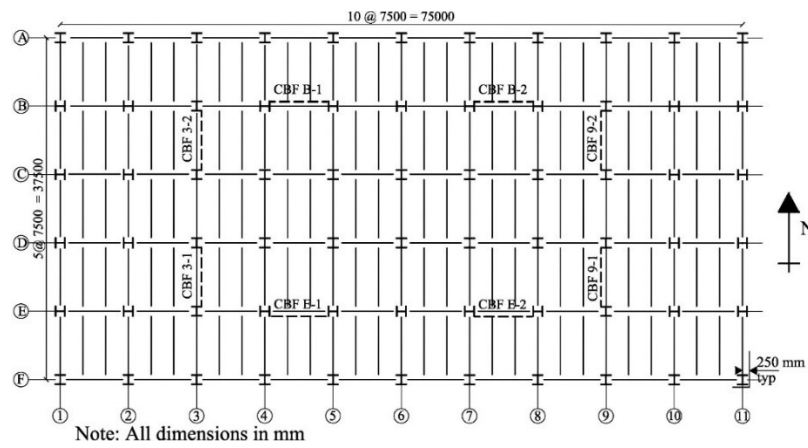
b. Plan "B"
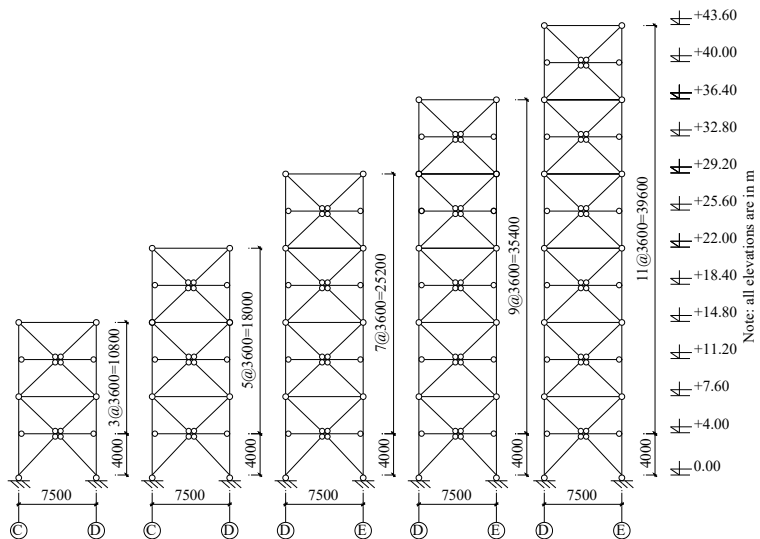
c. CBF elevations

Figure 3.1: Building plans and CBF elevations.

31

3.2. GRAVITY AND EARTHQUAKE DESIGN OF THE 12-STOREY BUILDING

3.2.1. Gravity System Design

For gravity design, the most critical load combinations are: $1.4D$, $1.25D + 1.5L + 1S$, and $1.25D + 1.5S + 1.0L$. The load patterns are assumed as shown in **Table 3.2**.

All flooring, such as the main beams and secondary beams are designed for strength and deflection requirements. Concerning the strength requirement, the size of beams was selected such that $M_f < M_r$, where M_f is the factored moment due to gravity load, and M_r is the moment resistance of the beam. All secondary beams placed in the E-W direction are designed to resist distributed load while the main beams are designed to carry the reaction of the secondary beams. These are also checked for deflection criterion, where the maximum allowable deflection is $l/360$ (l is the beam span). Only the service live loads are considered for the deflection verifications. All beams are made of W-shapes and are pinned at their ends.

For the gravity column design, the live load reduction factor was considered. For the cases where tributary area is greater than 20 m^2 and used for the purpose of office building when the live load is lesser than 4.8 kPa, the live load reduction factor is:

$$0.3 + \sqrt{9.8/B} \qquad\qquad (3\text{-}1)$$

where B is the tributary area.

According to CSA S16-2014, the slenderness of the columns under design is limited to 200 for compressive members. All gravity columns should be at least Class 3, be continuum over two floors, and be made of W-shapes.

Table 3.2: Assumed load patterns.

Load type	kPa
Dead load on roof	
Roofing	0.3
Insulation and vapor barrier	0.2
CANAM composite steel deck	1.89
Roof framing	0.41
Mechanical and ceiling	0.5
Total	3.3
Dead load on typical floor	
Partitions	1.0
Floor finishing	0.24
CANAM composite steel deck	1.86
Floor framing	0.4
Mechanical and ceiling	0.5
Total	4.0
Cladding	1.5
Live load on roof	1
Live load on typical floors	2.4
Snow on roof	2.48

3.2.2. Earthquake Design - General

The height of the 12-storey building is 43.6 m, hence less than 60 m and its location is in area where $I_E F_a S_a(0.2) = 0.595 > 0.35$, while for Site Class C, F_a is equal to $F(0.2) = 1.0$. Although the building height is lower than 60 m, its fundamental lateral period, T_a, maybe higher than 2.0 s (e.g. $2T_a = 0.05h_s = 2.18s$). In the case of $T_a > 2.0\ s$, the Dynamic Analysis Procedure is required. However, for a preliminary design, the Equivalent Static Force Procedure is applied.

All beam to column and brace to frame connections are pinned. Beams and columns are made of W-shapes steel with $F_u = 450\ MPa$ and $F_y = 350\ MPa$. Braces are made of HSS produced to ASTM A500 Grade C with $F_y = 345\ MPa$.

3.2.2.1. Preliminary Design by the Equivalent Static Force Procedure

The earthquake loads are resisted by 8 LD-CBFs distributed in each orthogonal direction. The ductility-related force modification factor and the overstrength-related force modification factor are $R_d = 2$ and $R_o = 1.3$, respectively. The earthquake loads determined by the Equivalent Static Force Procedure are computed with Equation (2-1). The importance factor, I_E, is 1.0 and the empirical fundamental period is:

$$T_a = 0.025 \times h_n = 0.025 \times 43.6 = 1.09 \ s$$

However, NBCC allows a higher value for the natural period of building with an upper limit of $2T_a = 2 \times 1.09 = 2.18 \ s$, which is used for the preliminary design. The higher mode factor, M_V, is equal to 1.0. The total dead load including 25% of snow load is $W = 266125 \ kN$. The base shear computed with Equation (2-1) is $V = 6630 \ kN$. This value is slightly smaller than the minimum base shear provided in Equation (2-2):

$$V = 6630 \ kN < V_{min} = 6960 \ kN$$

Therefore, in the first iteration, the base shear is determined as the minimum value: $V = 6690 \ kN$. The concentrated force applied at the roof level is $F_t = 0.07T_a V = 974 \ kN$.

Due to the building's symmetry, the base shear, V, is equally distributed among the 8 LD-CBFs. Then, the shear forces due to notional lateral loads, accidental torsion and P-Δ effects are added. The distribution of shear forces on the current building is given in **Table 3.3** and the distribution of shear forces on a braced frame in each orthogonal direction (e.g. LD-CBF 3-1 in N-S direction and on the LD-CBF E-1 in E-W direction) are given in **Table 3.4**. It is noted that the notional lateral load, N, at each level is equal to 0.5% of the total gravity load of that floor. To compute the notional lateral loads, the total gravity load

transferred to all column, C_{fx}, is determined for each level separately. Particularly, this value is equal to dead load, live load and snow load associated to the gravity components of earthquake load combination $1D + 0.5L + 0.25S$, where the live load reduction factor is used.

Table 3.3: Vertical distribution of earthquake loads along the 12-storey LD-CBF building with plan "A", Site Class C.

Story	h_x	W	F_x/V	F_x	V
	m	kN		kN	kN
12	43.6	23436	0.28	1936	1936
11	40	22052	0.12	830	2767
10	36.4	22052	0.11	756	3522
9	32.8	22052	0.1	681	4203
8	29.2	22052	0.09	606	4809
7	25.6	22052	0.08	531	5341
6	22	22052	0.07	457	5797
5	18.4	22052	0.05	382	6179
4	14.8	22052	0.04	307	6486
3	11.2	22052	0.03	232	6719
2	7.6	22052	0.02	158	6877
1	4	22165	0.01	83	6960
Total		**266125**	1	6960	

Table 3.4: Vertical distribution of earthquake shear including shears from notional lateral loads and accidental torsion on LD-CBF 3-1 (N-S direction) and LD-CBF E-1 (E-W direction) of the 12-st LD-CBF building with plan "A", Site Class C.

St.	V/ LD-CBF	N/ LD-CBF	(V+N)/ CBF	Shear from T/ LD-CBF (E-W)	Total shear/ LD-CBF (E-W)	Shear from T/ LD-CBF (N-S)	Total Shear/ LD-CBF (N-S)
12	**242**	14	256	5	261	107	363
11	**346**	31	377	7	384	153	530
10	**440**	48	488	9	497	195	683
9	**525**	65	590	11	601	233	823
8	**601**	82	683	13	696	266	949
7	**668**	99	767	14	780	296	1062
6	**725**	116	841	15	855	321	1161
5	**772**	132	904	16	921	342	1247
4	**811**	149	960	17	977	359	1319
3	**840**	166	1006	18	1024	372	1378
2	**860**	183	1043	18	1061	381	1423
1	**870**	200	1070	18	**1088**	385	**1455**

To consider the P-Δ effects in design, the stability coefficient, θ_x, at each level is calculated with Equation (2-8). If the stability coefficient, θ_x, is greater than 0.1, the P-Δ effects are taken into account by multiplying the earthquake shear of each floor level by the factor, U_2 (Equation (2-9)). If the stability coefficient, θ_x, is lesser than 0.1, the P-Δ effect is neglected. For the first design iteration, the interstorey drift values Δ_x are unknown and the P-Δ effect is not considered.

As specified in CSA S16-2014, CBF systems with different ductility levels are designed in accordance with capacity design principle. Thus, braces are considered to dissipate earthquake energy through their plastic behaviors. All other components are designed to withstand the effects resulted from this energy dissipation.

The HSS cross-sections are chosen for braces as recommended in CSA S16-2014. Firstly, braces are selected such that: $C_f < C_r$, and $T_f < T_r$ where C_f, T_f are the factored compressive and tensile forces, and C_r, T_r are the factored compressive and tensile resistance of braces. Secondly, the slenderness ratio, kL/r, and local buckling requirements, expressed as width-to-thickness ratio are verified. When the slenderness ratio is ≤ 200, the width-to-thickness ratio should be lower than or equal to $420/\sqrt{F_y}$, which is more severe than Class 1. When $KL/r \leq 100$, for HSS braces, the maximum width-to-thickness ratio is $330/\sqrt{F_y}$, which corresponds to Class 1. When $I_E F_a S_a(0.2) \geq 0.75$ or $I_E F_v S_a(1.0) \geq 0.3$, the slenderness of HSS braces shall not be less than 70 to avoid premature fracture under cyclic loading. The studied building is located in the earthquake area with $I_E F_a S_a(0.2) = 0.595 < 0.75$.

The factored compressive resistance, C_r, is computed by the following equation:

$$C_r = \emptyset A F_y (1 + \lambda^{2n})^{-1/n} \qquad (3\text{-}2)$$

where $\phi = 0.9$ for steel structure, which accounts for the variation expected in the properties of materials and section dimensions; $n = 1.34$; $\lambda = \sqrt{F_y/F_e}$; $F_e = \pi^2 E/(KL/r)^2$. The radius of gyration, r, is computed regarding the axis in which the brace bends about. The F_y is the specified minimum yield strength of the material, and F_e accounts for the possibility of torsional-flexural or torsional buckling of the cross-section of the brace and A is the area of the brace cross-section.

According to the same provisions, the factored tension resistance of a brace, is:

$$T_r = \emptyset A F_y \qquad (3\text{-}3)$$

All brace sections selected for the 12-storey LD-CBF located in E-W and N-S directions

are shown in **Table 3.5** and **Table 3.6**, respectively, where the probable capacity of the

braces computed with Equations (2-11), (2-12) and (2-13) are also summarized.

For sizing all CBF beam and column members, the brace capacity resistance is considered

in the following two loading scenarios:

- The compression acting braces attaining their probable compression resistance, C_u, in

  conjunction with the tension acting braces developing their probable tensile resistance,

  T_u,

- The compression acting braces attaining their probable post-buckling resistance, C'_u,

  in conjunction with the tension acting braces developing their probable tensile

  resistance, T_u.

Table 3.5: Brace sections, characteristics and probable resistances of the LD-CBF E-1 (E-W) of the 12-storey building with plan "A", Site Class C.

St.	Brace sections*	Ag	C_f/C_r	kL/r	T_u kN	C_u kN	C'_u kN
12	HSS114.3X114.3X6.4	2480	0.60	106.6	1112	523	222
11	HSS114.3X114.3X9.5	3540	0.76	110.3	1588	710	318
10	HSS114.3X114.3X9.5	3540	0.85	110.3	1588	710	318
9	HSS139.7X139.7X7.9	3770	0.78	87.3	1691	1034	338
8	HSS139.7X139.7X7.9	3770	0.81	87.3	1691	1034	338
7	HSS139.7X139.7X9.5	4440	0.85	88.6	1991	1196	398
6	HSS139.7X139.7X9.5	4440	0.87	88.6	1991	1196	398
5	HSS152.4X152.4X9.5	4890	0.81	80.8	2193	1464	439
4	HSS152.4X152.4X9.5	4890	0.81	80.8	2193	1464	439
3	HSS152.4X152.4X9.5	4890	0.9	80.8	2193	1464	439
2	HSS152.4X152.4X9.5	4890	0.88	80.8	2193	1464	439
1	HSS177.8X177.8X9.5	5790	0.76	72.2	2597	1942	519

*All sections are Class 1 and made of steel material ASTM A500 grade C ($F_y = 345 MPa$)

Table 3.6: Brace sections, characteristics and probable resistances of the LD-CBF 3-1 (N-S) of the 12-storey building with plan "A", Site Class C.

St.	Brace sections[*]	Ag	C_f/C_r	kL/r	T_u kN	C_u kN	C'_u kN
12	HSS114.3X114.3X7.9	3020	0.7	108.3	1354	623	271
11	HSS139.7X139.7X7.9	3770	0.82	87.3	1691	1034	338
10	HSS139.7X139.7X7.9	3770	0.8	87.3	1691	1034	338
9	HSS152.4X152.4X9.5	4890	0.82	80.8	2193	1464	439
8	HSS152.4X152.4X9.5	4890	0.78	80.8	2193	1464	439
7	HSS177.8X177.8X9.5	5790	0.73	68.5	2597	2038	519
6	HSS177.8X177.8X9.5	5790	0.69	68.5	2597	2038	519
5	HSS177.8X177.8X9.5	5790	0.84	68.5	2597	2038	519
4	HSS177.8X177.8X9.5	5790	0.78	68.5	2597	2038	519
3	HSS177.8X177.8X9.5	5790	0.92	68.5	2597	2038	519
2	HSS177.8X177.8X12.7	7480	0.67	70	3355	2582	671
1	HSS177.8X177.8X12.7	7480	0.84	73.9	3355	2456	671

*All sections are Class 1 and made of steel material ASTM A500 grade C ($F_y = 345MPa$)

Steel W-section is selected for all beams and columns. They are designed to resist the effects from both gravity and lateral forces due to the probable forces from the braces. These effects result in flexural and axial loads.

Frame members of Class 1 and Class 2 resisting both axial compressive force and bending moment applied in one direction (e.g. x direction) need to satisfy the following equation:

$$\frac{C_f}{C_r} + \frac{0.85U_{1x}M_{fx}}{M_{rx}} \leq 1 \tag{3-4}$$

The capacity of frame members subjected to axial compression and bending is examined for: a) cross-sectional strength (CSS), which applies for members in braced frames only, b) overall member strength (OMS), and c) lateral torsional buckling strength (LTBS). In the case of CSS verification, the compressive strength, C_r, is computed as prescribed in Equation (3-2) with $\lambda = 0$ and U_{1x} as shown below but not less than 1.0. In the case of

OMS verification, C_r is computed with Equation (3-2) and the calculation is based on the axis of bending, while the computation for U_{1x} is shown below. In the case of LTBS verification, C_r is computed based on the weak-axis of bending, while U_{1x} should not be lesser than 1.0. The moment resistance, M_r, for laterally supported Class 1 and Class 2 members is:

$$M_r = \emptyset Z F_y \tag{3-5}$$

where $\emptyset = 0.9$ and Z is the plastic section modulus.

The values of U_{1x} is determined as following:

$$U_1 = \left[\frac{\omega_1}{1 - \frac{C_f}{C_e}} \right] \tag{3-6}$$

where $C_e = \pi^2 EI / L^2$ and ω_1 is computed as:

- For members not subjected to transverse loads between support: $\omega_1 = 0.6 - 0.4k > 0.4$, where k is the ratio of the smaller to the larger factored moment at opposite ends of the member length.

- For members subjected to distributed loads or a series of point loads between supports: $\omega_1 = 1$.

- For members subjected to a concentrated load or moment between supports: $\omega_1 = 0.85$.

Members that withstand both axial tension and flexural loads need to satisfy the following equation:

$$\frac{T_f}{T_r} + \frac{M_f}{M_r} \leq 1 \tag{3-7}$$

where the factored tension resistance, T_r, of the member is computed with Equation (3-3). The axial forces in a CBF beam result from two scenarios: 1) T_u & C_u and 2) T_u & C'_u, when the probable tensile and compressive strength of braces or the probable tensile and post-buckling strength are projected on the beam axis. The class section of the CBF beams can be either Class 1 or Class 2. The sizes of the CBF beams are given in **Table 3.7**.

Similar to the design of CBF beams, the CBF columns are designed to carry the gravity loads together with the effects from brace forces associated with the aforementioned two scenarios. In any case, the brace forces need not exceed those associated with a storey shear corresponding to $R_d R_o = 1.3$. Columns are continuous over two storeys and have a constant cross-section. In terms of gravity effects, live load reduction factors are used and computed as shown in Equation (3-1). Here, the CBF column members are designed to carry a bending moment of minimum $0.2M_p$ and the corresponding axial compressive forces. All columns are selected to be minimum Class 2. Column sections are provided in **Table 3.8**.

Table 3.7: Beam sections of LD-CBF E-1 (E-W) and LD-CBF 3-1 (N-S) of the 12-storey building with plan "A", Site Class C.

St.	E-W direction				N-S direction			
	Beam sections*	A_g	T_u & C'_u		Beam sections*	A_g	T_u & C'_u	
			OMS Eq(3-4)	LTBS Eq(3-4)			OMS Eq(3-4)	LTBS Eq(3-4)
12	W460X74	9480	0.25	0.89	W460X106	13500	0.35	0.92
11	W460X128	16300	0.58	0.68	W460X128	16300	0.57	0.64
10	W460X128	16300	0.29	0.6	W460X144	18400	0.39	0.73
9	W460X106	13500	0.24	0.3	W460X128	16300	0.74	0.86
8	W460X128	16300	0.3	0.63	W530X150	19200	0.39	0.73
7	W460X74	9480	0.48	0.79	W460X106	13500	0.59	0.89
6	W460X128	16300	0.34	0.73	W460X158	20100	0.45	0.93
5	W460X74	9480	0.37	0.56	W460X89	11400	0.33	0.33
4	W460X128	16300	0.36	0.8	W530X165	21000	0.4	0.74
3	W460X106	13500	0.25	0.3	W460X89	11400	0.33	0.33
2	W460X144	18400	0.32	0.68	W530X165	21000	0.43	0.83
1	W460X82	10500	0.94	1.0	W460X89	11400	0.44	0.35

*All beam sections are Class 1

Table 3.8: Column sections of LD-CBF E-1 (E-W) and LD-CBF 3-1(N-S) of the 12-st building with plan "A", Site Class C.

Storey	E-W direction						N-S direction				
	Column sections*	A_g	T_u & C_u			Column sections*	A_g	T_u & C_u		
			CMS Eq(3-4)	OMS Eq(3-4)	LTBS Eq(3-4)			CMS Eq(3-4)	OMS Eq(3-4)	LTBS Eq(3-4)
12	W310X60	7550	0.37	0.32	0.50	W310X60	7550	0.41	0.36	0.56
11	W310X60	7550	0.49	0.44	0.69	W310X60	7550	0.53	0.48	0.75
10	W310X107	13600	0.62	0.57	0.70	W310X117	15000	0.68	0.64	0.77
9	W310X107	13600	0.68	0.64	0.78	W310X117	15000	0.73	0.69	0.84
8	W310X179	22700	0.69	0.65	0.79	W310X226	28800	0.69	0.65	0.78
7	W310X179	22700	0.73	0.69	0.83	W310X226	28800	0.72	0.68	0.81
6	W310X283	36100	0.69	0.64	0.77	W360X347	44200	0.71	0.66	0.76
5	W310X283	36100	0.71	0.67	0.80	W360X347	44200	0.73	0.68	0.78
4	W360X347	44200	0.76	0.72	0.82	W360X509	65200	0.69	0.63	0.73
3	W360X347	44200	0.78	0.73	0.84	W360X509	65200	0.7	0.65	0.74
2	W360X463	59000	0.75	0.70	0.80	W360X592	75500	0.76	0.7	0.8
1	W360X463	59000	0.77	0.72	0.83	W360X592	75500	0.77	0.72	0.83

*All column sections are Class 1

3.2.2.2. Linear Elastic Analysis by the Modal Response Spectrum Method

The numerical model for the 12-storey LD-CBF building located on Site Class C in Montreal is simulated in ETABS software to obtain the lateral deformations (interstorey drift) of the building and to check if P-Δ effect is required. The spectrum used in the analysis for Site Class C and Site Class B, as well as the peak ground acceleration, PGA and peak ground velocity, PGV is given in **Table 3.9**.

Table 3.9: Design spectral acceleration values, $S(T)$, for Site Class C and Site Class B in Montreal.

Montreal (City Hall)	Earthquake Data						
	$S(0.2)$	$S(0.5)$	$S(1.0)$	$S(2.0)$	$S(5.0)$	PGA	PGV
Site Class C	0.595	0.311	0.148	0.068	0.018	0.379	0.255
Site Class B	0.458	0.202	0.093	0.043	0.0115		

The dynamic base shear is computed separately for each orthogonal direction (e.g. N-S and E-W) and the torsional effects due to accidental eccentricity of $\pm 0.1 D_{nx}$ is added. After all braced frame members were sized according to the Equivalent Static Force Procedure and the size of gravity columns and beams were determined, the building was modelled in ETABS software as a 3-D model. The natural periods found in two major directions are: $T_{a,W-E} = 3.0 \ s$ and $T_{a,N-S} = 2.87 \ s$. These values are higher than the upper limit given by NBCC 2015 ($2T_a = 2.18 \ s$), which was initially used for the earthquake design of this building. From this analysis, the base shear is lower than V_{min}. However, another verification will be provided after the P-Δ effect is considered.

The interstorey drift computed from the 3-D model at any floor level under earthquake loading is multiplied by $R_d R_0 / I_E$. The interstorey drifts in both directions are provided in

Table **3.10**. In addition, in the same table the U_2 factor is given. As resulted, U_2 is greater than 1.1, therefore the P-Δ effect should be considered in design. Meanwhile, U_2 is lower than 1.4 which means the structure is stable.

Table 3.10: Interstorey drift and U_2 factor for the 12-storey LD-CBF building with plan "A", Site Class C.

	N-S direction			E-W direction		
Storey	Interstorey drift	Interstorey drift	U_2	Interstorey drift	Interstorey drift	U_2
	$\%h_s$	mm		$\%h_s$	mm	
12	1.06	38	1.116	0.69	25	1.076
11	0.97	35	1.160	0.69	25	1.114
10	1.03	37	1.202	0.69	25	1.136
9	1.00	36	1.220	0.67	24	1.147
8	1.03	37	1.246	0.67	24	1.160
7	0.86	31	1.222	0.64	23	1.165
6	0.89	32	1.245	0.67	24	1.183
5	0.78	28	1.228	0.53	19	1.155
4	0.81	29	1.251	0.56	20	1.173
3	0.67	24	1.220	0.42	15	1.138
2	0.69	25	1.244	0.44	16	1.156
1	0.45	18	1.168	0.39	14	1.131

After the P-Δ effect was added in the preliminary design by means of the Equivalent Static Force Procedure, a few brace members required slightly larger cross-sections which are provided in **Table 3.11** and **Table 3.12**. The same cross-sections provided in **Table 3.7** for CBF beams and in **Table 3.8** for CBF columns were used because they satisfied the strength demand.

Table 3.11: Increased brace sizes of LD-CBF E-1 (E-W) of the 12-st building with plan "A", Site Class C and their characteristics.

St.	Brace sections[*]	A_g	C_f/C_r	kL/r	T_u kN	C_u kN	C'_u kN
12	HSS114.3X114.3X6.4	2480	0.64	106.6	1112	523	222
11	HSS114.3X114.3X9.5	3540	0.83	110.3	1588	710	318
10	HSS114.3X114.3X9.5	3540	0.96	110.3	1588	710	318
9	HSS139.7X139.7X9.5	4440	0.76	88.6	1991	1196	398
8	HSS139.7X139.7X9.5	4440	0.81	88.6	1991	1196	398
7	HSS152.4X152.4X9.5	4890	0.8	80.8	2193	1464	439
6	HSS152.4X152.4X9.5	4890	0.83	80.8	2193	1464	439
5	HSS152.4X152.4X9.5	4890	0.92	80.8	2193	1464	439
4	HSS152.4X152.4X9.5	4890	0.94	80.8	2193	1464	439
3	HSS177.8X177.8X9.5	5790	0.72	68.5	2597	2038	519
2	HSS177.8X177.8X9.5	5790	0.72	68.5	2597	2038	519
1	HSS177.8X177.8X9.5	5790	0.84	72.2	2597	1942	519

Table 3.12: Increased brace sizes of LD-CBF E-1 (N-S) of the 12-st building with plan "A", Site Class C and their characteristics.

St.	Brace sections*	A_g	C_f/C_r	kL/r	T_u kN	C_u kN	C'_u kN
12	HSS114.3X114.3X7.9	3020	0.78	108.3	1354	623	271
11	HSS139.7X139.7X9.5	4440	0.79	88.6	1991	1196	398
10	HSS139.7X139.7X9.5	4440	0.82	88.6	1991	1196	398
9	HSS152.4X152.4X9.5	4890	0.97	80.8	2193	1464	439
8	HSS152.4X152.4X9.5	4890	0.97	80.8	2193	1464	439
7	HSS177.8X177.8X9.5	5790	0.87	68.5	2597	2038	519
6	HSS177.8X177.8X9.5	5790	0.85	68.5	2597	2038	519
5	HSS177.8X177.8X12.7	7480	0.79	70	3355	2582	671
4	HSS177.8X177.8X12.7	7480	0.77	70	3355	2582	671
3	HSS177.8X177.8X12.7	7480	0.86	70	3355	2582	671
2	HSS177.8X177.8X12.7	7480	0.82	70	3355	2582	671
1	HSS203.2X203.2X12.7	8710	0.72	63.9	3906	3245	781

When the increased brace sections were used in the ETABS model, the periods of the building in two orthogonal directions decrease to: $T_{1,N-S} = 2.38\ s$ and $T_{1,E-W} = 2.66\ s$. However, these values of the first-mode period are larger than 2.0 s, while the associated base shear is lower than V_{min} computed for $S(2.0)$. Therefore, according to Clause 4.1.8.12(8) of NBCC 2015, for a regular building, it is accepted that $V_{dyn} \geq 0.8V$. In the case that V_{dyn} is less than 80% of the lateral earthquake force V (e.g. in this case study, $V = V_{min}$), then V_{dyn} shall be scaled up to $0.8V$. In the case that the building is irregular, V_{dyn} shall be equal to V. Therefore, the next step is to verify if the building structure is regular or irregular.

According to NBCC 2015, there are 9 types of structure irregularities. By visual inspection, structure irregularity Types 3, 4, 5 and 8 can be verified. From building's geometry, the horizontal dimension of each CBF is constant over the building height. Therefore, structure irregularity Type 3 (vertical geometric irregularity), Type 4 (In-plane discontinuity in vertical lateral-force-resisting element irregularity) and Type 5 (Out-of-plane offsets) do not occur. All CBFs are placed perpendicular to each other in both orthogonal directions, which eliminates the Type 8 irregularity (Non-orthogonal systems). The other types of structure irregularities 1, 2, 6, 7 and 9 need to be verified.

Type 1 or the vertical stiffness irregularity occurs when the lateral stiffness of LFRS at a storey is less then 70% of the stiffness of any adjacent storey or less than 80% of the average stiffness of three storeys above or below. The normalized storey stiffness to the maximum storey stiffness is shown in **Figure 3.2**, which indicates that there is no Type 1 irregularity.
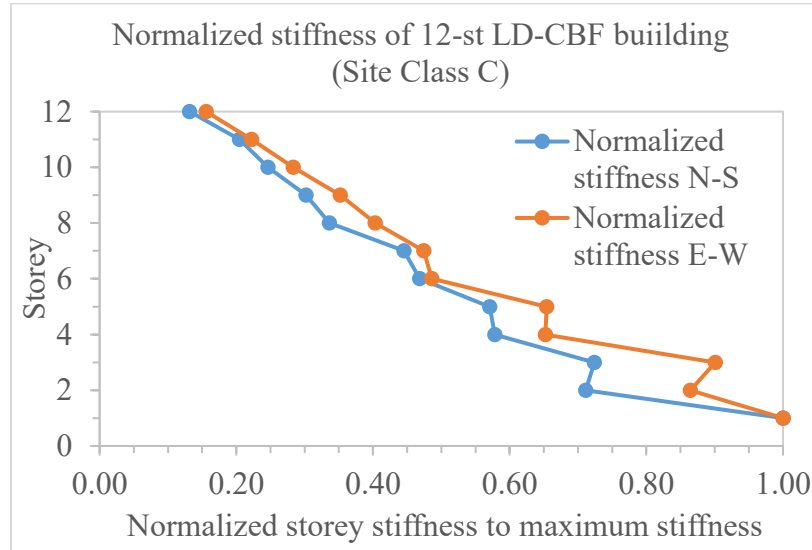
Figure 3.2: Normalized storey stiffness to max. storey stiffness in N-S and E-W directions

There is no Type 2 or mass irregularity because the mass of each floor is the same with the exception of top floor. Regarding type 6 irregularity or "weak storey", there is not a floor where the shear strength of the floor above is larger than that of the floor below as illustrated in **Table 3.11** and **Table 3.12**. In addition, there is no gravity-induced irregularity (Type 9) in the studied building.

To check irregularity Type 7 (Torsional sensitivity), the B_x value is computed with Equation (2-6). When B_x is less than 1.7 at all floors and in both directions, there is no irregularity Type 7.

The building is regular and the storey shear forces resulted from the ETABS output should be scaled up to $0.8V$ which is $0.8 \times 6960 = 5568 \, kN$. The distribution of storey shear forces associated to base shear V and $0.8V$ resulted from the Equivalent Static Force Procedure as well as the shear forces resulted from the ETABS model in both directions are provided in **Figure 3.3**. These shear forces do not include notional lateral loads, shear

caused by torsion and shear due to P-Δ effect. In the N-S direction the resulted base shear from ETABS is $6630\ kN$ and in E-W direction is $5694\ kN$. Therefore, both values of base shear resulted from ETABS are greater than $0.8V$ and lower than V. The main period from ETABS is $T_{E-W} = 2.66\ s$ and $T_{N-S} = 2.38\ s$. As resulted from **Figure 3.3,** the dynamic distribution of shear force along the building height is different than that from the equivalent static force procedure. It is shown that the dynamic demand is lower in middle floors than that resulted from the inverted-triangular distribution used with the Equivalent Static Force Procedure.
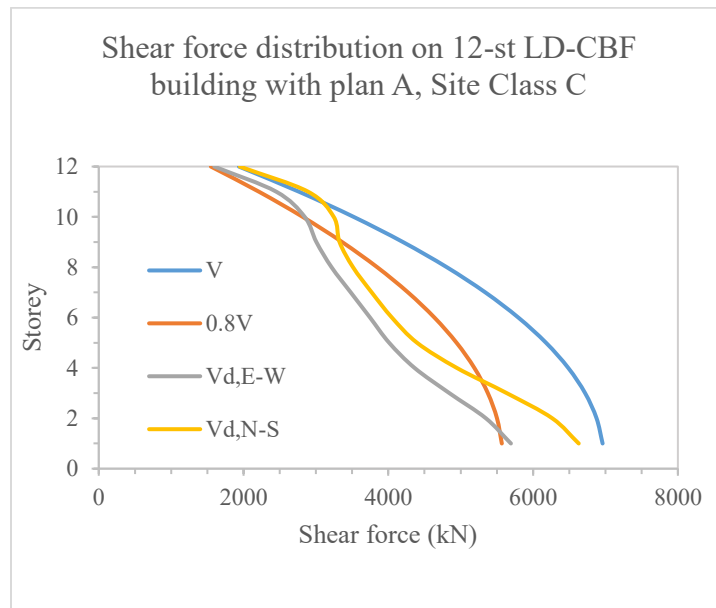
Figure 3.3: Storey shear distribution over the building height resulted for the 12-st LD-CBF with plan "A", Site Class C.

3.3. DESIGN OF THE OTHER BUILDINGS

The same gravity and earthquake design steps used in Section 3.2. are applied to design all the other buildings listed in **Table 3.1**.

In terms of gravity design, the gravity load for all buildings as shown in **Table 3.2**.

The structure irregularities are checked and all buildings are regular. In each main loading direction, the CBF are designed for the maximum earthquake forces considering those resulted from notional loads, torsional and P-Δ effects.

The sections of braced frame members are provided for all studied buildings given in **Table 3.1** and their shears distributed along building height resulted from both Equivalent Static Force Procedure and Dynamic Analysis Procedure as well as the corresponding fundamental periods in both orthogonal directions are also provided in Appendix A.

Chapter 4

WIND LOADING ISSUES

After all buildings have been designed and earthquake loads have been determined, wind loads are computed. However, it is noted in Chapter 2 that the provisions given by NBCC 2015 are not clear enough to determine the wind loads in these buildings. Therefore, several recommendations are provided in the current thesis to resolve these issues. The adequacy of these methods is verified by comparisons with the ASCE/SEI 7-10 provisions and previous wind tunnel test results.

The verification is carried out on buildings given in four past studies and five buildings considered in the current thesis. To compute wind loads, building natural frequency needs to be predetermined. Therefore, these buildings are designed (for gravity and earthquake loads) before being analyzed to obtain their natural frequencies.

After having clarified the methodology given in NBCC 2015, final recommendations are provided and will be used in Chapter 5 to compute wind loads on the buildings listed in **Table 3.1**.

4.1. WIND LOADING ISSUES AND POTENTIAL RECOMMENDATIONS – NBCC 2015

This section attempts to address and give a solution for the ambiguities addressed in Chapter 2 in determining wind-induced torsions for medium-rise buildings and the probable underestimation for low-rise buildings.

4.1.1. Medium-Rise Buildings

For medium-rise buildings, torsional effects are computed by considering Case B and Case D. The tributary areas that could produce the maximum torsions are recommended by using a mathematical method. The detailed illustration for Case D is shown in **Figure 4.1** (Nguyen et al., 2017). The same approach can be adopted for Case B.
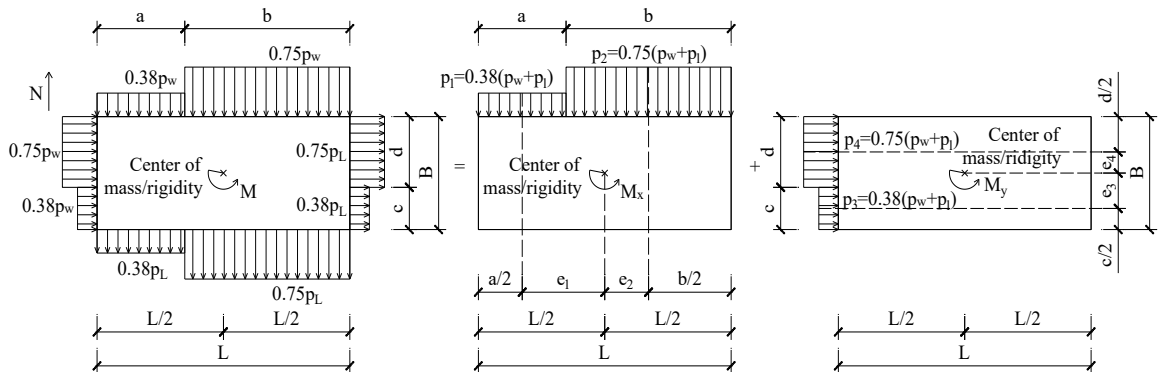
Figure 4.1: Load Case D for medium-rise buildings analyzed in E-W and N-S directions.

As mentioned in Chapter 2, the tributary area of the uniformly distributed wind force acting on a particular storey is given as: $A = l \times h$, where h is the height of the story under consideration, and l is the horizontal distribution length of the wind load. However, according to NBCC 2015, the horizontal distribution lengths (mentioned as *a, b, c* and *d* in **Figure 4.1**) are unknown. These values need to be determined such that the corresponding

wind forces create a maximum moment, M, which is the summation of the moments formed

in both orthogonal directions:

$$M = M_x + M_y \tag{4-1}$$

Herein, M is maximum when M_x and M_y reach their highest values. The moment due to

wind load along N-S direction is given by:

$$M_x = p_2 b h e_2 - p_1 a h e_1 \tag{4-2}$$

where p_1 and p_2 are uniform wind forces acting on the wall faces in N-S direction; e_1 and

e_2 are the eccentricities corresponding to p_1 and p_2, respectively; and a and b are the

horizontal distribution lengths of p_1 and p_2, respectively. The eccentricities, e_1 and e_2, are:

$e_1 = L/2 - a/2$, $e_2 = L/2 - b/2$, where $a = L - b$. By substituting these parameters in

Equation (4-2), one gets:

$$
\begin{aligned}
M_x &= p_2 bh \left(\frac{L}{2} - \frac{b}{2} \right) - p_1 ah \left(\frac{L}{2} - \frac{a}{2} \right) \\[2mm]
&= p_2 bh \frac{L}{2} - p_2 h \frac{b^2}{2} - p_1 ah \frac{L}{2} + p_1 h \frac{a^2}{2} \\[2mm]
&= p_2 bh \frac{L}{2} - p_2 h \frac{b^2}{2} - p_1 (L-b) h \frac{L}{2} + p_1 h \frac{(L-b)^2}{2} \\[2mm]
&= p_2 bh \frac{L}{2} - p_2 h \frac{b^2}{2} - p_1 h \frac{L^2}{2} + p_1 bh \frac{L}{2} \\[2mm]
&\quad + p_1 h \frac{b^2 + L^2 - 2Lb}{2} \\[2mm]
&= p_1 h \frac{b^2}{2} - p_2 h \frac{b^2}{2} + p_2 bh \frac{L}{2} - p_1 bh \frac{L}{2} \\[2mm]
&= \left(\frac{p_1}{2} - \frac{p_2}{2} \right) b^2 h + \left(\frac{p_2 L}{2} - \frac{p_1 L}{2} \right) bh
\end{aligned}
\tag{4-3}
$$

M_x is a quadratic function of variable b. This function reaches its maximum value when its differentiation with respect to b is equal to 0, i.e.:

$$M'_x = (p_1 - p_2)bh + 0.5(p_2 - p_1)Lh = 0 \tag{4-4}$$

$$\Leftrightarrow b = \frac{L}{2}$$

Therefore, the maximum wind-induced torsion along N-S direction occurs when $b = a = L/2$. Similarly, M_y is maximum when $c = d = B/2$.

Applying the same procedure, torsion in Case B is maximum when pressures are applied on half of the wall faces. In conclusion, it was found that by deducting wind load on half of the wall face, one gets maximum torsions in Case B and Case D. This recommendation will be verified in this chapter.

4.1.2. Low-Rise Buildings

In terms of low-rise buildings, only two cases, namely A and B, are present in NBCC, when torsion is caused by a higher concentration of wind loads in each wall corner. As opposed to partial loading cases for medium-rise buildings, the tributary areas of wind forces are defined explicitly in the case of low-rise buildings (as exhibited in **Figure 4.2**). Torsion in this case is computed by the following equation:

$$M = (p_1 + p_4)e_1(L - y)h - (p_{1E} + p_{4E})e_{1E}yh \tag{4-5}$$

where y is the width of the end zone computed as the greater of 6 m and $2z$; z is the lesser of 10% of the least horizontal dimension or 40% of height, H, but not less than 4% of the least horizontal dimension or 1 m.

According to a study of Stathopoulos et al. (2013), the wind-induced torsions resulted by following this procedure may not be appropriate. Therefore, the adequacy of the current procedure is to be verified in the following sections.
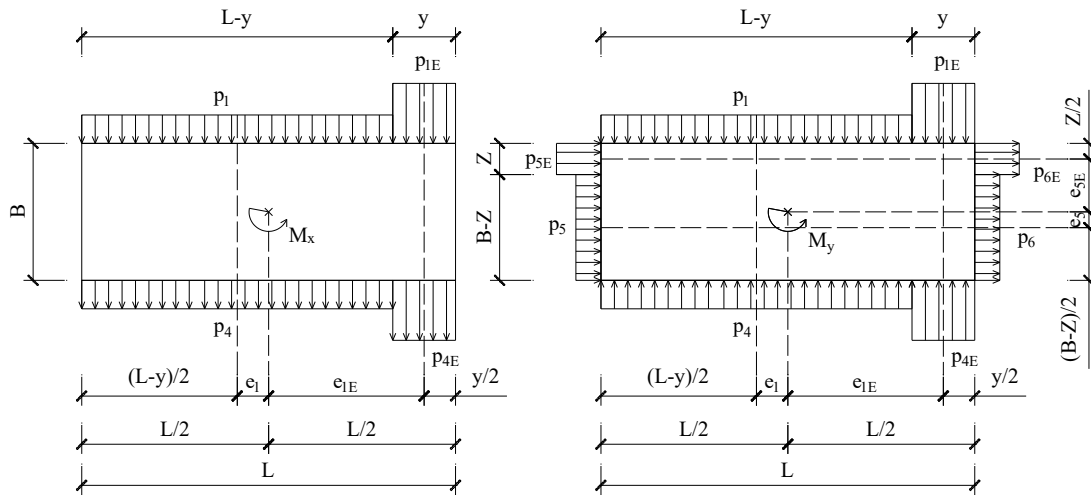
Load case A: winds generally perpendicular to ridge   Load case B: winds generally parallel to ridge

End-zone width y should be the greater of 6m or 2z, where z is the gable wall end zone defined for Load Case B below. Alternatively, for buildings with frames; the end zone y may be the distance between the end and the first interior frame

End-zone width z is the lesser of 10% of the least horizontal dimension or 40% of height, H, but not less than 4% of the least horizontal dimension or 1m

Figure 4.2: Load cases for low-rise flat roof buildings - NBCC 2015.

4.2. RECOMMENDATION VERIFICATIONS

4.2.1. Shear and Torsional Coefficients

The adequacy of the procedures provided in Sections 4.1.1. and 4.1.2. are to be verified by comparisons with the results from ASCE/SEI 7-10 standard and with wind tunnel test results. Generally, four past studies for a variety of building configurations have been chosen in the current thesis. The NBCC 2015 and ASCE/SEI 7-10 provisions are used to compute two maximum wind-induced base shears in two orthogonal directions and the greatest torsional moment in each building. These results are normalized in non-

dimensional forms called: shear and torsional coefficients for comparing purpose with the wind tunnel tests.

However, the definitions of the coefficients provided by four studies vary. For that reason, shear and torsional coefficients are defined in the current thesis (Equations (4-6) and (4-7)) and the results from all other studies are transformed to the corresponding definitions so that comparisons can be carried out.

$$C_V = \frac{V}{q_H B L} \tag{4-6}$$

$$C_T = \frac{T}{q_H B^2 L} \tag{4-7}$$

$$q_H = q C_e \tag{4-8}$$

where C_V and C_T are shear and torsional coefficients; V and T are the base shear and torsion; B and L are the shorter and longer horizontal dimensions of the building; q_H is the mean dynamic wind pressure at roof height H; q is the reference velocity pressure based on the mean hourly wind speed; and C_e is the exposure factor.

4.2.2. Building Design and Wind Load Computations

All buildings are designed under gravity and earthquake loads as shown in Chapter 3. Due to the lack of information in the chosen studies, some assumptions have been made in this thesis. All buildings are assumed to be steel and enclosed structures using LD-CBF as LFRS. According to NBCC 2015, the height limit for a building with the LD-CBF under an earthquake region that has $0.35 \leq I_E F_a S_a(0.2) \leq 0.75$, is 60 m. Location of the buildings is Montreal and they are on ground categorized as Site class C (firm soil), the value $I_E F_a S_a(0.2)$ is equal to 0.55. At the same time, the tallest building among all studies

is 60 m high, which satisfies this limit. This Chapter only shows and discusses the resulted shear and torsional coefficients. The detailed wind design of these buildings is demonstrated in Appendix B.

4.2.3. Comparisons Conducted

4.2.3.1. Comparisons of NBCC 2015 Provisions and Wind Tunnel Tests

In this section, the comparisons between the shear and torsional coefficients resulted from wind tunnel tests and the corresponding code results are depicted in graphs where the vertical axis shows shear or torsional coefficients from wind tunnel tests, while those from NBCC 2015 are placed on the horizontal axis. Each pair of results (experimental and code-based) is represented by a point. The closer the point is to the balance line (forming an angle of 45^0 with the axes), the better the agreement between code provisions and experimental results is.

Due to the diversity of coefficient definitions among the past studies, all coefficients given have all been transformed to be consistent with those of the current study. The transformation Equations used for each study are provided in **Table 4.1**.

.

Table 4.1: Original and transformed definition of shear and torsional coefficients in previous studies.

Study (Experimental)	Shear coefficient		Torsion coefficient	
	Original definition	Transformed definition	Original definition	Transformed definition
Isyumov and Case (2000)			$C_T = \dfrac{T}{q_H BLH}$	$C_T = \dfrac{T}{q_H BLH} \times \dfrac{H}{B} = \dfrac{T}{q_H B^2 L}$
Tamura et al. (2003)	$C_V = \dfrac{V}{q_H LH}$	$C_V = \dfrac{V}{q_H LH} \times \dfrac{H}{B} = \dfrac{V}{q_H BL}$	$C_T = \dfrac{T}{q_H LHR}$	$C_T = \dfrac{T}{q_H LHR} \times \dfrac{HR}{B^2} = \dfrac{T}{q_H B^2 L}$ $R = (B^2 + L^2)^{0.5}/2$
Keast et al. (2012)	$C_V = \dfrac{V}{q_H LH}$	$C_V = \dfrac{V}{q_H LH} \times \dfrac{H}{B} = \dfrac{V}{q_H BL}$	$C_T = \dfrac{T}{q_H L^2 H}$	$C_T = \dfrac{T}{q_H H^2 L} \times \dfrac{H^2}{B^2} = \dfrac{T}{q_H B^2 L}$
Stathopoulos (2013)	$C_V = \dfrac{V}{q_H B^2}$	$C_V = \dfrac{V}{q_H B^2} \times \dfrac{B}{L} = \dfrac{V}{q_H BL}$	$C_T = \dfrac{T}{q_H B^2 L}$	$C_T = \dfrac{T}{q_H B^2 L}$

Figure 4.3 compares the torsional coefficients in two separate categories, namely low-rise and medium-rise buildings. Clearly, NBCC 2015 greatly underestimates torsional effects on low-rise buildings in all cases. Thus, all points shown in the graph for low-rise buildings are at noticeable distances from the balance line (experimental results are 6 to 10 times higher than those from NBCC 2015). The largest disagreement is found in the study of Tamura et al. (2003).

Moreover, the underestimation in torsional effects of NBCC 2015 for low-rise buildings can be witnessed through the case of the two buildings of Stathopoulos et al. (2013). These two buildings are 20.0 m high (low-rise building) and 30.0 m high (medium-rise building) and have the same horizontal dimensions and exposure conditions. According to the Canadian code computations, the torsional coefficient increases tenfold from 0.024 (20.0 m – low-rise building) to 0.26 (30.0 m - medium-rise building). The values from the wind tunnel tests are 0.15 and 0.27, correspondingly, making a smaller jump of about just 1.8 times.

For medium-rise buildings, all studies give similar results with the computations from NBCC 2015, except for the case of the building of Tamura et al. (2003) in urban-terrain area.

In conclusion, torsional effects on low-rise buildings are not assessed properly by NBCC 2015. In contrast, good assessments have been shown in medium-rise buildings with the application of partial loading. Therefore, it was decided to test the effectiveness of the medium-rise building methodology for low-rise buildings although, according to NBCC 2015, partial loading cases are not required for them. Particularly, the wind pressure acting on all low-rise buildings is computed as similar to that of the medium-rise buildings. After

that, the partial loading cases are carried out. Here, only the torsional cases are considered. Cases B and D are applied to all the low-rise buildings of the previous studies to obtain the maximum torsions. The tributary area width of wind pressure in these cases is taken as half of the wall face. The torsional coefficients resulted from this process are exhibited in **Figure 4.4**. The abbreviation "PL" in the figure implies the results from the partial loading Cases B and D. As can be seen, if partial loading cases are applied as for the case of medium-rise buildings, the torsional effects on low-rise buildings can be evaluated more appropriately, although somewhat underestimated.
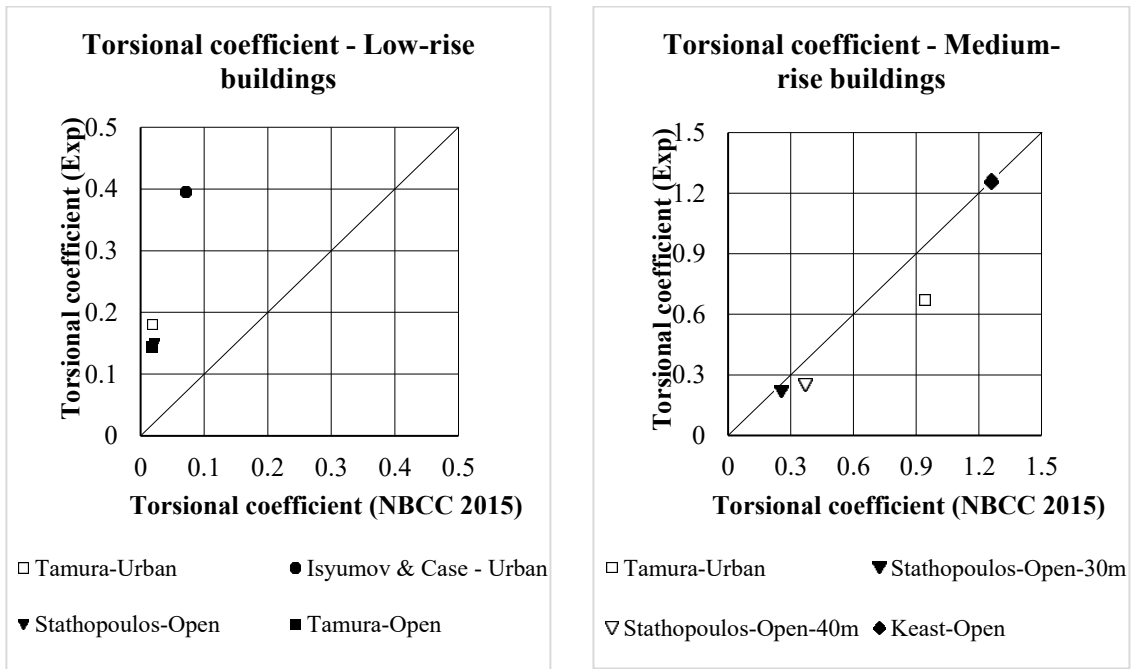
Figure 4.3: Comparison of torsional coefficients for low-rise and medium-rise buildings in NBCC 2015 with experimental results from previous studies.
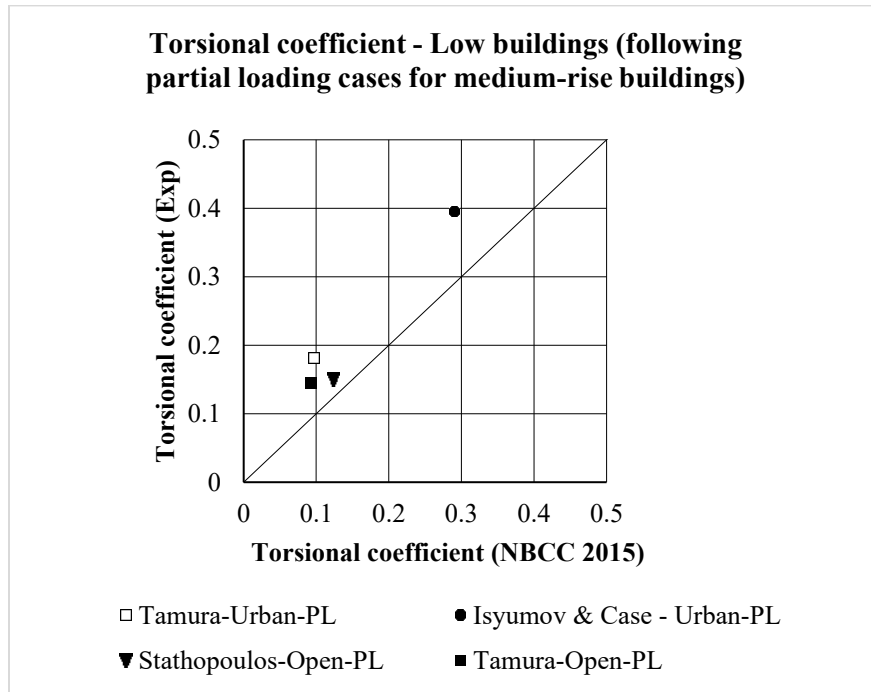
Figure 4.4: Comparison of torsional coefficients for low-rise buildings in NBCC 2015 (following partial loading cases, PL) with experimental results from previous studies.

Figure 4.5 presents the comparisons between shear coefficients obtained from NBCC 2015 and wind tunnel tests. The shear coefficients are computed in two principal wind directions: North-South (N-S) and East-West (E-W). In general, good similarities between the code computations and the test results are present. For low-rise buildings, four out of six shear coefficients computed from NBCC 2015 are nearly equal to the experimental coefficients. However, an underestimating trend is demonstrated. Additionally, the shear coefficient adequacy decreases in N-S direction (the longer wall face). For medium-rise buildings, there is an excellent agreement in seven out of eight cases. The best agreement is found with the results of Stathopoulos et al. (2013) for both terrains (only roughly 1% difference). The largest difference found was approximately 16%, in the case of the 60.0 m high

building in the study of Keast et al. (2012), which is also the highest building among all studies.

In brief, apart from the underestimated torsional effects for low-rise buildings, NBCC 2015 seems to evaluate adequately the impact of wind loads on low-rise (shear effects) and medium-rise buildings. Potential remedies can be taken in the case of torsional effects on low-rise buildings by applying the partial loading cases, similar to the case of medium-rise buildings.
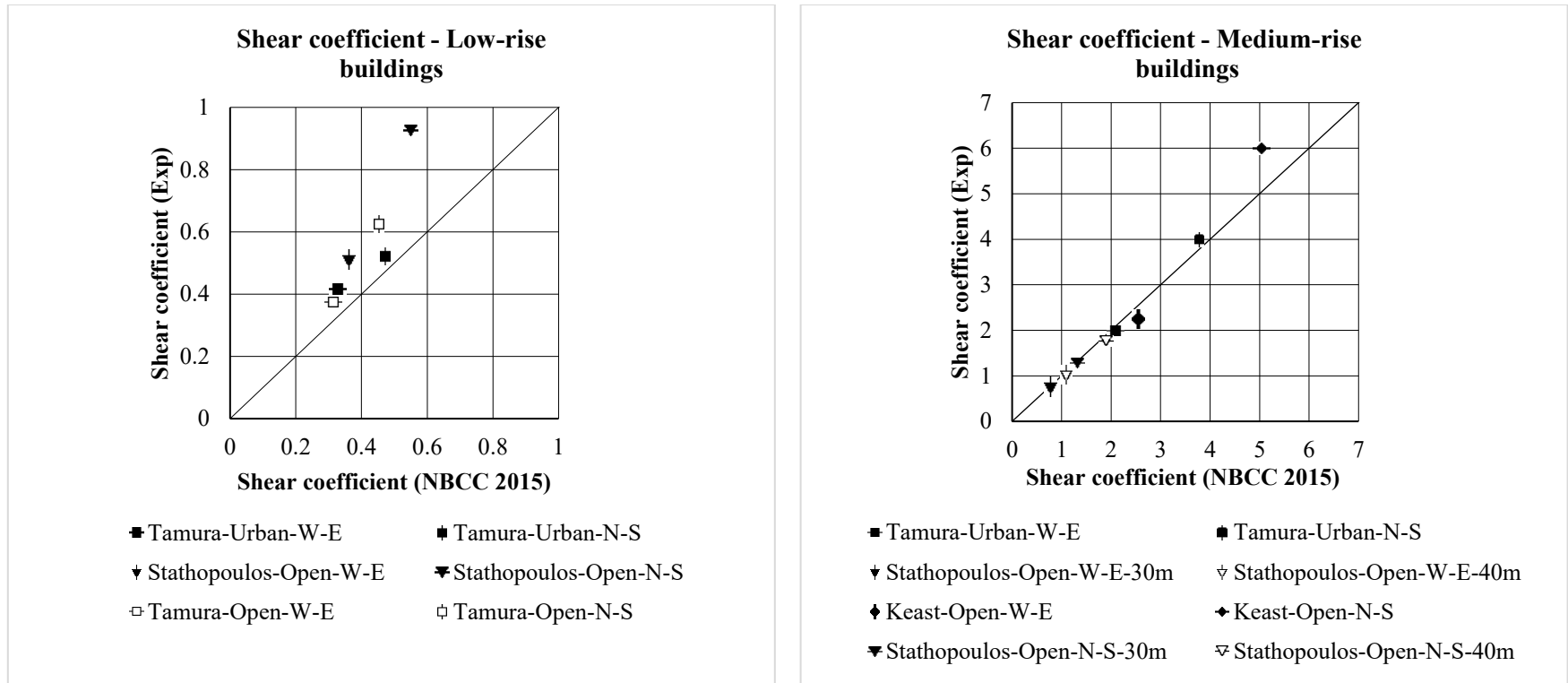
Figure 4.5: Comparison of shear coefficients for low-rise and medium-rise buildings in NBCC 2015 with experimental results from previous studies.

- **Discussion on the discrepancies of results from NBCC 2015 and wind tunnel tests**

The underestimation in torsion for low-rise buildings is due to the fact that the code does not take partial loading into account. As can be seen in **Figure 4.2**, the higher wind pressures (the factor that produces the torsional effects) are only placed in a small area $y \times h$ in the building's corners, where y is the maximum of 6 m or $2z$. This value, in most cases, is not comparable to half of the wall dimension perpendicular to wind directions to produce the maximum torsion. This inappropriate pressure distribution also results in small shear coefficients, as illustrated in **Figure 4.3**.

Discrepancies between shear and torsional coefficients in medium-rise buildings provided by NBCC 2015, as shown in **Figure 4.3** and **Figure 4.5**, may be attributed to the lowest natural frequency of the building, f_n. Dynamic procedure was applied for all medium-rise buildings. Wind loads determined by the dynamic procedure are controlled by the building natural frequency, which may not be similar for buildings in the current study and those in previous studies due to the differences in building materials and LFRS. The assumptions made in the current study may result in different building material, LFRS and damping ratios to those in the past studies. As a result, dissimilar natural frequencies between buildings are resulted and directly affect the values of the size reduction factor s, and gust energy ratio at the natural frequency of the structure F, and consequently the gust factor C_g.

Computations with steel and concrete structures with different types of LFRS were carried out to examine the differences between their wind-induced shears and torsions. The 30.0 m height building of Stathopoulos et al. (2013) is taken as an example. As mentioned previously, this building was assumed to be a steel structure, with limited ductile braced-

frames as lateral force-resisting systems. Two other cases were considered, as the buildings were assumed to be moment resisting frame concrete structure and concrete building without a lateral force-resisting system. These buildings were designed for gravity and earthquake loads and a structural analysis software was used to determine their fundamental frequencies.

The three buildings have different damping ratio values, ranging from 2% to 5%, and natural frequencies ranging from 0.5 Hz to 1.0 Hz. Although they produce different gust factors C_g, similar torsional coefficients were found for the steel braced-frame building, the concrete building with moment resisting frame and the concrete building without lateral force-resisting system (0.37, 0.369, and 0.35, respectively). In addition, the corresponding shear coefficients computed in both directions were almost identical. Clearly, although building material and LFRS directly affect the wind-induced shear and torsion of a building, the differences they create are not significant.

4.2.3.2. Comparisons of ASCE/SEI 7-10 Provisions and Wind Tunnel Tests

This section presents similar comparisons with those illustrated previously in **Figure 4.3** and **Figure 4.5**.

Figure 4.6 shows similar torsional coefficients between the past studies and ASCE/SEI 7-10 standard. For low-rise buildings, the American standard has generated almost the same results as the experimental values on three out of four studies. The study of Tamura et al. (2003) is the only one that gives a considerable discrepancy - the code result is just half the value of the experimental data.
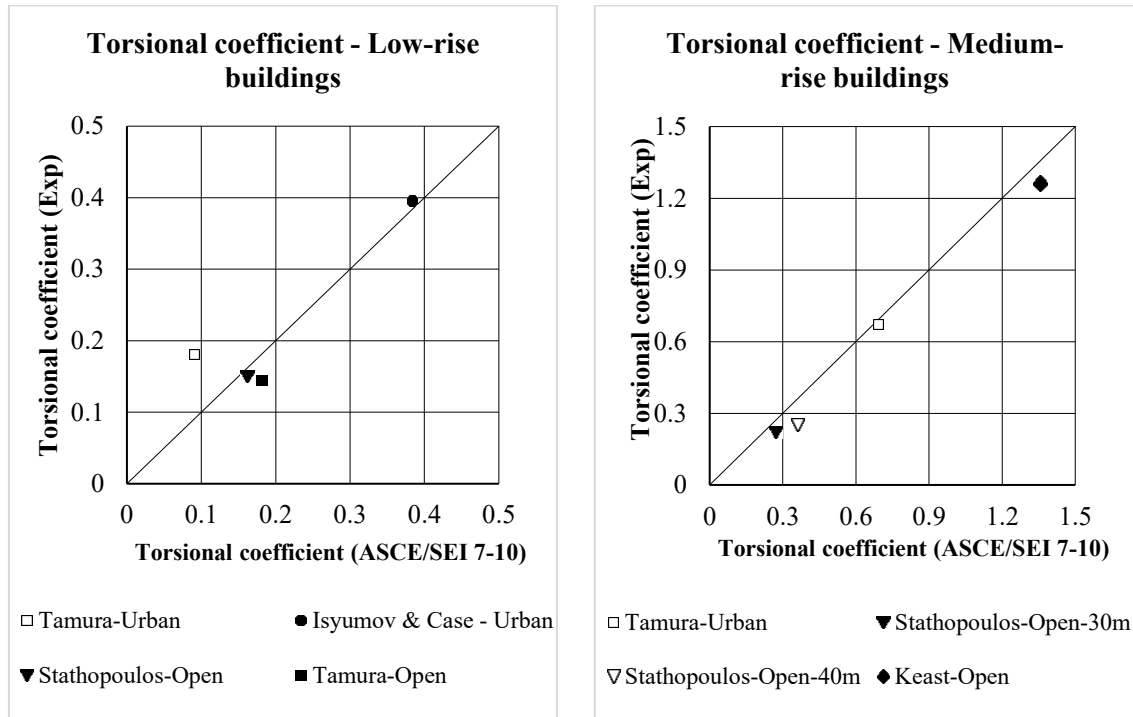
Figure 4.6: Comparison of torsional coefficients for low-rise and medium-rise buildings in ASCE/SEI 7-10 with experimental results from previous studies.

Better agreement has been illustrated in the results for medium-rise buildings. The highest difference is from the study of Stathopoulos et al. (2013), where an experimental coefficient is found equal to 75% of that from the American provisions. Other findings are very similar: experimental results are roughly 95% of the value of code computations.

Figure 4.7 compares shear coefficients on low-rise and medium-rise buildings obtained using ASCE/SEI 7-10 provisions and the wind tunnel results. Generally, the discrepancies induced in low-rise buildings are slightly higher than those in medium-rise buildings. All points shown in the graph of medium-rise buildings almost overlap with the 45° line. Stathopoulos et al. (2013) have again given identical values to those provided by the American standard. This resemblance tendency has been previously identified in the case

of NBCC 2015 (see **Figure 4.5**). Dissimilar results were found in the comparisons with

Tamura et al. (2003). Overall, ASCE/SEI 7-10 provisions have given analogous shear

results compared to the wind tunnel results.
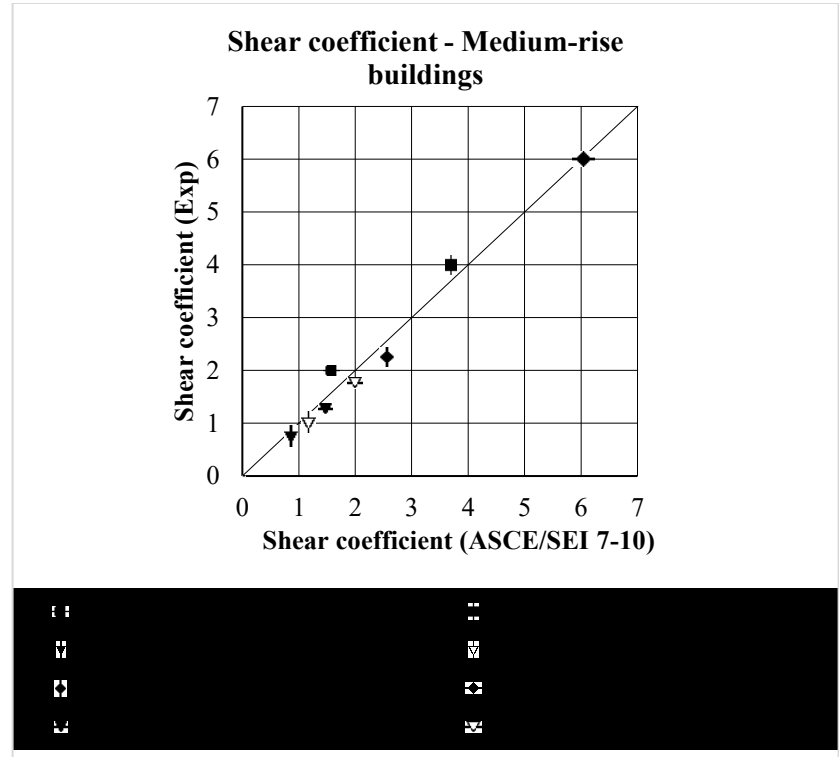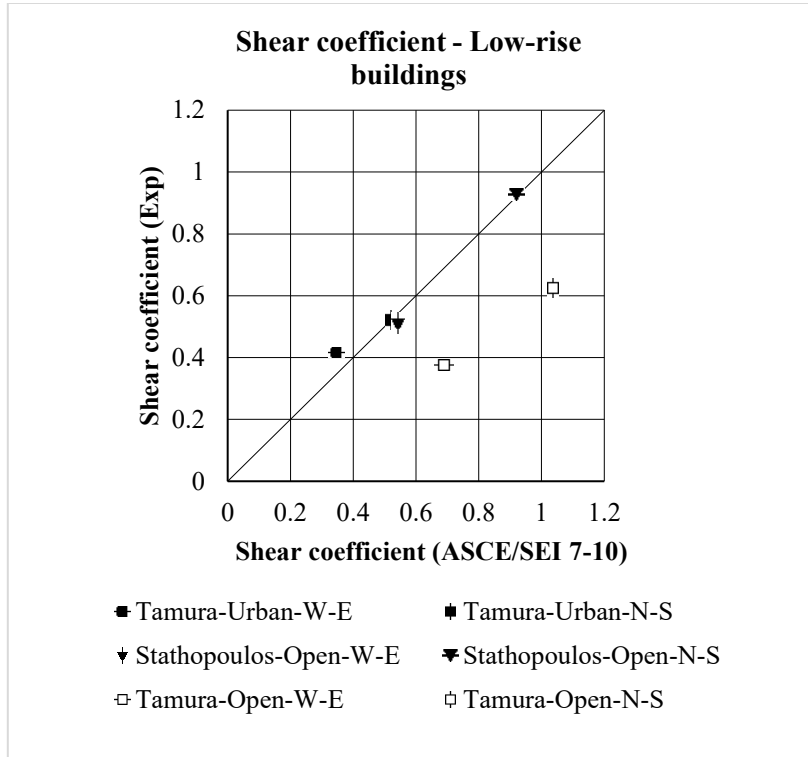
Figure 4.7: Comparison of shear coefficients for low-rise and medium-rise buildings in ASCE/SEI 7-10 with experimental results from previous studies.

4.2.3.3. Comparisons of NBCC 2015 and ASCE/SEI 7-10

In this section, the NBCC 2015 and ASCE/SEI 7-10 wind provisions are applied to the five buildings of group G1.C on Site Class C (**Table 3.1**). It is interesting to study the changes of shear and torsional coefficients when building heights increase. Also, the discrepancies of results between a low-rise building and a medium-rise building, and between two medium-rise buildings with the same height increment can be witnessed through this comparison.

These buildings were designed under gravity and earthquake loads as described in Chapter 3. Based on these building configurations and natural frequencies, the wind static procedure is applied for low-rise buildings and the dynamic procedure is applied for medium-rise buildings, according to NBCC 2015. In terms of the American standard, the Directional Procedure is applied for all buildings. The Envelope Procedure can only be carried out for the low-rise buildings. The summary of computation procedures regarding both standards is given in **Table 4.2**.

Table 4.2: Computation procedure for the buildings in the current study according to NBCC and ASCE.

Study	f_n	H/w	H (m)	Procedure	
				NBCC 2015	ASCE/SEI 7-10
Current study	1.25	0.39	14.8	Static	Envelope/Directional
	0.79	0.58	22	Dynamic	Directional
	0.61	0.77	29.2	Dynamic	Directional
	0.49	0.96	36.4	Dynamic	Directional
	0.38	1.15	43.6	Dynamic	Directional

All partial loading cases are carried out to seek the highest wind-induced shears and torsions provided by both codes. The results are shown in **Figure 4.8**.
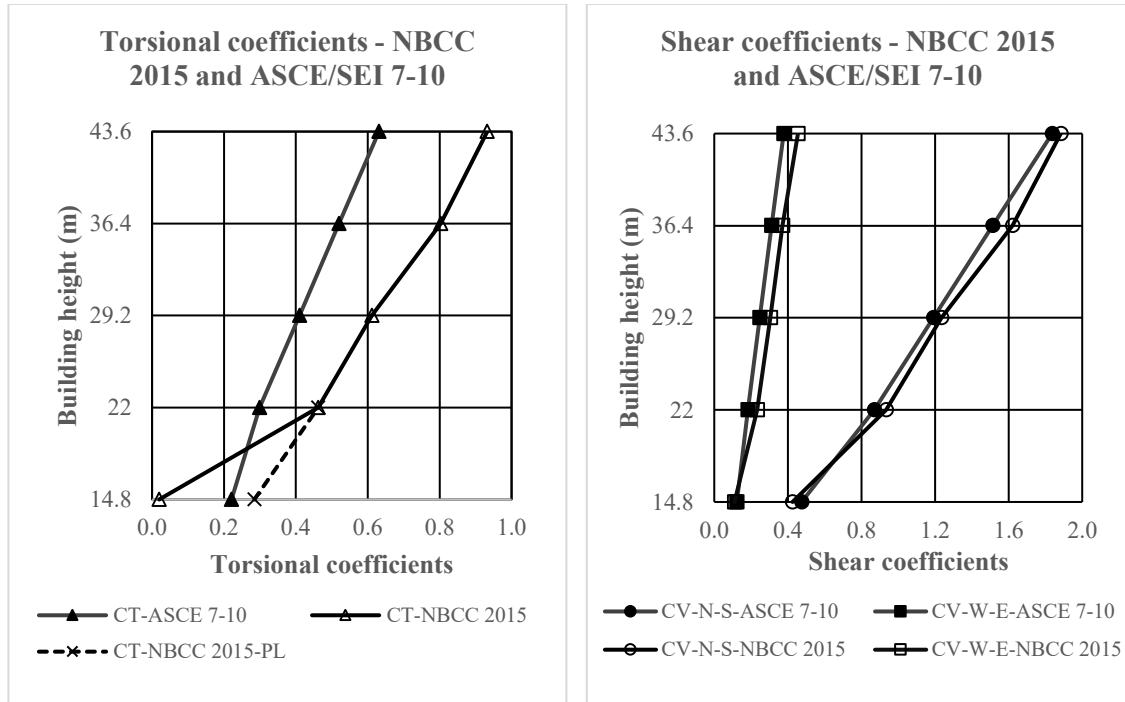
Figure 4.8: Shear and torsional coefficients according to NBCC 2015 & ASCE/SEI 7-10.

A very small torsional coefficient is produced for the low-rise building. The torsional coefficient rises immensely when building class changes from low-rise to medium-rise building (14.8 m to 22.0 m) and can be witnessed easily from the sudden change in the C_T line's alignment in **Figure 4.8**. Moreover, this jump seems to be noticeably high compared to the average of 1.3 times different between the results according to the same height steps of the other buildings. In terms of shear coefficients, the differences are apparently less remarkable. The difference between the low-rise and medium-rise buildings is just slightly greater than that between two consecutive medium-rise buildings in N-S direction and decreases largely when it comes to E-W direction.

Through the good agreement with experimental values (**Figure 4.6** and **Figure 4.7**), ASCE/SEI 7-10 wind provisions are believed to have successfully predicted the wind effects in low- and medium-rise buildings and can be considered a good reference to evaluate the adequacy of other codes. Therefore, the coefficients found in NBCC 2015 are compared with the values provided by the ASCE/SEI 7-10 provisions on the same set of buildings. Significant discrepancies are found regarding torsional coefficients, especially in the case of the low-rise building. Firstly, the torsional coefficient of NBCC 2015 for low-rise building is much smaller than that of ASCE/SEI 7-10, implying a significant underestimation of NBCC 2015 in evaluating the wind-induced torsional effects on low-rise buildings. Secondly, for medium-rise buildings, NBCC 2015 has created torsional coefficients roughly 1.5 times higher than those of ASCE/SEI 7-10. This trend increases with the building height and is greater than the 6% difference shown in **Figure 4.3** and **Figure 4.6** where the same computations were made for smaller buildings. Indeed, the longer horizontal dimension of the buildings in this section (150.5 m) is more than double of the maximum building dimension from previous comparisons (61.0 m) with wind tunnel test results, where NBCC 2015 has produced better results. Therefore, it can be concluded that the recommended tributary area is conservative for determining the torsional effects of large and high buildings.

In contrast, in terms of shear coefficients, **Figure 4.8** shows that both codes have given similar results regardless of building height. Thus, although the discrepancies fluctuate with the ascending building heights, the two codes only give differences within 10%. Excluding the results of low-rise buildings, all shear coefficients resulted from NBCC 2015 are higher than those from ASCE/SEI 7-10. It is also noticeable that the gap between the

shear coefficients of the 14.8 m high building (low-rise) and the 22.0 m high building (medium-rise) is significantly higher comparing to those between the other medium-rise buildings. In particular, with the same increases in building height, while the shear coefficients of the 14.8 m high building in two major directions are on average about 50% of those of the 22.0 m high building, the average between the medium-rise buildings is almost 80%. However, this difference does not imply any underestimation in shear computations in low-rise building as a similar trend between code provisions and wind tunnel test results has been found in the previous section.

4.3. RECOMMENDATIONS FOR WIND LOADING TO BE INCLUDED IN NBCC

In conclusion, although having a tendency of being conservative, the wind load assessment given by NBCC 2015 for medium-rise buildings with the tributary area given in Equation (4-4) is still considerably good. Therefore, this method is applied in this thesis to compute wind loading on medium-rise buildings.

On the other hand, the wind-induced shears and torsions resulted are underestimated by the procedure stipulated for low-rise buildings. It was thus decided that the methodology given in ASCE/SEI 7-10 be used to compute wind loads on the set of low-rise buildings.

Chapter 5

WIND DESIGN

In this chapter, the recommendations from Chapter 4 for the NBCC 2015 wind load provisions are used to design wind load on the set of buildings listed in **Table 3.1**. The wind-induced interstorey drifts are then obtained to see if P-Δ effects should be examined. However, in all cases, P-Δ effects are not needed as all stability coefficients, θ_x, are smaller than 0.1. The load combination $(1.25D \text{ or } 0.9D) + 1.4W + 0.5L \text{ or } 0.5S$ is used. The detailed wind calculation of the plan "A", 12-storey, LD-CBF building on Site Class C is illustrated in an example as follows.

5.1. DYNAMIC PROCEDURE

Based on modal analysis, the natural frequency of the building is $f_n = 1/T_{dyn} = 1/2.66 = 0.38 \ Hz$. The height of the building is 43.6 m, which is lower than 60 m, and it has the ratio $1 < H/w = 43.6/38 = 1.15 < 4$. Therefore, the dynamic procedure is chosen for wind design. Equation (2-14) is used to determine the wind external pressure. The design process is similar to that shown for the building of Tamura et al. (2013) in Appendix B. The gust factors, C_g, are 2.47 and 1.94 in E-W direction and N-S direction, respectively. The exposure factors and the external factors are computed considering open terrain, which consequently yields the following values:

$$C_{e,H} = \left(\frac{42.3}{10}\right)^{0.28} = 1.51$$

$$\begin{cases} C_{p,ww,E-W} = 0.27 \times \left(\dfrac{42.3}{150.5} + 2 \right) = 0.62 \\ C_{p,lw,E-W} = -0.27 \times \left(\dfrac{42.3}{150.5} + 0.88 \right) = -0.32 \end{cases}$$

$$\begin{cases} C_{p,ww,N-S} = 0.8 \\ C_{p,lw,N-S} = -0.5 \end{cases}$$

The wind-induced base shears of Case A are $W_{A,E-W} = 1974/8 = 247 \ kN$ and $W_{A,N-S} = 8636/8 = 1079 \ kN$. In Case C, the forces are equal to 75% of Case A, which are $W_{C,E-W} = 185 \ kN$ and $W_{C,N-S} = 810 \ kN$. Half of the wind load in Case A are reduced in Case B, which are given as: $W_{B,W-E} = 130 \ kN$ and $W_{B,N-S} = 1137 \ kN$. Regarding Case D, the base shears are $W_{D,E-W} = 183 \ kN$ and $W_{D,N-S} = 844 \ kN$. The results of all 4 partial loading cases are reported in **Table 5.1**.

.

Table 5.1: Wind computation following NBCC 2015 provisions for dynamic procedure –

12-storey LD-CBF building, plan "A", Site Class C.

St	p	W-E direction				p	N-S direction			
		1.4W					1.4W			
		Case A	Case B	Case C	Case D		Case A	Case B	Case C	Case D
	kN/m²	kN	kN	kN	kN	kN/m²	kN	kN	kN	kN
12	1.52	13	7	10	10	1.68	57	60	43	44
11	1.48	38	20	29	28	1.64	168	177	126	131
10	1.44	63	33	47	47	1.60	276	291	207	216
9	1.40	87	46	65	65	1.55	381	401	286	298
8	1.36	110	58	83	82	1.50	482	508	362	377
7	1.31	133	70	99	98	1.45	580	611	435	453
6	1.25	154	81	116	114	1.39	674	710	505	527
5	1.19	174	92	131	130	1.32	763	804	572	597
4	1.12	194	102	145	144	1.24	847	893	635	662
3	1.04	211	111	159	157	1.15	925	974	694	723
2	1.01	229	120	171	170	1.11	1000	1054	750	782
1	1.01	**247**	130	185	183	1.11	1079	**1137**	810	844

5.2. STATIC PROCEDURE

Although only the dynamic procedure is required, the Static Procedure is also applied for comparative purposes. Equation (2-14) is also used for the Static Procedure. Except the gust factor, C_g, and the exposure factor, C_e, the other parameters remain unchanged comparing to the Dynamic Procedure. The gust factor is determined to be equal to 2 because the current building is considered as a whole. In terms of the exposure factor, the following equation is used for open terrain:

$$C_e = \left(\frac{h}{10}\right)^{0.2} \geq 0.9 \tag{5-1}$$

The resulted wind loads corresponding to all four Cases are shown in **Table 5.2**.

Table 5.2: Wind computation following NBCC 2015 provisions for static procedure – 12-storey LD-CBF building, plan "A", Site Class C.

St	p	W-E direction				p	N-S direction			
		1.4W					1.4W			
		Case A	Case B	Case C	Case D		Case A	Case B	Case C	Case D
	kN/m²	kN	kN	kN	kN	kN/m²	kN	kN	kN	kN
12	1.05	9	5	7	7	1.47	50	52	37	39
11	1.04	27	14	20	21	1.44	147	155	110	115
10	1.02	44	23	33	35	1.41	243	256	182	189
9	0.99	61	32	46	48	1.38	337	355	253	262
8	0.97	78	41	58	61	1.35	428	452	321	334
7	0.95	94	49	70	74	1.32	518	546	388	403
6	0.92	110	58	82	86	1.28	604	637	453	471
5	0.89	125	66	94	98	1.23	688	725	516	536
4	0.85	139	73	104	110	1.18	768	809	576	598
3	0.80	153	80	115	120	1.12	843	889	633	657
2	0.74	166	87	124	130	1.03	913	963	685	712
1	0.71	**178**	94	134	140	0.98	984	**1037**	738	767

The differences between the two procedures can be illustrated after comparing **Table 5.1** and **Table 5.2**. The maximum base shear per CBF is approximately 10% and 40% higher in N-S and E-W directions, respectively. Therefore, it is important to determine the appropriate wind computation procedure.

Chapter 6

COMPARISONS BETWEEN EARTHQUAKE- AND WIND-INDUCED SHEAR AND TORSION

The maximum wind-induced and earthquake-induced shear forces in each CBF of the 22 buildings shown in **Table 3.1** are compared to decide the type of lateral load that governs the CBFs design. The lateral deflections resulted from each case is also verified. Particularly, the interstorey drifts due to earthquake and wind loads are compared with the limits given in NBCC 2015. The comparisons are conducted in both orthogonal directions.

6.1. COMPARISONS BETWEEN WIND FORCE AND EARTHQUAKE ELASTIC FORCE AT THE BASE OF BUILDING STRUCTURE

In this section, the factored base shear force from earthquake load is compared to that from factored wind load. In the earthquake load combination, the earthquake load factor is 1.0. In the wind load combination, the wind load factor is 1.4. Furthermore, the CBF design for wind loads needs to assure an elastic response while for earthquake load, inelastic response is permitted when $R_d > 1.5$. For comparison purposes, the inelastic base shear resulted from earthquake load is transposed into elastic base shear computed with $R_d \times R_o = 1$.

Table 6.1 to **Table 6.3** show the base shear forces computed for one CBF in N-S direction and one CBF in E-W direction for all 22 buildings based on the following load cases:

i. The elastic base shear resulted from earthquake load when the Equivalent Static Force Procedure was applied, V_e;

ii. The elastic base shear plus shear due to torsional effect, $(V_e + T)$;

iii. The elastic base shear plus shear due to torsional effect, as well as shear due to notional lateral load and P-Δ effect, expressed by U_2 factor, $(V + N + T) \times U_2$;

iv. The factored wind base shear $(1.4W)$ computed for 4 loading cases: W_A, W_B, W_C, W_D and

v. The maximum base shear value among the 4 wind loading cases plus the notional lateral load per one CBF, $(W_{max} + N)$.

It is noted that the elastic base shear computed from the equivalent static force procedure corresponds to $T_a = 2 \times 0.025 h_n$. The tables provide the fundamental period of studied buildings in both orthogonal directions resulted from dynamic analysis by means of acceleration response spectra using ETABS.

Table 6.1: Maximum earthquake and wind base shear of LD- and MD-CBF with plan "A", Site Class C.

St. no.	Dir	T_{dyn}	T_a	Base Shear of 1 CBF (kN)									Observation
				1.0 Earthquake			1.4 Wind						
				V_e	V_e+T	$(V_e+T+N)U_2$	W_A	W_B	W_C	W_D	$(W_{max}+N)$	V_e/W_A	
				Plan "A", Site Class C, $R_d=2$									
12-st	E-W	2.66	2.18	**2262**	2309	2767	**345**	182	259	257	529	6.56	E governs
	N-S	2.38		**2262**	3264	**4759**	1511	**1591**	1133	1182	1797	1.49	E governs
10-st	E-W	2.04	1.82	**2287**	2335	2683	**244**	128	183	184	433	9.36	E governs
	N-S	1.88		**2287**	3300	3815	1131	**1198**	848	879	1398	2.02	E governs
8-st	E-W	1.65	1.46	**2473**	2525	2839	**176**	92	132	131	299	14.03	E governs
	N-S	1.58		**2473**	3568	4076	772	**818**	579	600	950	3.20	E governs
6-st	E-W	1.27	1.1	**2342**	2391	2617	**116**	60	87	85	217	20.19	E governs
	N-S	1.14		**2342**	3379	3710	**477**	506	358	371	615	4.91	E governs
4-st	E-W	0.80	0.74	**2610**	2665	2909	**28**	-	-	-	105	93.21	E governs
	N-S	0.72		**2610**	3766	4065	**121**	-	-	-	198	21.57	E governs
				Plan "A", Site Class C, $R_d=3$									
12-st	E-W	2.76	2.18	**2262**	2309	2862	**354**	185	266	262	538	6.55	E governs
	N-S	2.51		**2262**	3264	**4074**	1514	**1603**	1135	1177	1800	1.49	E governs
10-st	E-W	2.09	1.82	**2287**	2299	2715	**244**	127	183	184	433	9.39	E governs
	N-S	2.03		**2287**	2546	**3092**	1134	**1201**	851	881	1402	2.01	E governs
8-st	E-W	1.75	1.46	**2473**	2525	2914	**177**	93	133	131	300	13.96	E governs
	N-S	1.63		**2473**	3568	4231	768	**813**	576	597	945	3.22	E governs
6-st	E-W	1.27	1.1	**2342**	2391	2671	**118**	62	89	87	219	19.82	E governs
	N-S	1.293		**2342**	3379	3809	**484**	**513**	363	377	622	4.84	E governs
4-st	E-W	0.86	0.74	**2610**	2624	2812	**28**	-	-	-	105	93.21	E governs
	N-S	0.77		**2610**	2899	3228	**121**	-	-	-	198	21.57	E governs

Table 6.2: Maximum earthquake and wind base shear LD- and MD-CBF buildings with plan "A", Site Class B.

St. no.	Dir	T_{dyn}	$T_{a,}$	V_e	V_e+T	$(V_e+T+N)U_2$	W_A	W_B	W_C	W_D	$(W_{max}+N)$	V_e/W_{max}	Observation
							Base Shear of 1 CBF (kN)						
				1425	1455	1871	**362**	189	272	268	546	3.93	E governs
12-st	N-S	2.68	2.18	**1425**	2056	**2668**	**1543**	**1637**	1157	1201	**1835**	0.92	$V_e < W_A$; $(V_e + T) > W_B$; Check W & E
10-st	E-W	2.36	1.82	1441	1471	1802	**255**	133	191	191	443	5.66	E governs
	N-S	2.16		1441	2079	**2492**	1150	**1220**	863	894	**1421**	1.25	E governs
8-st	E-W	1.84	1.46	**1558**	1591	1873	**180**	94	135	133	303	8.66	E governs
	N-S	1.63		1558	2248	**2611**	768	**815**	576	597	**947**	2.02	E governs
							Plan "A", Site Class B, $R_d=3$						
	E-W	2.90		**1425**	1455	2006	**361**	188	271	267	544	3.94	E governs
12-st	N-S	2.62	2.18	**1425**	2056	2723	**1535**	**1628**	1151	1194	**1825**	0.92	$V_e < W_A$; $(V_e + T) > W_B$; Check W & E
10-st	E-W	2.38	1.82	**1441**	1471	1844	**255**	133	191	191	444	5.65	E governs
	N-S	2.14		1441	2079	**2551**	1148	**1218**	861	893	**1419**	1.25	E governs
8-st	E-W	1.90	1.46	**1558**	1591	2012	**182**	95	136	134	304	8.57	E governs
	N-S	1.75		1558	2248	2812	777	**824**	583	605	**957**	2.00	E governs

(Header spanning note: columns "V_e, V_e+T, $(V_e+T+N)U_2$" are under "1.0 Earthquake"; columns "W_A, W_B, W_C, W_D, $(W_{max}+N)$" are under "1.4 Wind"; row "Plan "A", Site Class B, $R_d=2$" precedes the first data block.)

Table 6.3: Maximum earthquake and wind base shear of MD-CBF buildings with plan "B", on Site Class C and Site Class B.

St. no.	Dir	T_{dyn}	T_a	Base Shear on 1 CBF (kN)									Observation
				1.0 Earthquake			1.4 Wind						
				V_e	V_e +T	$(V_e$ +T+N$)U_2$	W_A	W_B	W_C	W_D	$(W_{max}$+N$)$	V_e /W_A	
				Plan "B", Site Class C, R_d=3									
12-st	E-W	2.79	2.18	2310	2591	3405	**822**	488	617	641	1009	2.81	E governs
	N-S	2.63		2310	2806	**3921**	**1706**	1517	1280	1237	**1907**	1.35	E governs
10-st	E-W	2.20	1.82	2335	2619	3271	**576**	342	432	454	768	4.05	E governs
	N-S	2.01		2335	2836	**3635**	**1249**	1114	937	905	**1453**	1.87	E governs
8-st	E-W	1.79	1.46	2524	2831	3364	**388**	230	291	305	513	6.51	E governs
	N-S	1.63		**2524**	3066	3728	**831**	**741**	623	602	966	3.04	E governs
				Plan "B", Site Class B, R_d=3									
12-st	E-W	2.92	2.18	1455	1553	2013	**837**	497	627	655	1024	1.74	E governs
	N-S	2.82		**1455**	1846	**2655**	**1764**	1573	1323	1279	**1965**	0.83	*V_e<W_A; $(V_e + T) > W_B$; Check W & E*
10-st	E-W	2.45	1.82	**1471**	1570	2131	**598**	355	449	472	791	2.46	E governs
	N-S	2.30		1471	1866	**2624**	**1308**	1166	981	948	**1512**	1.12	E governs
8-st	E-W	1.88	1.46	**1590**	1698	2156	**399**	**237**	299	314	540	3.99	E governs
	N-S	1.83		1590	2017	**2679**	**858**	765	643	621	**1008**	1.85	E governs

As can be seen from **Table 6.1**, earthquake load combination governs the design of buildings with plan "A" located on Site Class C, regardless the type of CBF. As resulted in the case of buildings designed with $R_d = 2$, the dynamic fundamental period is about 10% larger than the static period computed from the empirical equation and about 20% larger for buildings designed with $R_d = 3$. When the direction of earthquake loading is perpendicular to the building's long dimension, larger shear force resulted due to torsional effects (which increases shear force by 150%). The maximum wind force in a CBF in E-W direction resulted from wind Case A, while Case B created the maximum values in N-S direction.

For the plan "A", LD-CBF, Site Class C, the 12-storey building (N-S direction) has the ratio $V_e/W_A = 1.41$, while that for the 10-storey building is 1.91. Although the earthquake combination governs the design, the wind load combination needs to be checked because brace members are designed based on the inelastic earthquake-induced shear, which is much lower than the elastic shear when the value $R_d \times R_o$ increases. This matter will be discussed further in this chapter.

When buildings are located on Site Class B (**Table 6.2**), wind load almost remains similar in comparison with the case of Site Class C. However, with harder soil, earthquake load decreases. For the 12-storey building with plan "A" located on Site Class B, having both LD-CBF and MD-CBF (N-S direction calculation), the ratio $V_e/W_A = 0.87$ and 0.88, while that for the similar 10-storey building and 8-storey building are > 1, respectively. As resulted, for the 12-storey building, in the N-S direction, the wind load combination governs the design when torsional effects are not considered. However, when the shear due to earthquake plus shear due to torsion ($V_e + T$) is checked, the earthquake controls the

design (e.g. $V_e + T = 2056\ kN > W_B = 1637\ kN$). Therefore, when designing buildings higher than 10 storeys (36.4 m) on Site Class B, based on elastic earthquake-induced shear, caution should be given to both earthquake and wind design.

When buildings with plan "B" ($L/B = 2$) are considered, the maximum wind load is provided by wind Case A in all considered cases (**Table 6.3**). Again, for the CBF design in the N-S direction, the 12-storey building on Site Class B presents $V_e/W_A = 0.83$. However, when shear plus shear caused by torsion ($V_e + T$) is checked against W_B, it is the earthquake load combination that controls the design. Therefore, caution should be given when designing buildings taller than 10 storeys in Montreal on stiffer Site Class (e.g. Site Class B). A potential recommendation could be to choose LD-CBF over MD-CBF, which results in small changes in member sizes when wind and earthquake demands are considered.

In conclusion, when the factored elastic shear from earthquake load is compared with the factored shear from wind load, attention should be given when verifying 12-storey buildings on Site Class B (in Montreal), regardless of CBF's ductility type.

6.2. COMPARISONS BETWEEN WIND AND EARTHQUAKE INDUCED SHEAR AND TORSION AT DESIGN LEVEL

6.2.1. Shear Distributions Normalized to Braces' Compressive and Tensile Resistance

In this study, both types of LFRS, which are LD-CBF and MD-CBF, are selected. Following the Equivalent Static Load Procedure, the distribution of earthquake design storey shear, V_d, (computed either with $R_d \times R_0 = 2 \times 1.3$ or $R_d \times R_0 = 3 \times 1.3$), against the distribution of wind load computed for each case, is shown in **Figure 6.1** to **Figure 6.22**.

In these figures, the distribution of only design base shear V_d; the V_d plus shear caused by torsion, $(V_d + T)$; and the total design shear including shear caused by notional load, torsion and P-Δ effects, i.e. $(V_d + N + T) \times U_2$, are shown.

To compare the distribution of shear along the building height for all cases, shears are normalized to brace members' resistance, T_r and C_r, projected to horizontal axis as follows:

$$\frac{V}{(C_r + T_r) \times cos\alpha} \tag{6-1}$$

where V is either shear from earthquake or wind loads, C_r and T_r are brace compressive and tensile resistance, α is the brace angle with a horizontal line.

Figure 6.1 to **Figure 6.5** show the normalized shear force distribution on buildings with plan "A", $R_d = 2$, located on Site Class C. In all cases but two, the ratio of normalized shear force, V_d to shear provided by brace resistance is always larger than that of the normalized shear computed from wind load. The two exceptions are the 12-storey and 10-storey buildings when the direction of loading is N-S. For the bottom two floors of the 10-storey building, the normalized shear included shear from torsion almost equates the normalized shear computed from wind Case B. Although these two buildings (12-storey and 10-storey) are more sensitive to wind load cases, the ratio of normalized shear due to wind load is < 1.0.

Figure 6.1: Normalized shear force distribution of the 12-storey building with plan "A", $R_d=2$, Site Class C.

Figure 6.2: Normalized shear force distribution of the 10-storey building with plan "A", $R_d=2$, Site Class C.

Figure 6.3: Normalized shear force distribution of the 8-storey building with plan "A", R_d=2, Site Class C.

Figure 6.4: Normalized shear force distribution of the 6-storey building with plan "A", R_d=2, Site Class C.
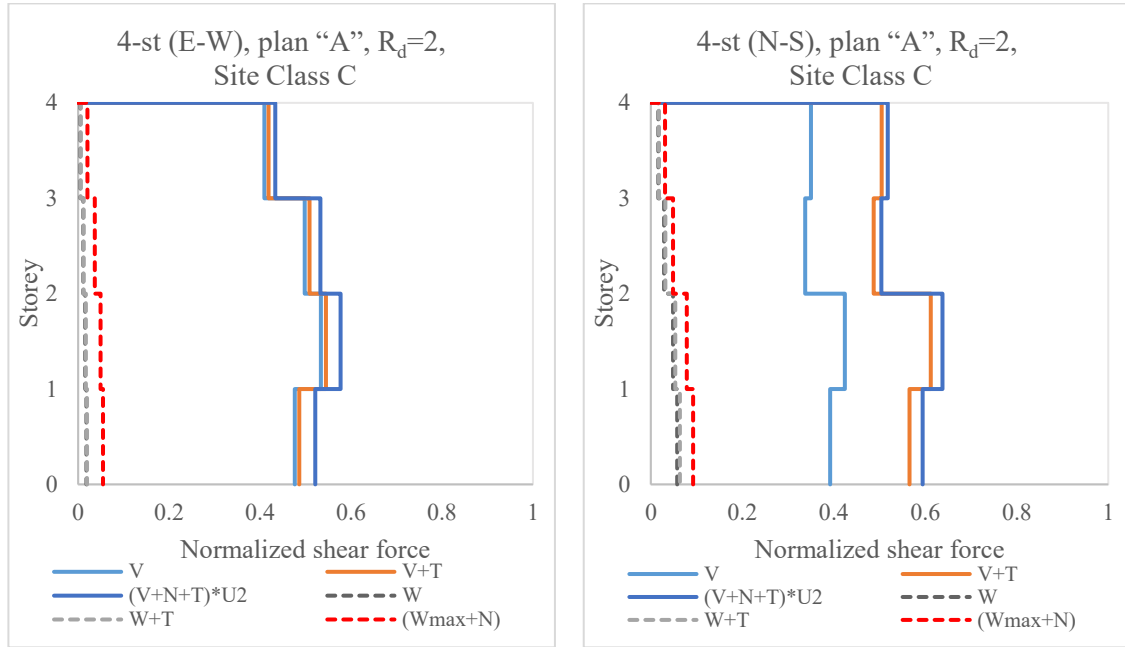
Figure 6.5: Normalized shear force distribution of the 4-storey building with plan "A", R_d=2, Site Class C.

From the figures above (**Figure 6.1** to **Figure 6.5**), wind load has a tendency of exceeding earthquake loads, especially for the 12-storey building. In the following figures (**Figure 6.6** to **Figure 6.10**), it is interesting to observe the decrease in earthquake shear when MD-CBF ($R_d = 3$) is considered instead of LD-CBF ($R_d = 2$).
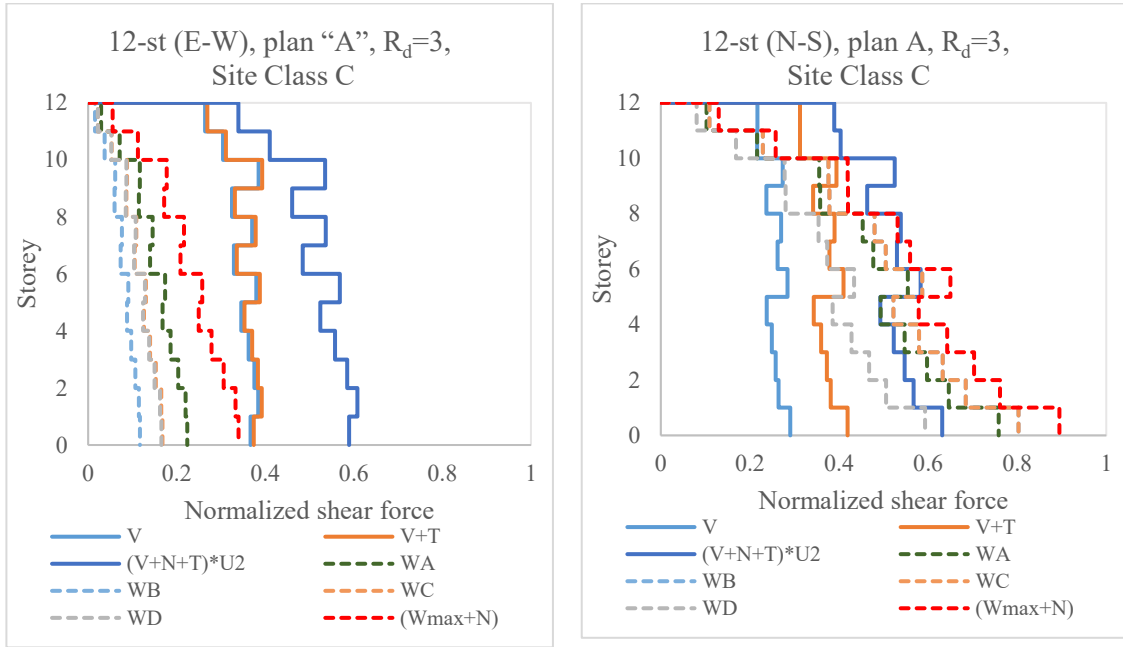
Figure 6.6: Normalized shear force distribution of the 12-storey building with plan "A", $R_d=3$, Site Class C.
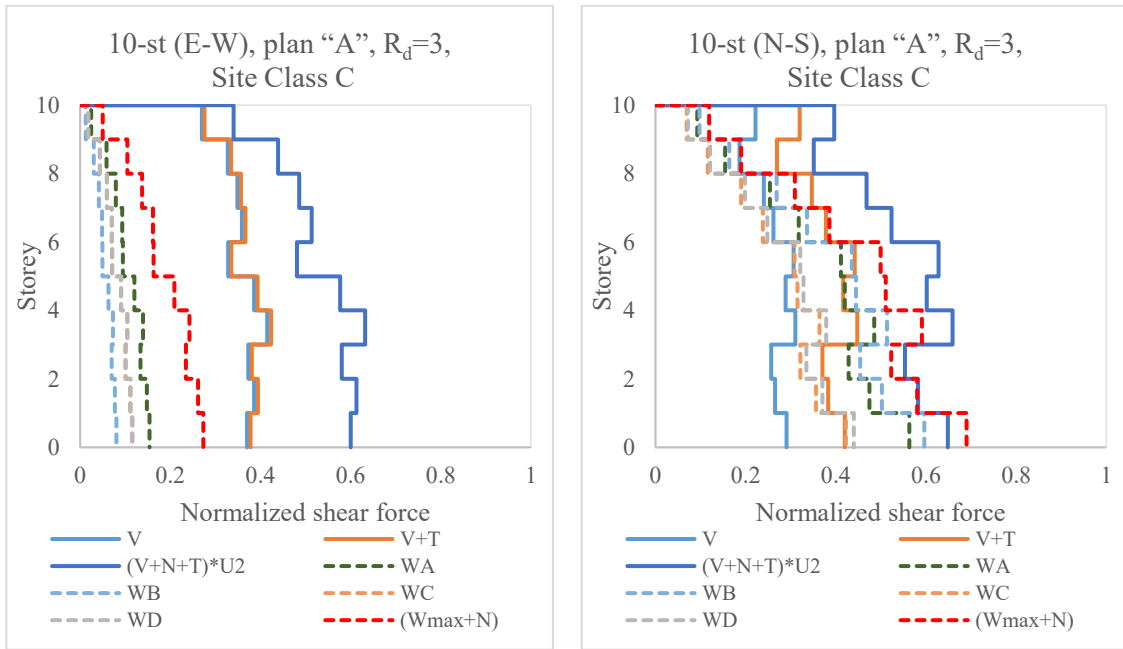
Figure 6.7: Normalized shear force distribution of the 10-storey building with plan "A", $R_d=3$, Site Class C.
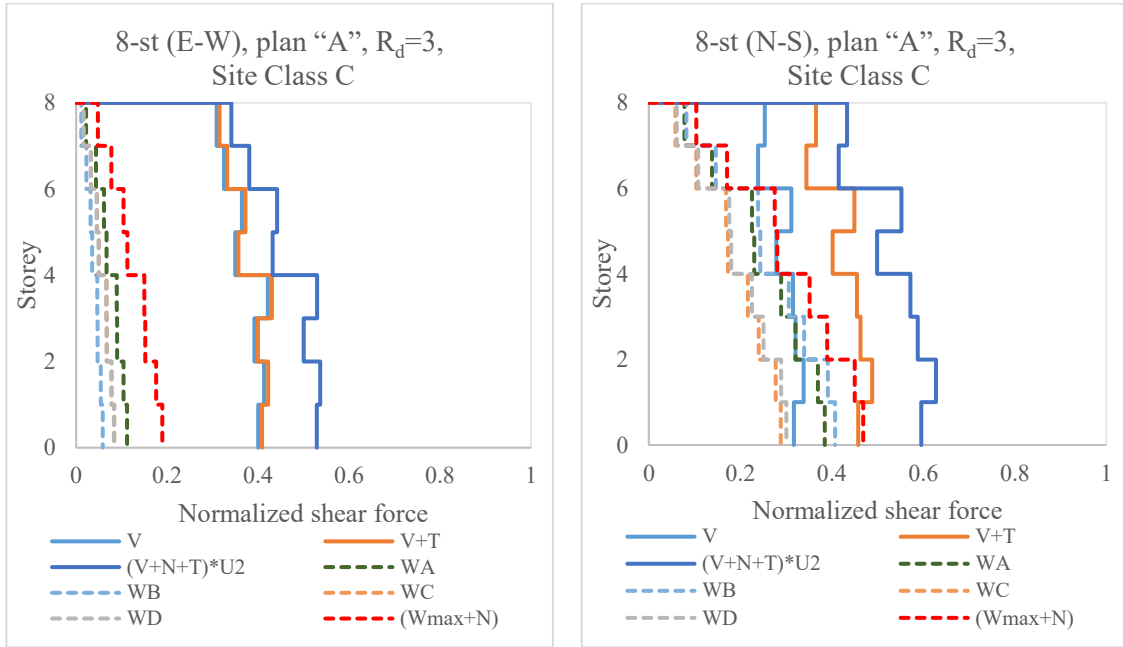
Figure 6.8: Normalized shear force distribution of the 8-storey building with plan "A", R_d=3, Site Class C.
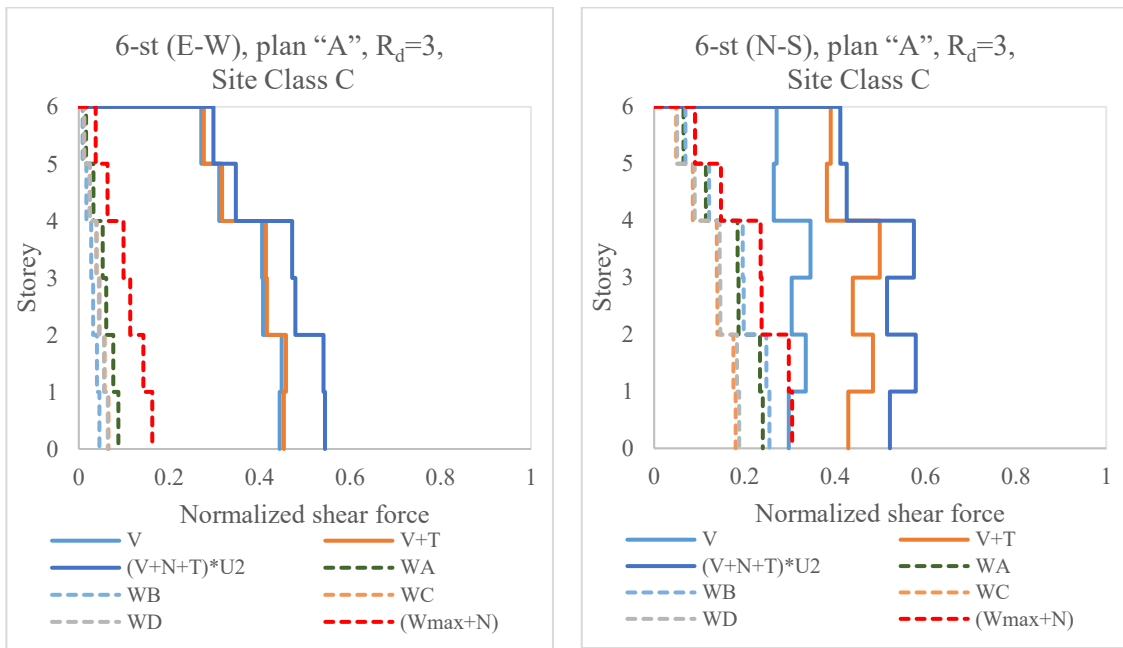
Figure 6.9: Normalized shear force distribution of the 6-storey building with plan "A", R_d=3, Site Class C.
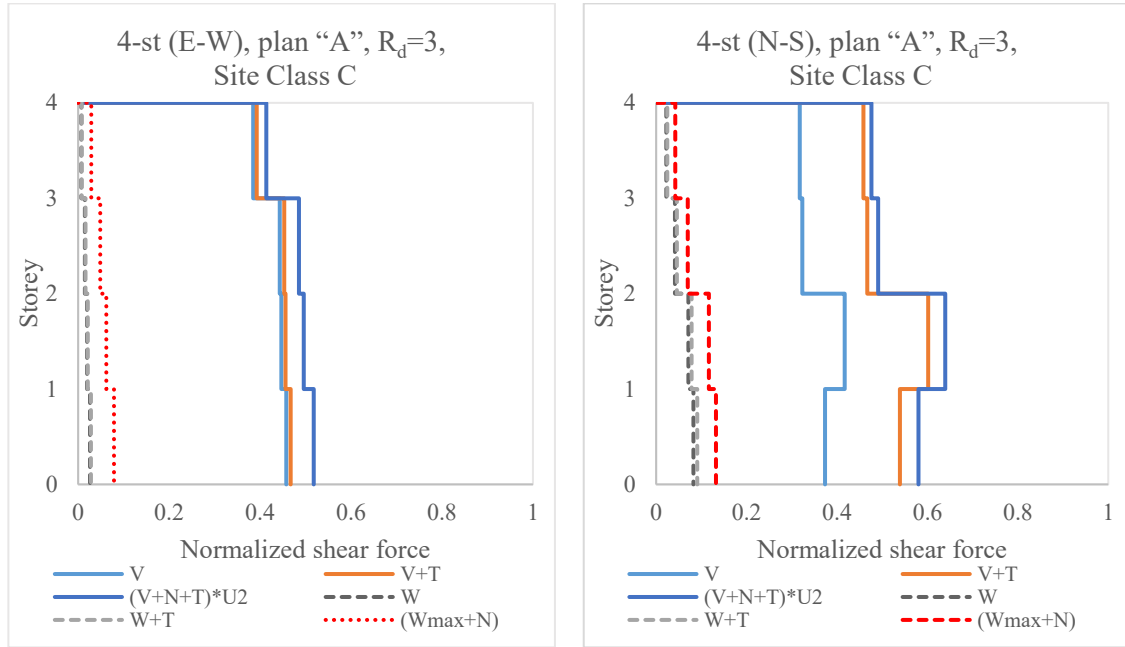
Figure 6.10: Normalized shear force distribution of the 4-storey building with plan "A", R_d=3, Site Class C.

As shown in **Figure 6.6** to **Figure 6.10**, the ratio of normalized shear force, V_d to shear provided by braces resistance is greater than those due to wind load in the case of lower buildings (e.g. 6-storey and 4-storey buildings). For the 8-storey building, in N-S direction, at the ground floor, the ratio of normalized shear included shear from torsion exceeds the normalized shear computed from wind Case B. However, no brace strength exceedance is witnessed. At the lower half floors of the 12-storey building (N-S), the ratio of normalized shear due to wind load Case B is larger than that of the normalized shear due to earthquake load even when the shear is composed from pure shear, shear due to torsion, shear due to notional lateral loads and P-Δ effect.

The normalized shear from earthquake and wind loads are also computed for the same buildings with plan "A" located on Site Class B. Only the 12-storey, 10-storey and 8-storey

buildings are considered herein because they are more sensitive to wind load. For buildings with LD-CBF, the results are illustrated in **Figure 6.11** to **Figure 6.13**. As illustrated, due to the reduction in earthquake demand, wind becomes more critical.

Figure 6.11: Normalized shear force distribution of the 12-storey building with plan "A", R_d=2, Site Class B.

Figure 6.12: Normalized shear force distribution of the 10-storey building with plan "A", $R_d=2$, Site Class B.

Figure 6.13: Normalized shear force distribution of the 8-storey building with plan "A", $R_d=2$, Site Class B.

In all cases, earthquake loads are much higher than wind loads when acting perpendicular to the shorter dimension of building (E-W direction). As illustrated in **Figure 6.13**, for the 8-storey building (N-S), at the bottom floor, the ratio of normalized wind shear exceeds the ratio of normalized earthquake shear plus shear due to torsion ($V_d + T$). In the case on 10-storey building (N-S direction), wind loads are dominant at the bottom four storeys. However, the ratio is still lesser than 1.0. This statement is also true for the 12-storey building (N-S) even when the wind loads govern the bottom eight floors of the building as shown in **Figure 6.11**.

Similarly, the same study is conducted for the 12-storey, 10-storey and 8-storey buildings with plan "A" located on Site Class B and designed with higher ductility factor ($R_d = 3$). The results as illustrated in **Figure 6.14** to **Figure 6.16**. In N-S direction, the ratio of normalized shear due to wind is larger than that from earthquake design at almost all floors of the 12-storey (**Figure 6.14**) and 10-storey building (**Figure 6.15**). However, for the 12-storey building the ratio of normalized shear due to wind load exceeds 1.0 at the 2nd floor level. This case shows a significant increase in wind-induced demand and will be discussed in detail in the next section.

Figure 6.14: Normalized shear force distribution of the 12-storey building with plan "A", R_d=3, Site Class B.

Figure 6.15: Normalized shear force distribution of the 10-storey building with plan "A", R_d=3, Site Class B.
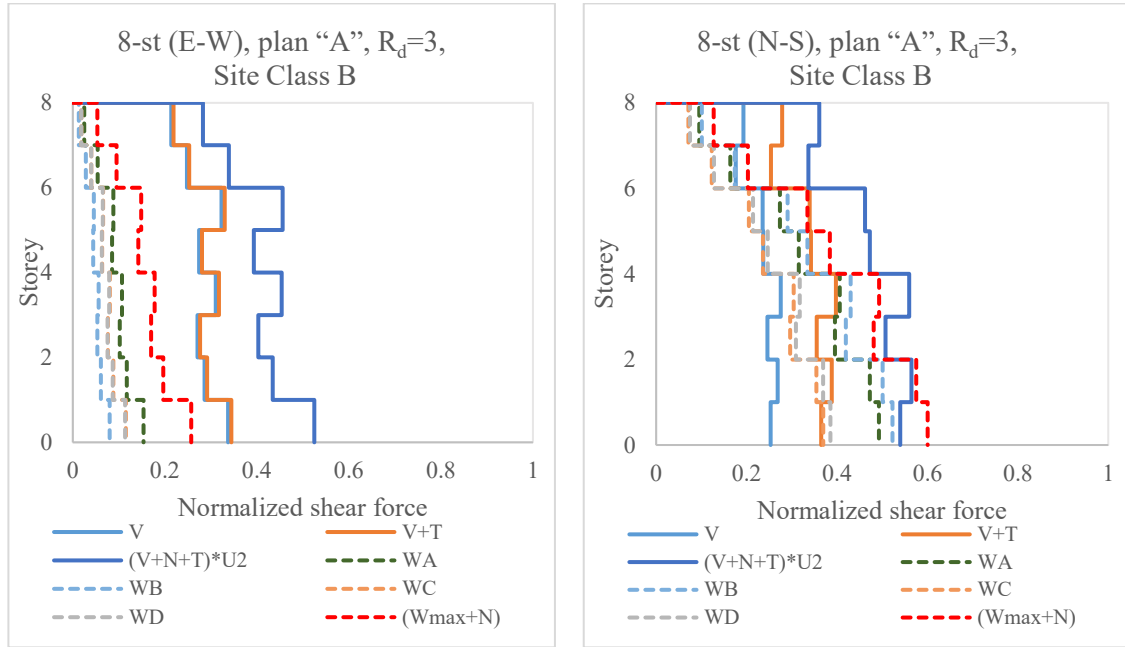
Figure 6.16: Normalized shear force distribution of the 8-storey building with plan "A", R_d=3, Site Class B.

The current study also presents the finding when a building with smaller floor area labelled plan "B", corresponding to $L/B = 2$, is investigated under the earthquake and wind load. Herein, the 12-storey, 10-storey and 8-storey MD-CBF buildings located in Montreal on Site Class C (**Figure 6.17** to **Figure 6.19**) and Site Class B (**Figure 6.20** to **Figure 6.22**) are considered.
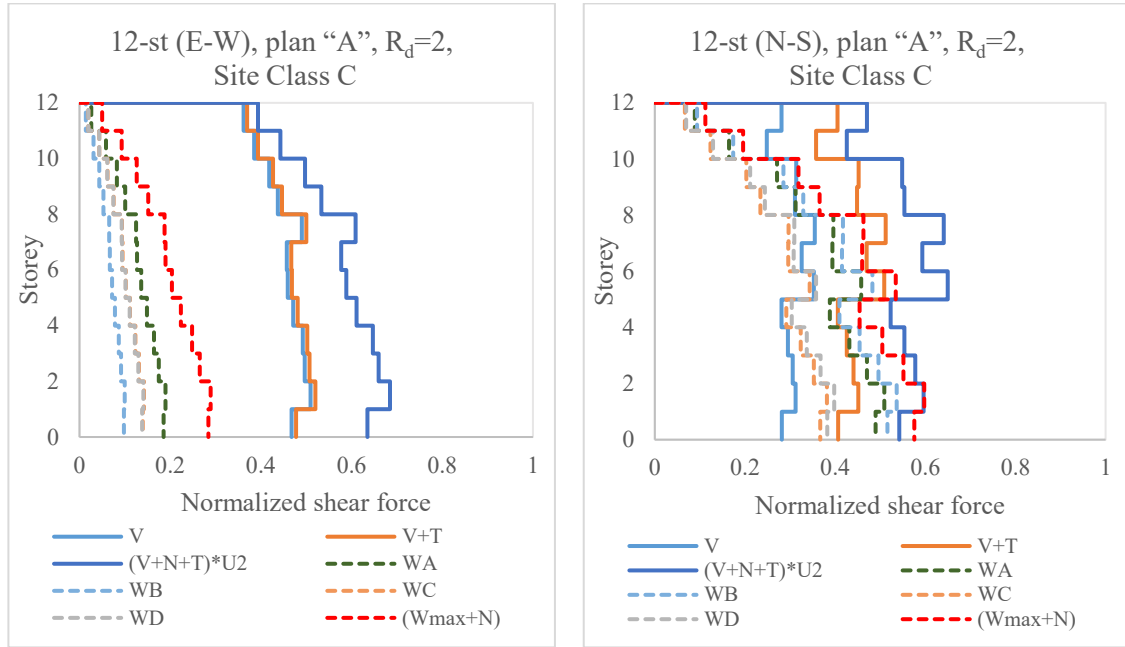
Figure 6.17: Normalized shear force distribution of the 12-storey building with plan "B", R_d=3, Site Class C.
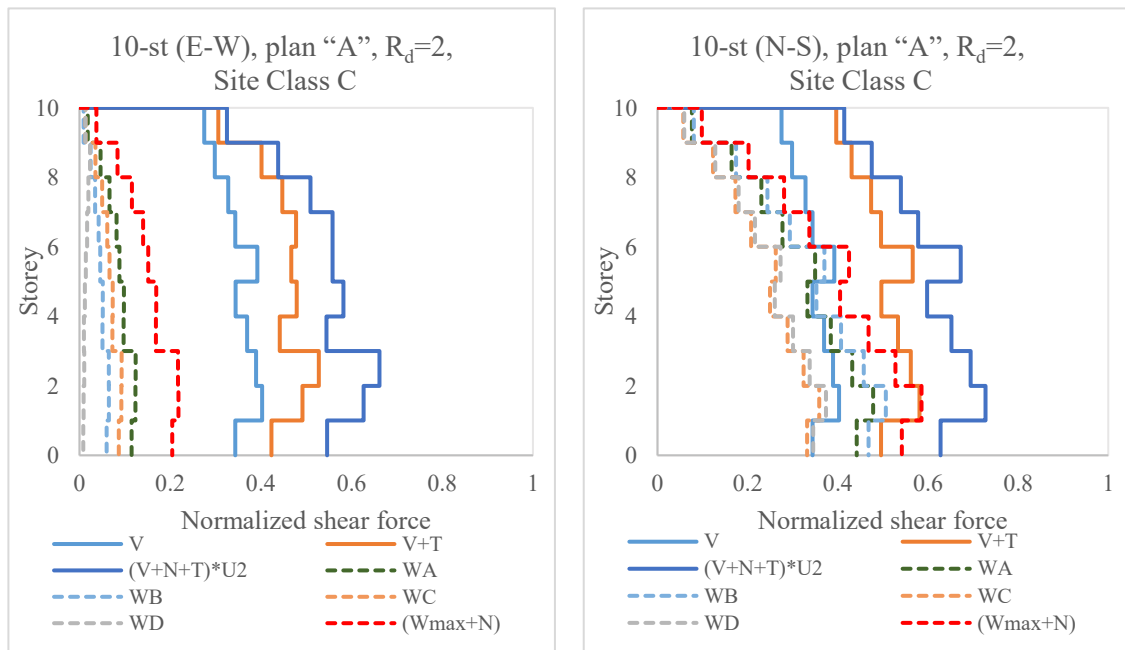

Figure 6.18: Normalized shear force distribution of the 10-storey building with plan "B", R_d=3, Site Class C.
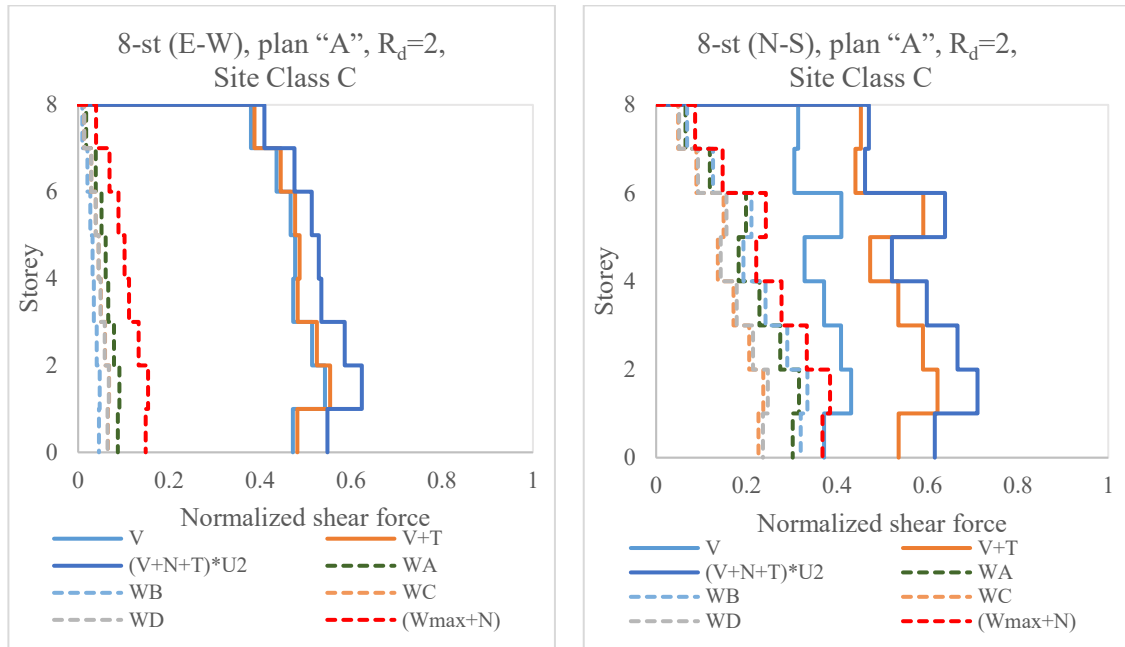
Figure 6.19: Normalized shear force distribution of the 8-storey building with plan "B", R_d=3, Site Class C.

Figure 6.20: Normalized shear force distribution of the 12-storey building with plan "B", R_d=3, Site Class B.

Figure 6.21: Normalized shear force distribution of the 10-storey building with plan "B", $R_d=3$, Site Class B.

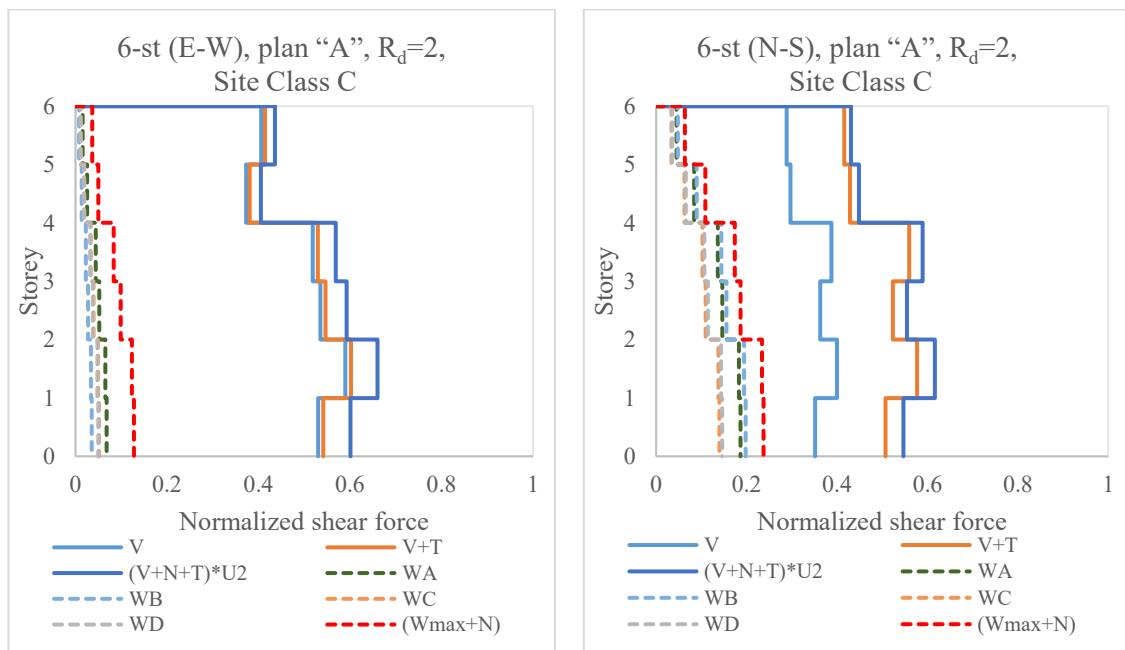**Figure 6.22:** Normalized shear force distribution of the 8-storey building with plan "B", $R_d=3$, Site Class B.

As illustrated in **Figure 6.17** and **Figure 6.18**, the ratio of normalized shear caused by wind loads is larger than that resulted from earthquake design in most of the floors. However, the ratio is smaller than 1.0. The same conclusions are also true for the 10-storey building located on Site Class B and illustrated in **Figure 6.21**. The most critical case is the 12-storey building located on Site Class B (**Figure 6.20**) where the ratios are greater than 1 at the bottom four floors. However, in the cases presented above, the normalized storey shear force of a CBF with tension-compression braces to the horizontal projection of braces' compressive and tensile resistances is not significant in the inelastic range after the buckled braces lost their compression strength. Therefore, although the ratio is higher than 1, no conclusions can be made about adjusting the cross-section of braces. This matter is discussed in detail in the following section.

6.2.2. Shear Distributions Normalized to Braces' Compressive Resistance

When ductility is considered in design and braces are sized to behave in tension-compression, they should comply to the following criteria: $C_f \leq C_r$ and $T_f \leq T_r$ where C_f and T_f are the factored compressive and tensile forces, respectively triggered in braces. However, only the former is critical to the brace design. In this section, the shear force resulted from earthquake design and wind load cases is normalized to the horizontal projection of $2 \times C_r$ as follows:

$$\frac{V}{2C_r cos\alpha} \tag{6-2}$$

The earthquake shears are presented separately in terms of V_d; then V_d plus shear due to notional lateral load, torsion and P-Δ as $(V_d + N) \times U_2$ and $(Vd + T + N) \times U_2$. Only the

normalized shear due to wind load Cases A and B are provided as they are dominant wind load cases. Braces are required to behave in elastic range under wind load, therefore, when the ratio of normalized shear force is greater than 1, the corresponding brace's cross-section needs to be increased.

Figure 6.23 to **Figure 6.27** show the comparisons between the normalized shear resulted from earthquake and wind loads for the 12-storey, 10-storey, 8-storey, 6-storey and 4-storey building with plan "A", $R_d = 2$, on Site Class C. In E-W direction, the earthquake load governs the design. In N-S direction, wind-induced shear has approached that from earthquake load in the 1st floor of the 12-storey building. However, no changes in brace cross-sections are required to assure elastic behaviour under wind loads as in all cases, the ratio is smaller than 1.
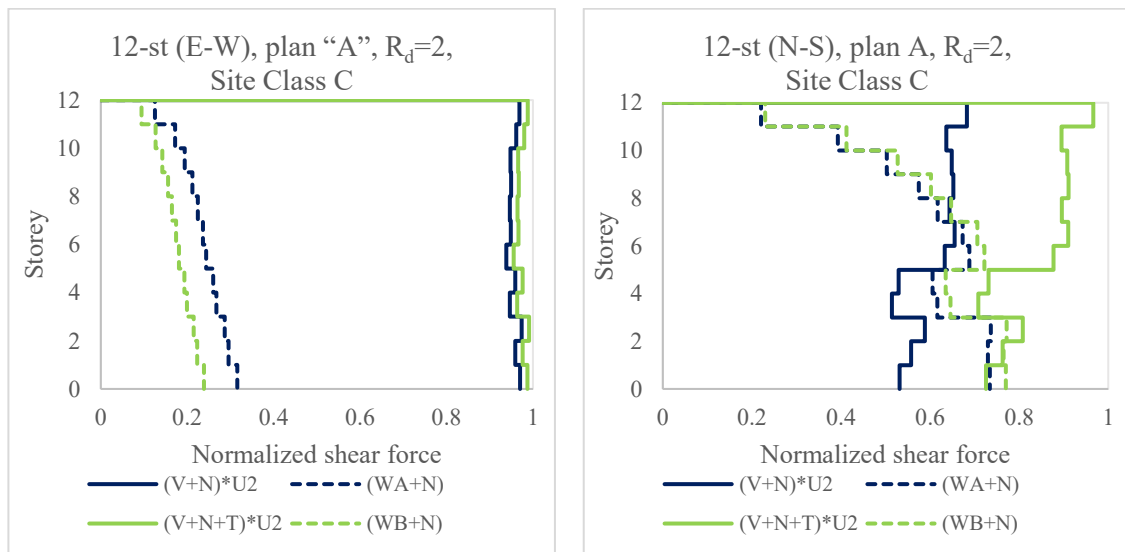
Figure 6.23: Normalized shear force distribution of the 12-storey building with plan "A", R_d=2, Site Class C.
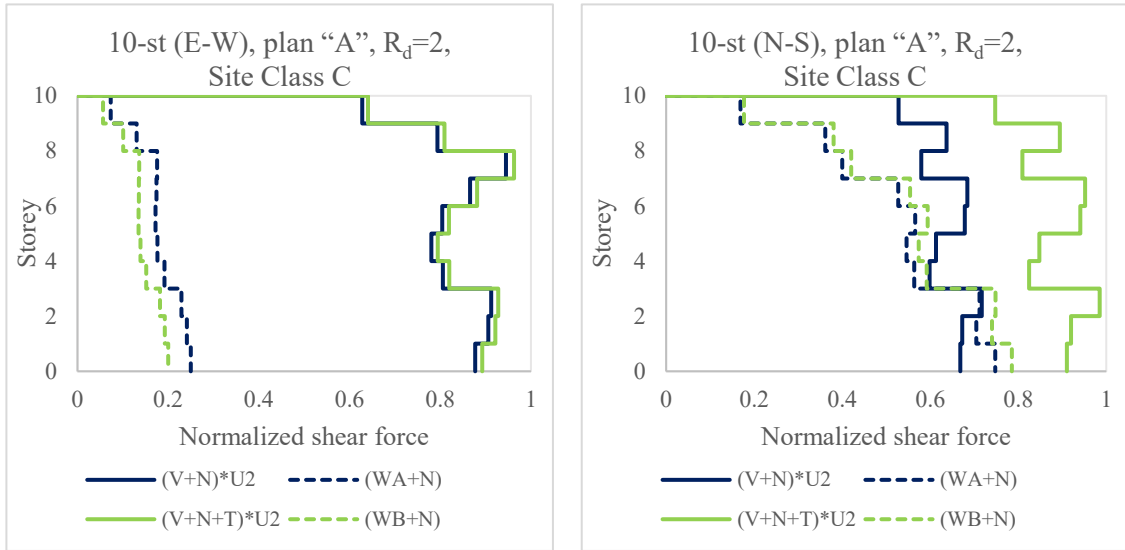
Figure 6.24: Normalized shear force distribution of the 10-storey building with plan "A", $R_d=2$, Site Class C.
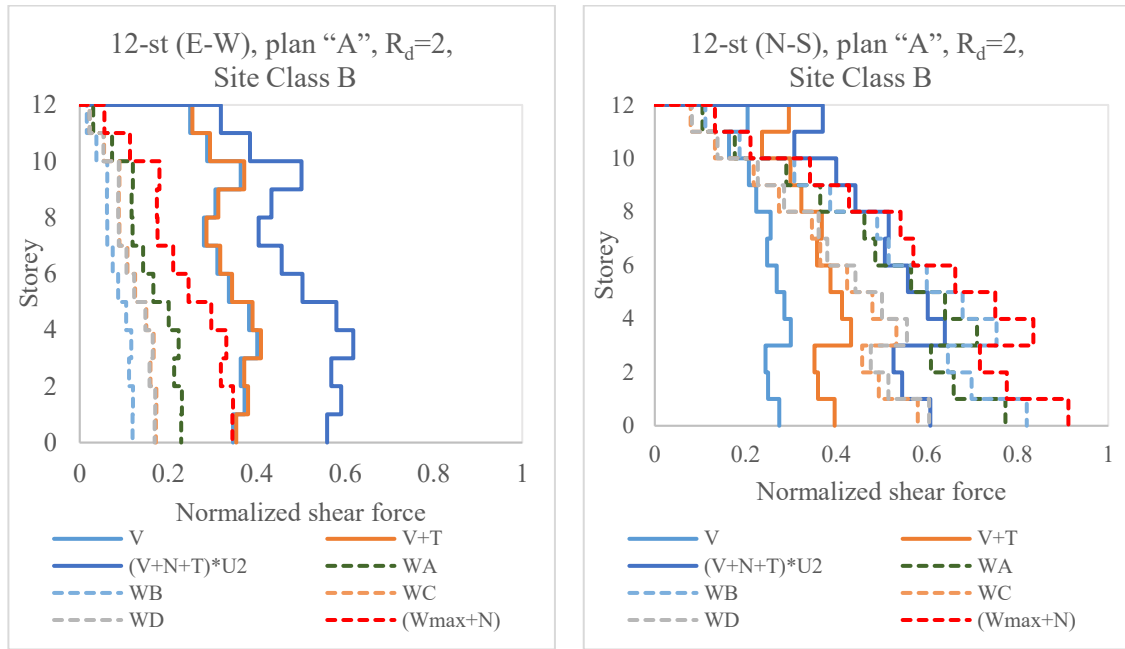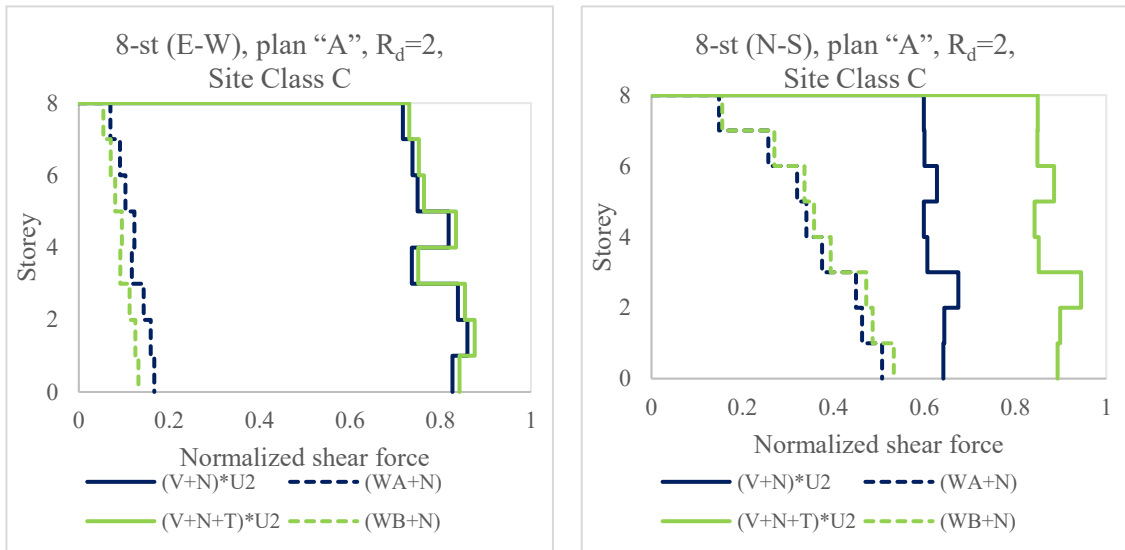

Figure 6.25: Normalized shear force distribution of the 8-storey building with plan "A", $R_d=2$, Site Class C.
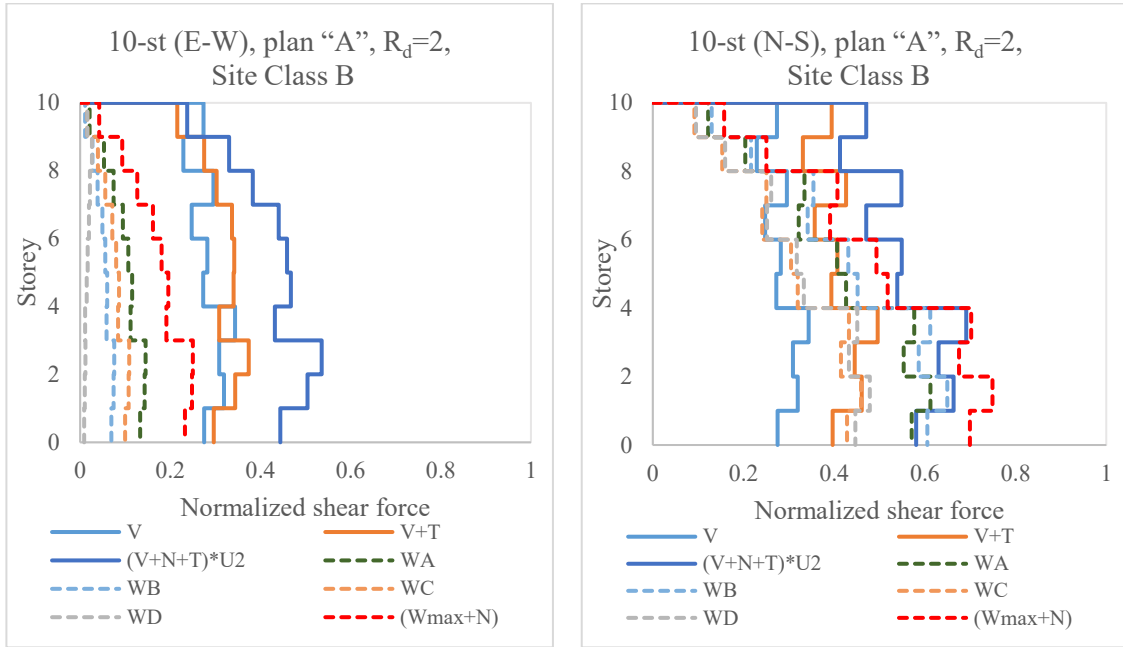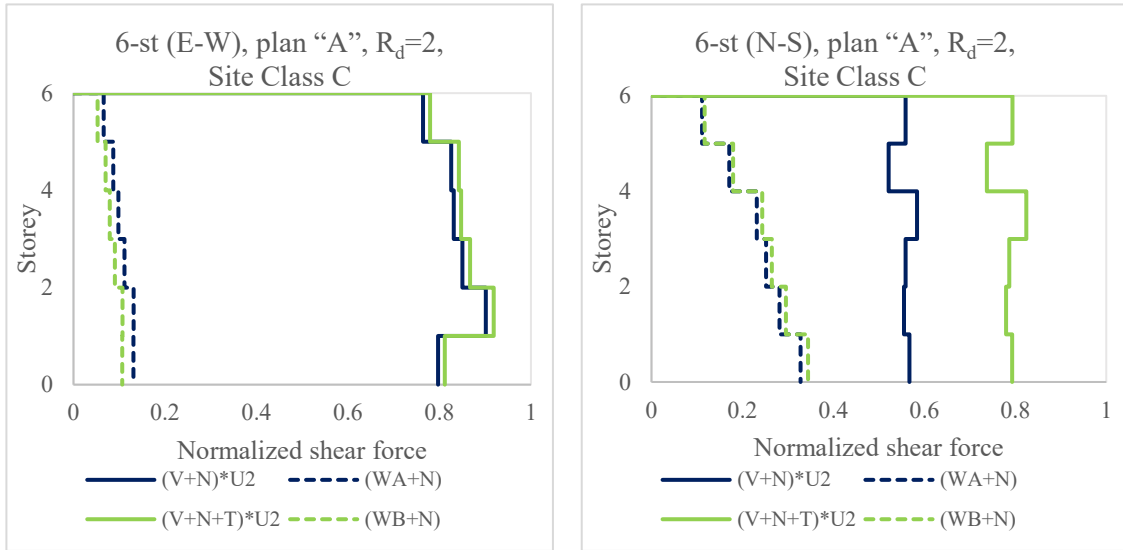
Figure 6.26: Normalized shear force distribution of the 6-storey building with plan "A", R_d=2, Site Class C.
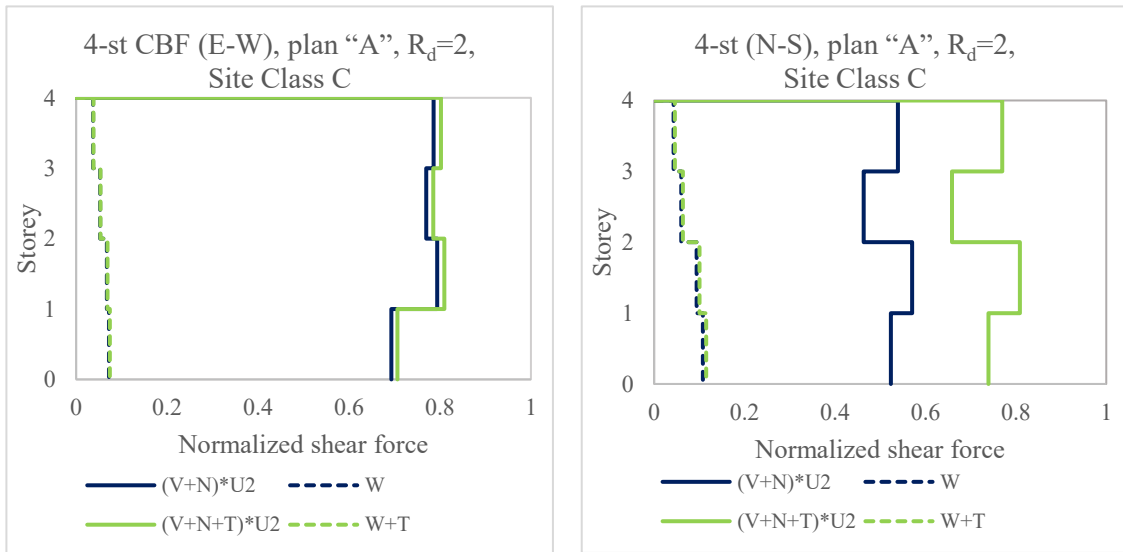
Figure 6.27: Normalized shear force distribution of the 4-storey building with plan "A", R_d=2, Site Class C.

The same 12-storey, 10-storey, 8-storey, 6-storey and 4-storey buildings with moderately ductile CBF ($R_d = 3$) are considered and the normalized shear along the building height is

showed in **Figure 6.28** to **Figure 6.32**. In general, the wind demand increases comparing to that of earthquake. However, no adjustment in brace sizes is needed for MD-CBF located in E-W direction. For the N-S direction, the size of ground floor braces of the 12-storey and 10-storey building need to be increased to assure elastic response under the wind load (**Figure 6.28** and **Figure 6.29**).
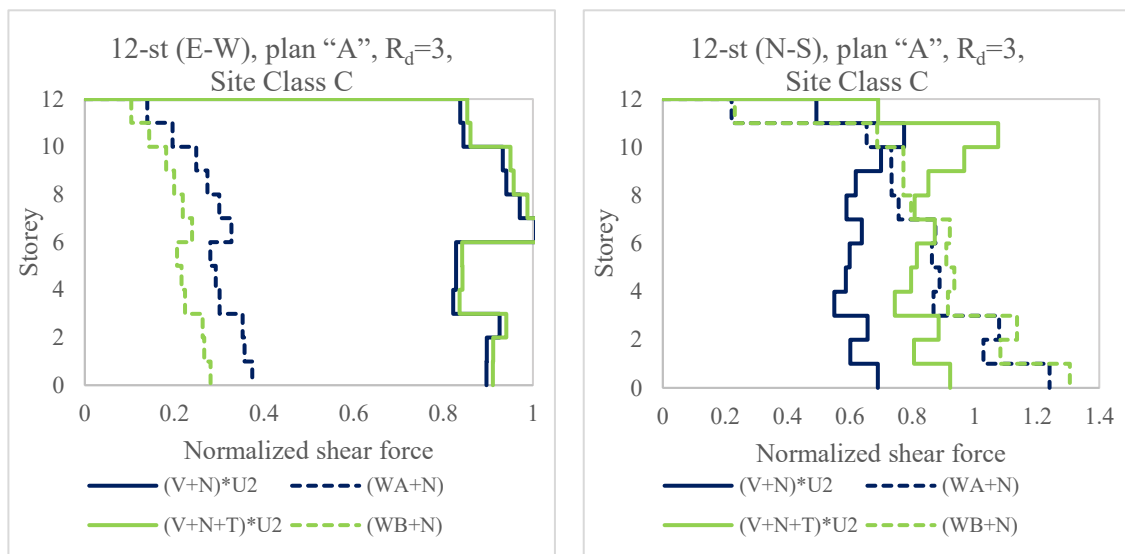
Figure 6.28: Normalized shear force distribution of the 12-storey building with plan "A", R_d=3, Site Class C.
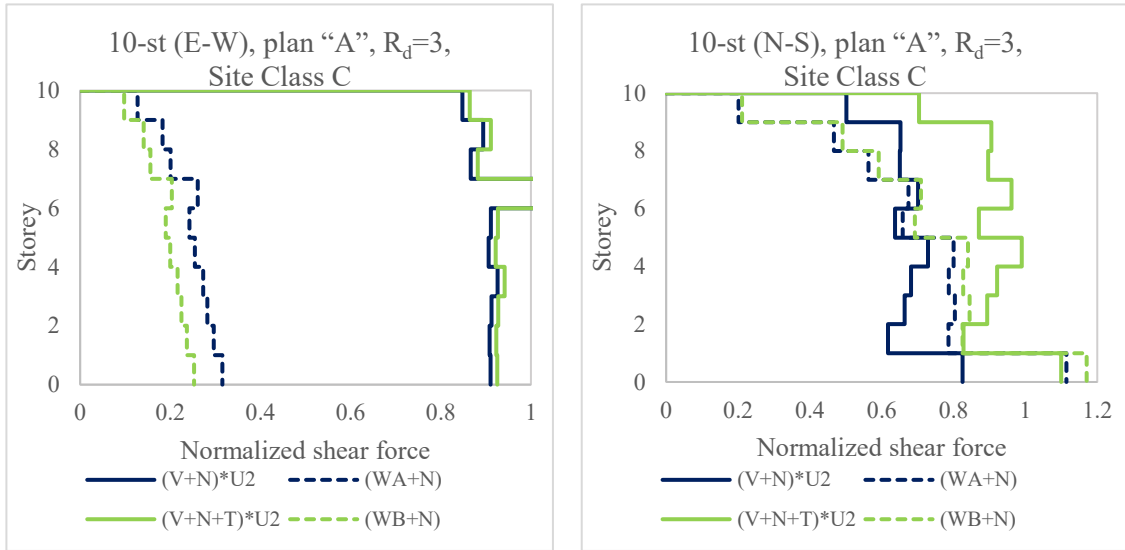
Figure 6.29: Normalized shear force distribution of the 10-storey building with plan "A", R_d=3, Site Class C.
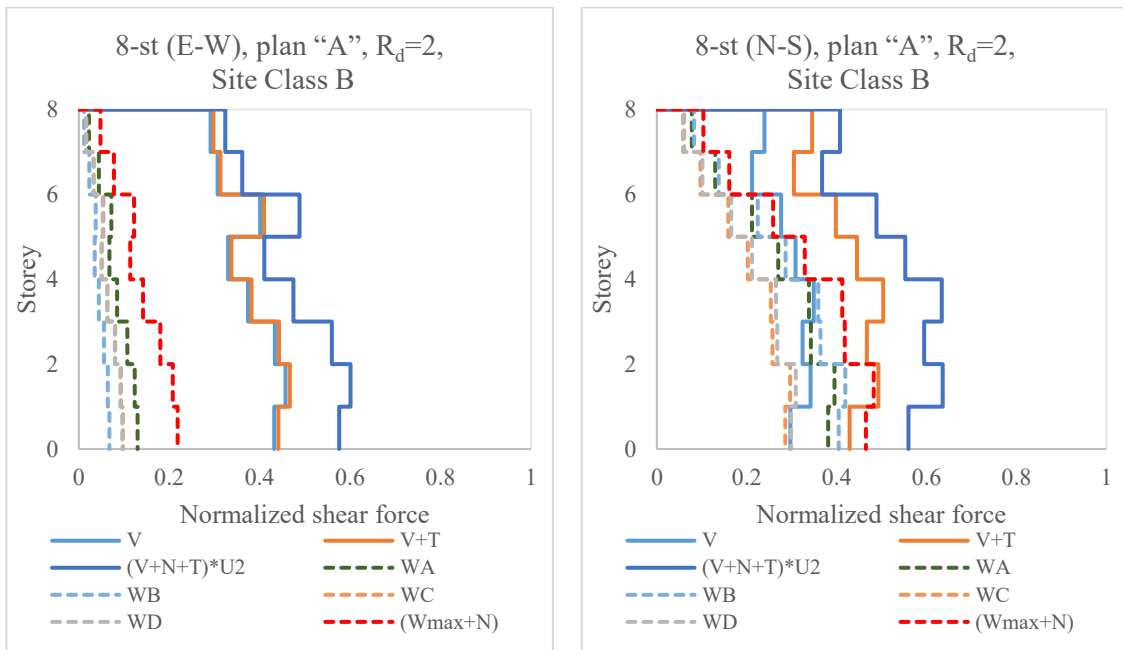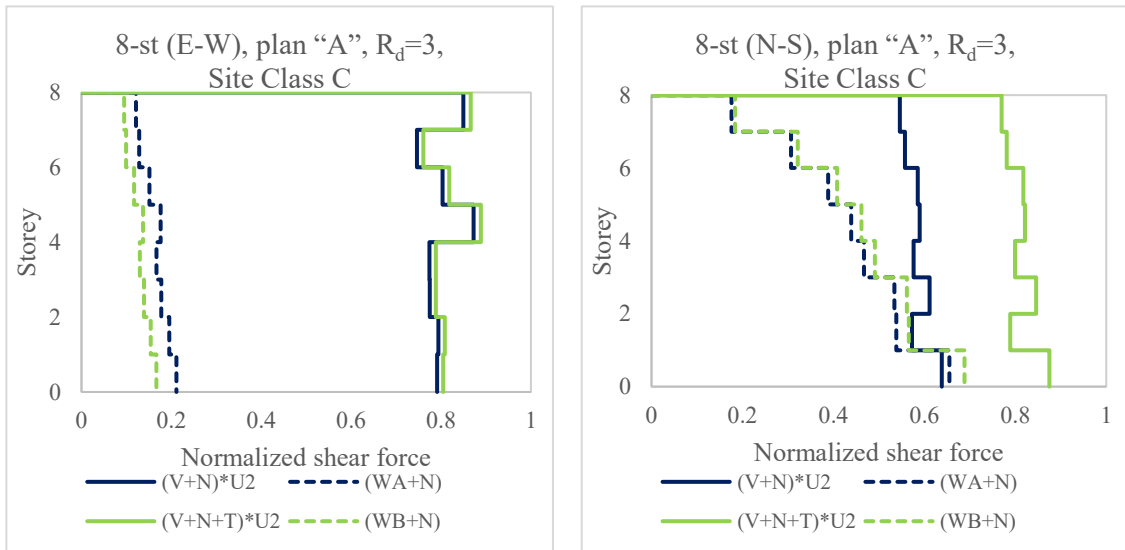

Figure 6.30: Normalized shear force distribution of the 8-storey building with plan "A", R_d=3, Site Class C.
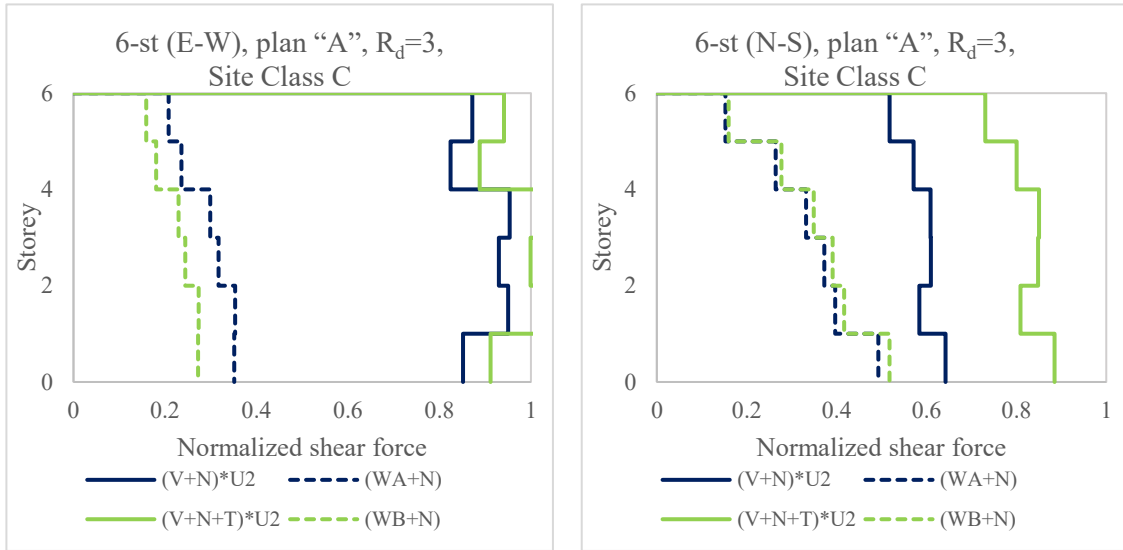
Figure 6.31: Normalized shear force distribution of the 6-storey building with plan "A", R_d=3, Site Class C.
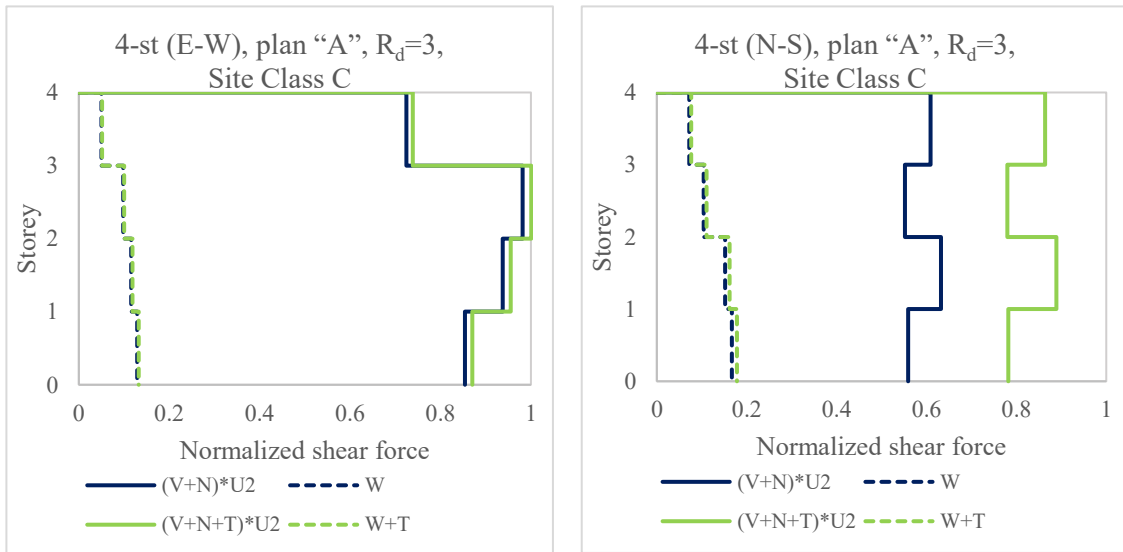
Figure 6.32: Normalized shear force distribution of the 4-storey building with plan "A", R_d=3, Site Class C.

The normalized shear force distribution of the 12-storey, 10-storey and 8-storey buildings with plan "A", $R_d = 2$, located on Site Class B are exhibited in **Figure 6.33**, **Figure 6.34**

and **Figure 6.35**. The wind demand increases compared to the previous cases. Again, the braces of LD-CBF in E-W direction behave in elastic range when subjected to wind load. However, braces in the five bottom floors of the 12-storey buildings and three bottom storeys of the10-storey buildings, in N-S direction, need to be substantially increased to behave elastically under the wind load.
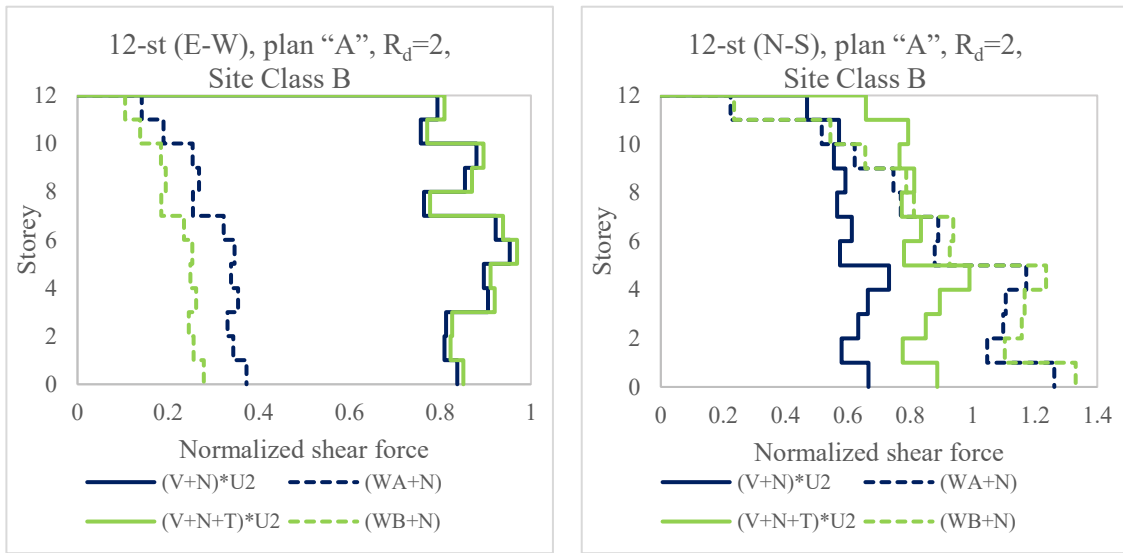
Figure 6.33: Normalized shear force distribution of the 12-storey building with plan "A", R_d=2, Site Class B.
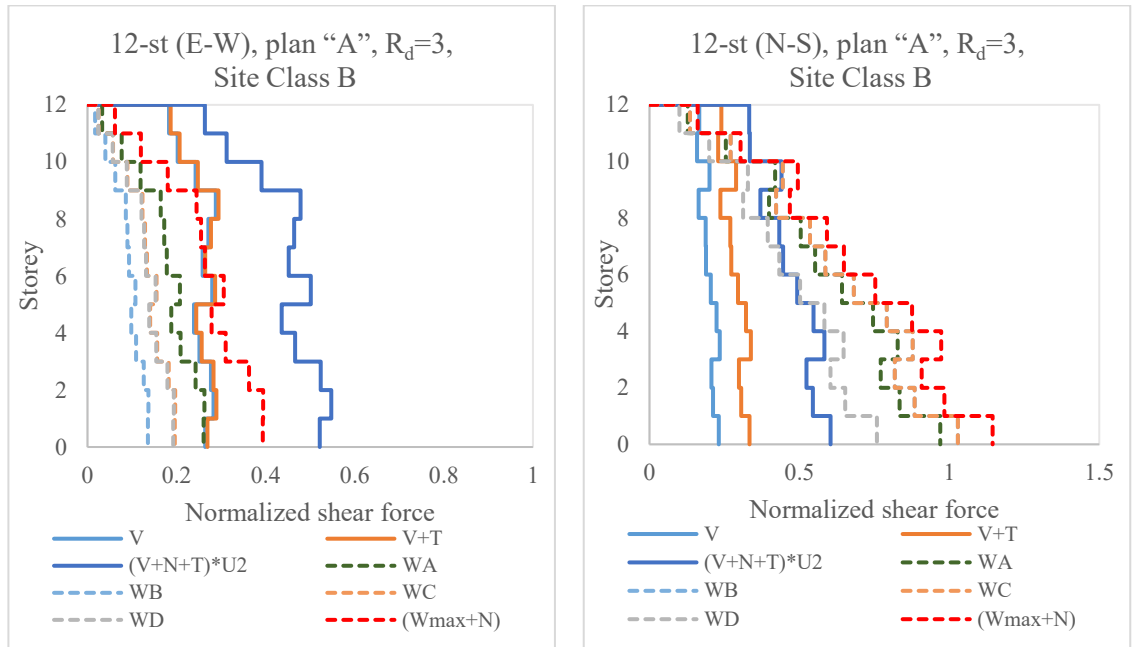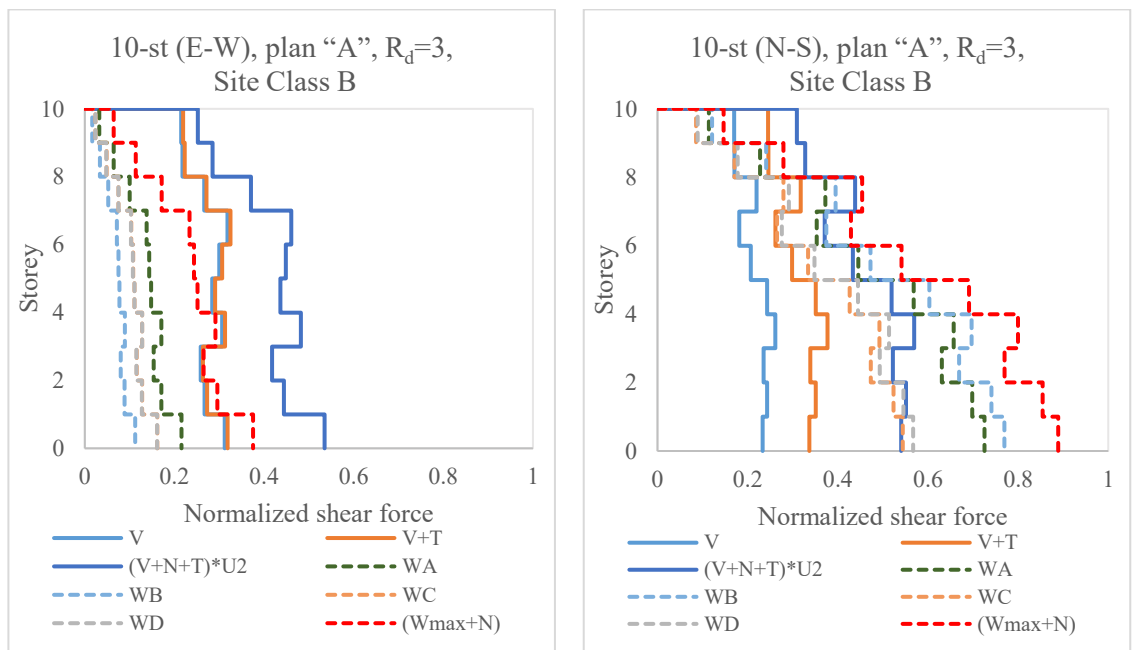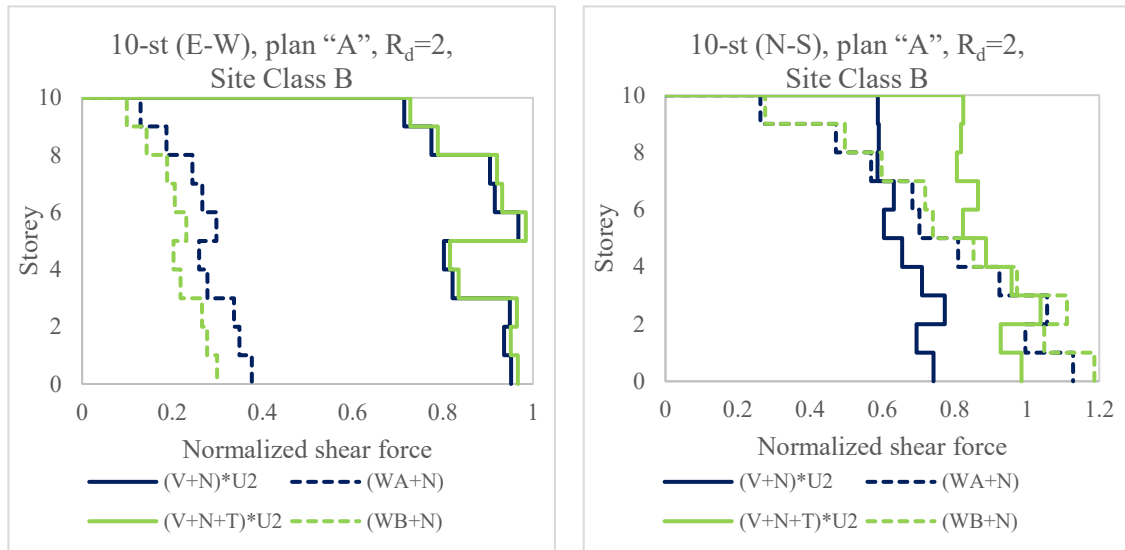
Figure 6.34: Normalized shear force distribution of the 10-storey building with plan "A", R_d=2, Site Class B.
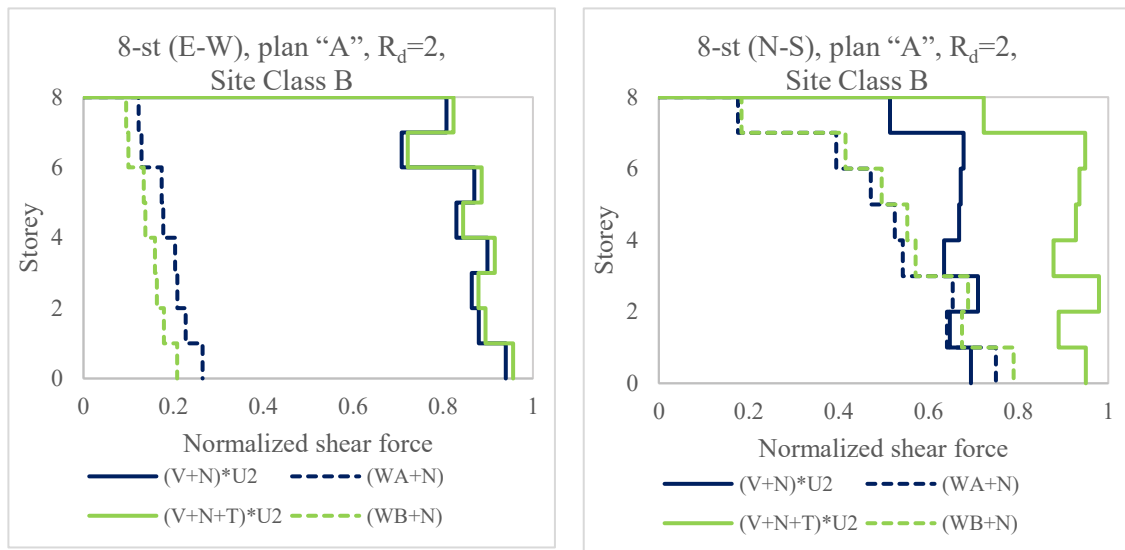
Figure 6.35: Normalized shear force distribution of the 8-storey building with plan "A", R_d=2, Site Class B.

Figure 6.36 to **Figure 6.38** show the normalized shear distribution of the 12-storey, 10-storey and 8-storey buildings with plan "A", $R_d = 3$, located on Site Class B. As illustrated

in **Figure 6.36**, brace cross-sections of all floors but three top floors of the 12-storey building (N-S) need to be increased due to wind load demand. Great attentions should be given to bottom floor where wind load is almost double than the brace's compressive resistance. In the case of 10-storey building, in N-S direction, excepting the top three floors, the brace sizes of all bottom floor levels need to be increased (**Figure 6.37**). For the 8-storey building (N-S direction) only the brace of the 1st storey should be slightly increased.
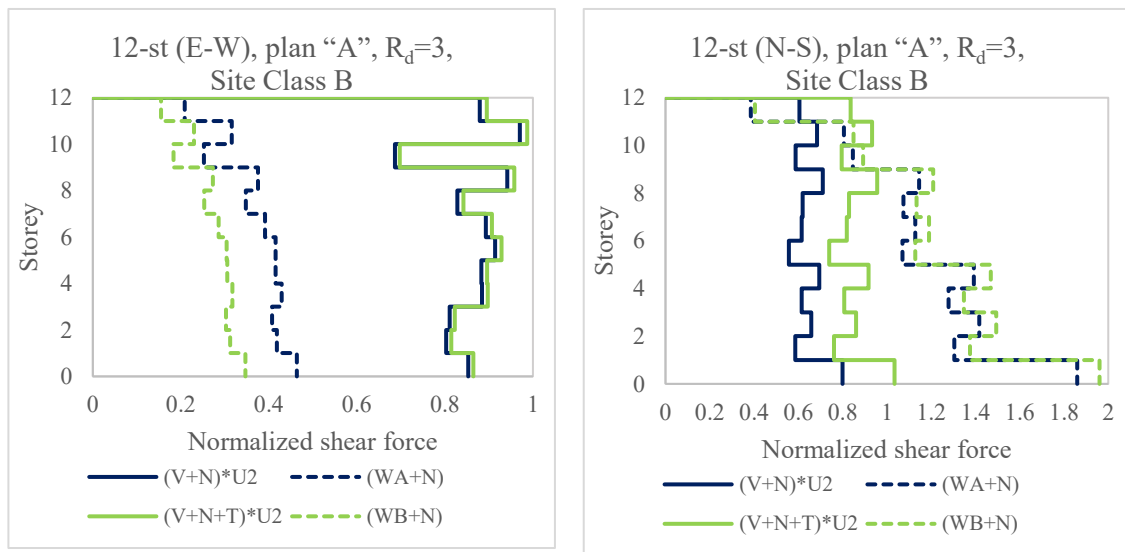
Figure 6.36: Normalized shear force distribution of the 12-storey building with plan "A", R_d=3, Site Class B.
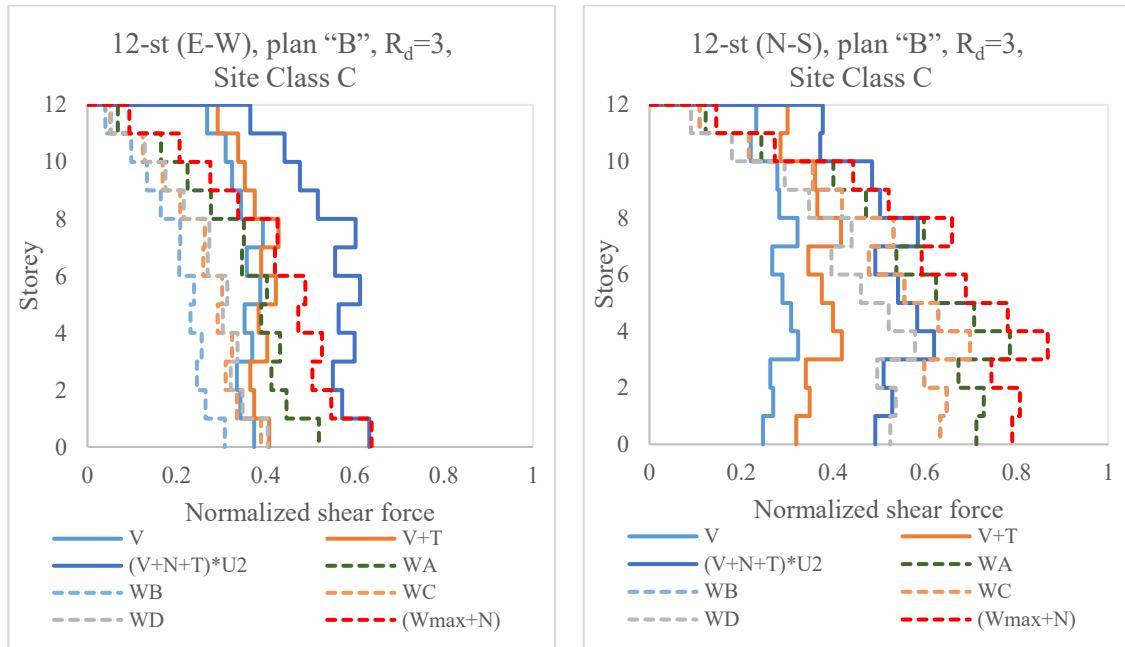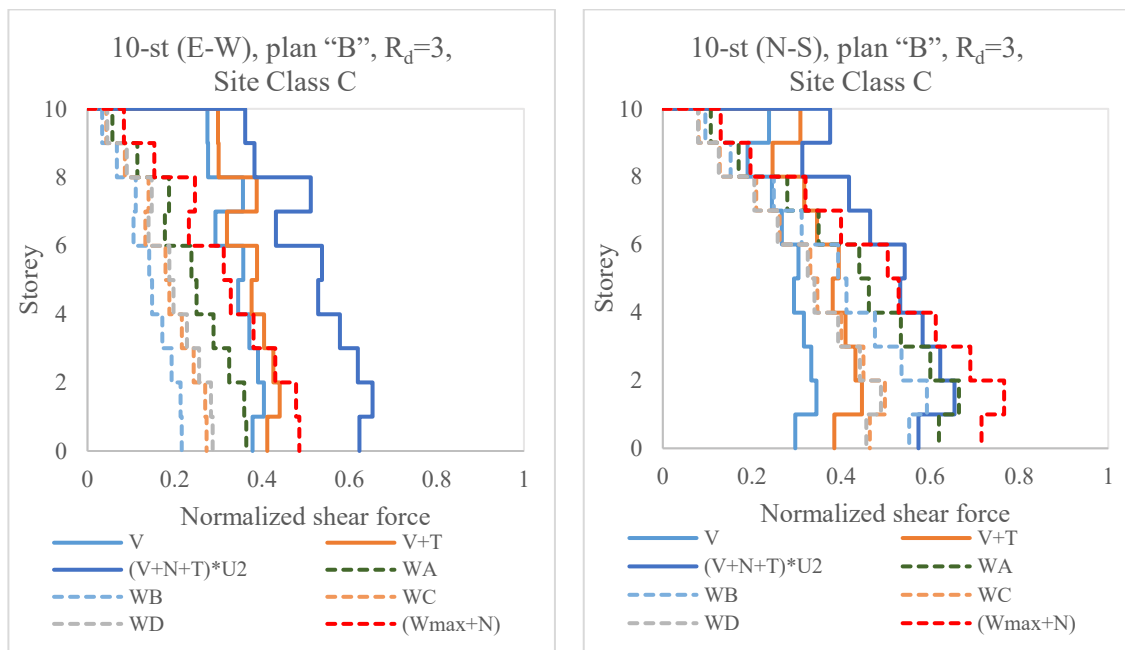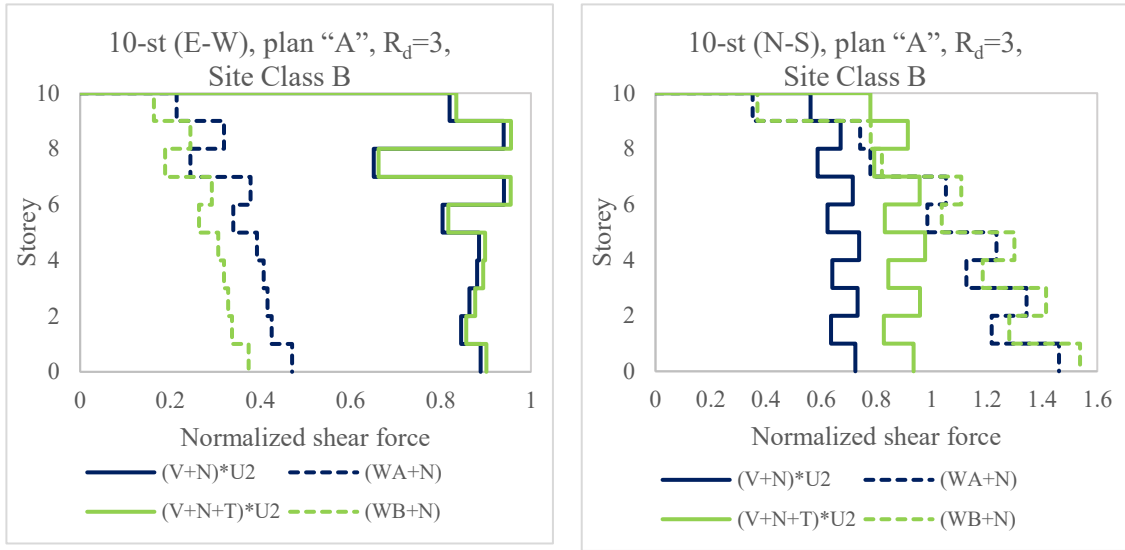
Figure 6.37: Normalized shear force distribution of the 10-storey building with plan "A", R_d=3, Site Class B.
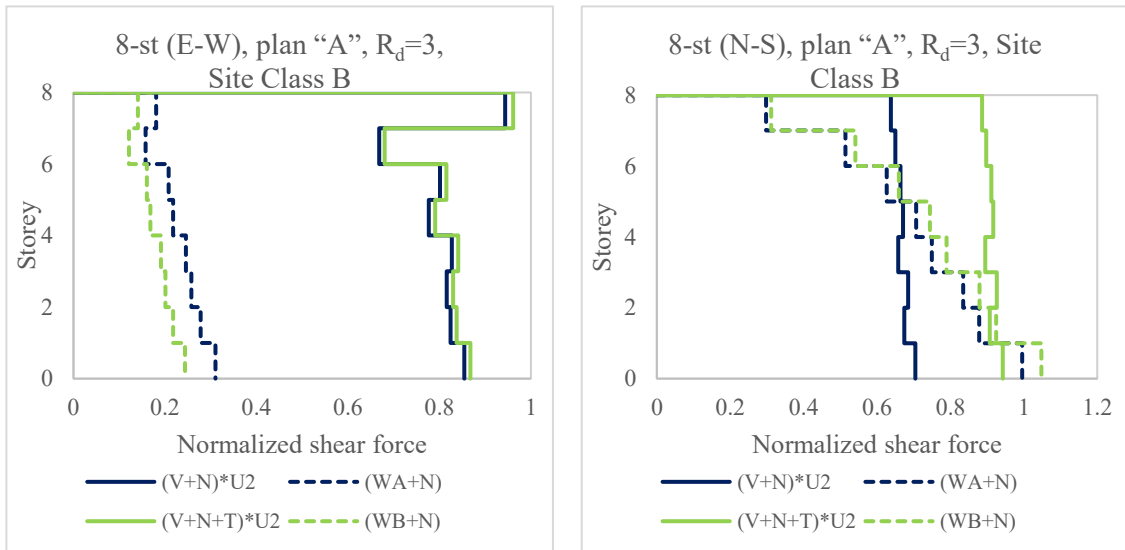
Figure 6.38: Normalized shear force distribution of the 8-storey building with plan "A", R_d=3, Site Class B.

The normalized shear distribution of the 12-, 10- and 8-storey buildings with plan "B", $R_d = 3$, on Site Class C are illustrated in **Figure 6.39** to **Figure 6.41** and that resulted from the same buildings located on Site Class B is given in **Figure 6.42** to **Figure 6.44**.
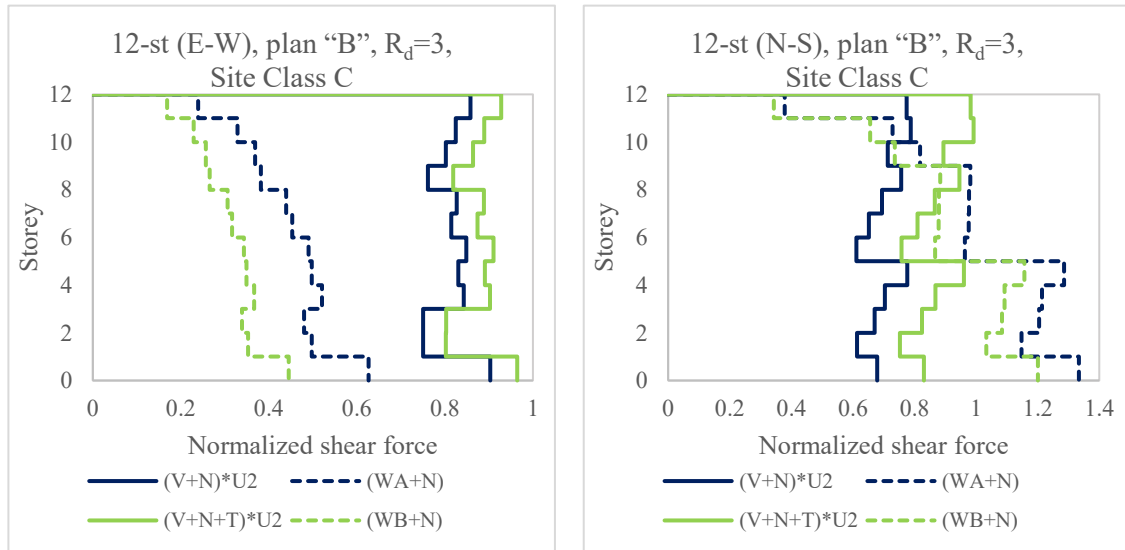
Figure 6.39: Normalized shear force distribution of the 12-storey building with plan "B", R_d=3, Site Class C.
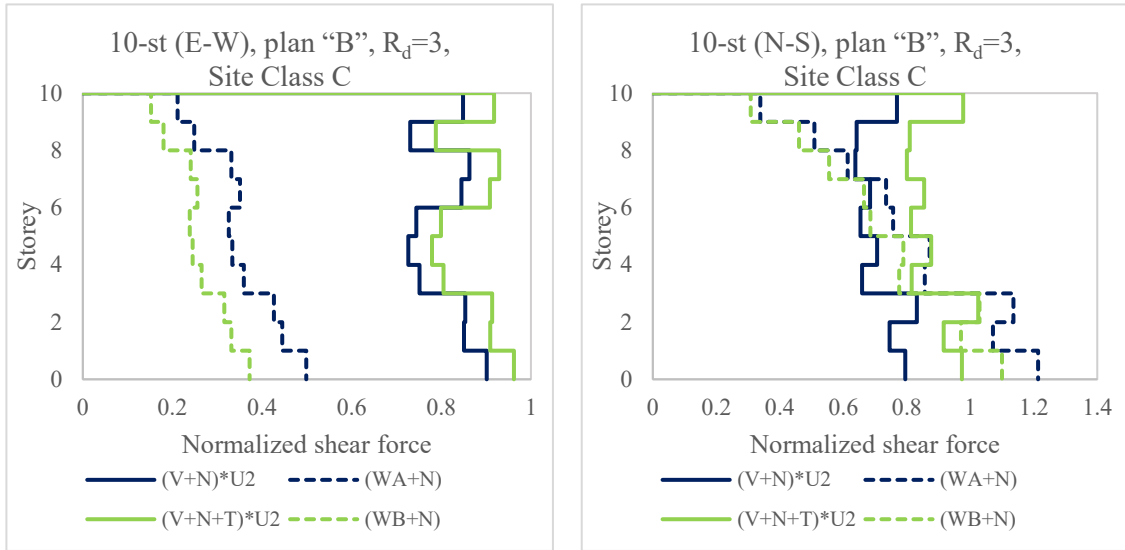
Figure 6.40: Normalized shear force distribution of the 10-storey building with plan "B", $R_d=3$, Site Class C.
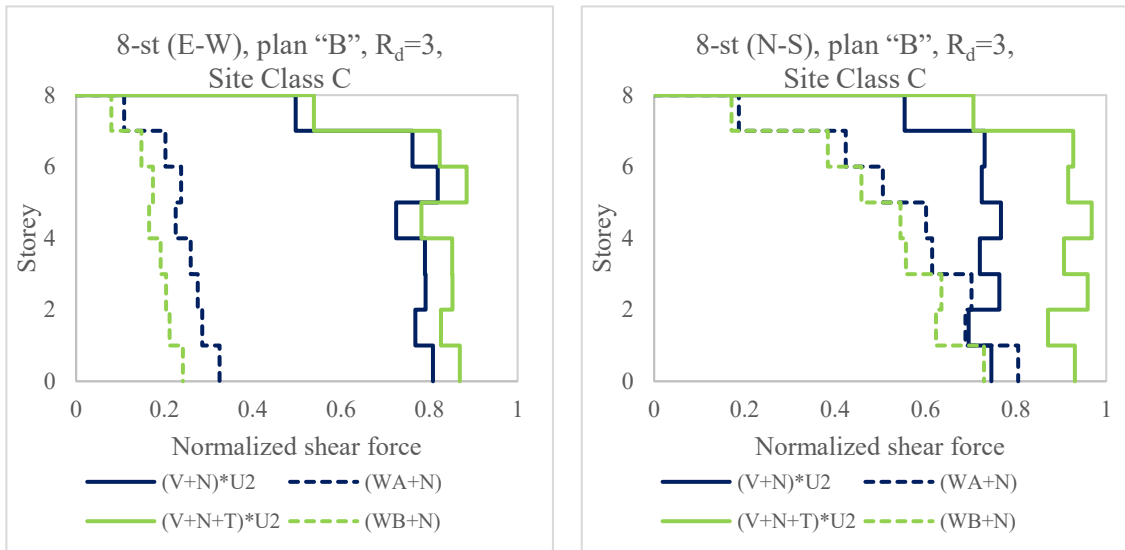
Figure 6.41: Normalized shear force distribution of the 8-storey building with plan "B", $R_d=3$, Site Class C.
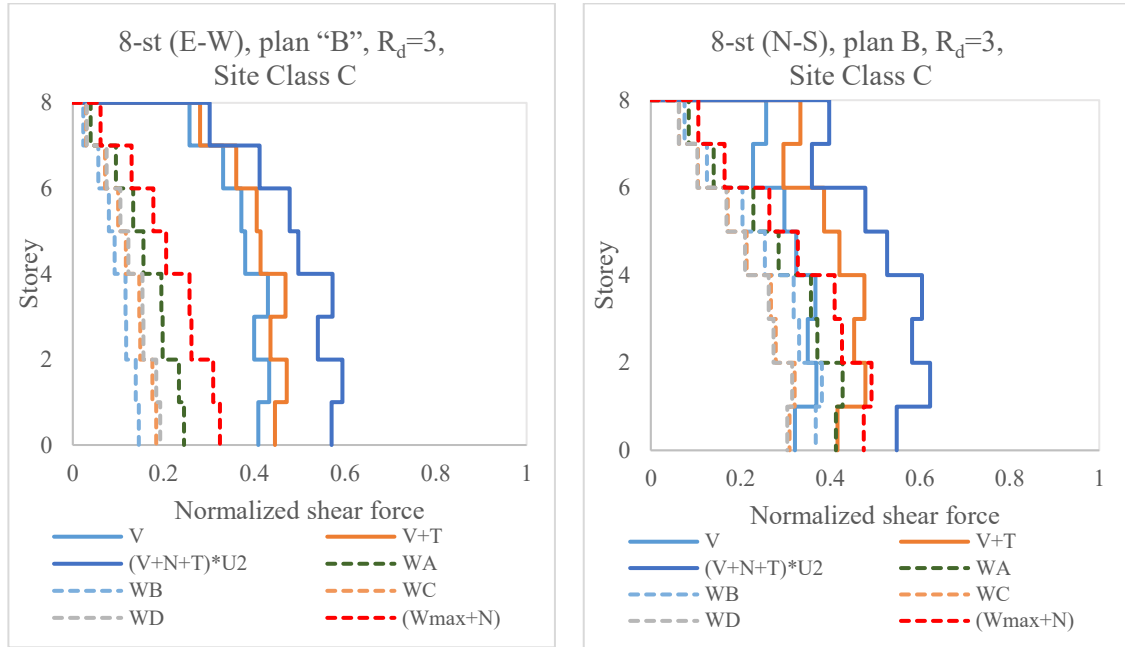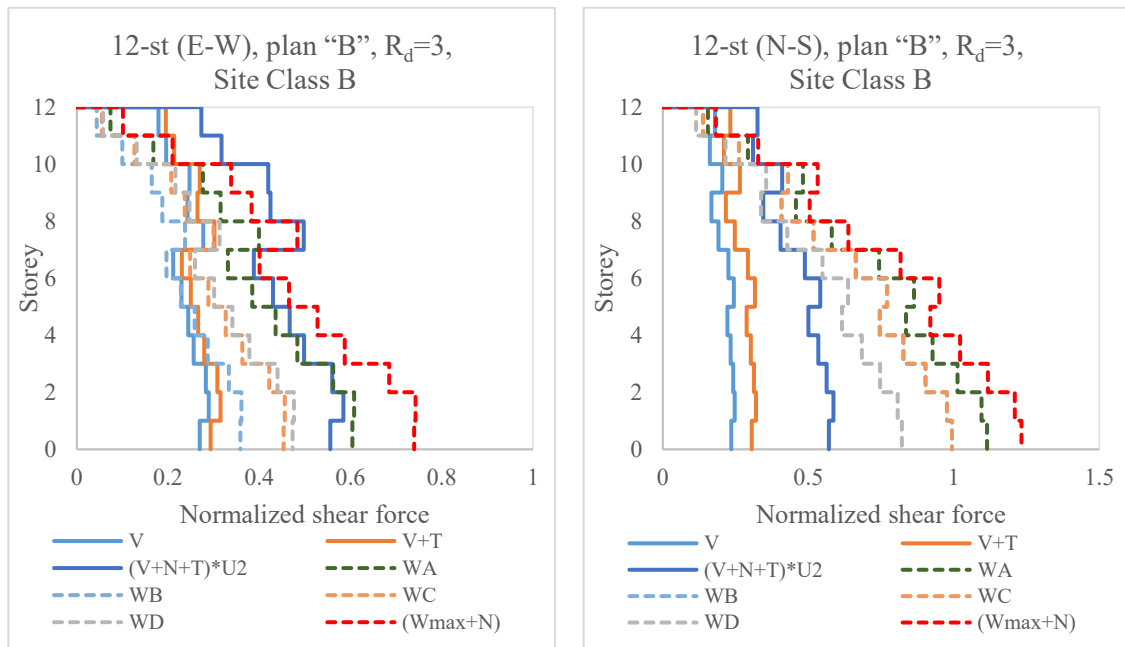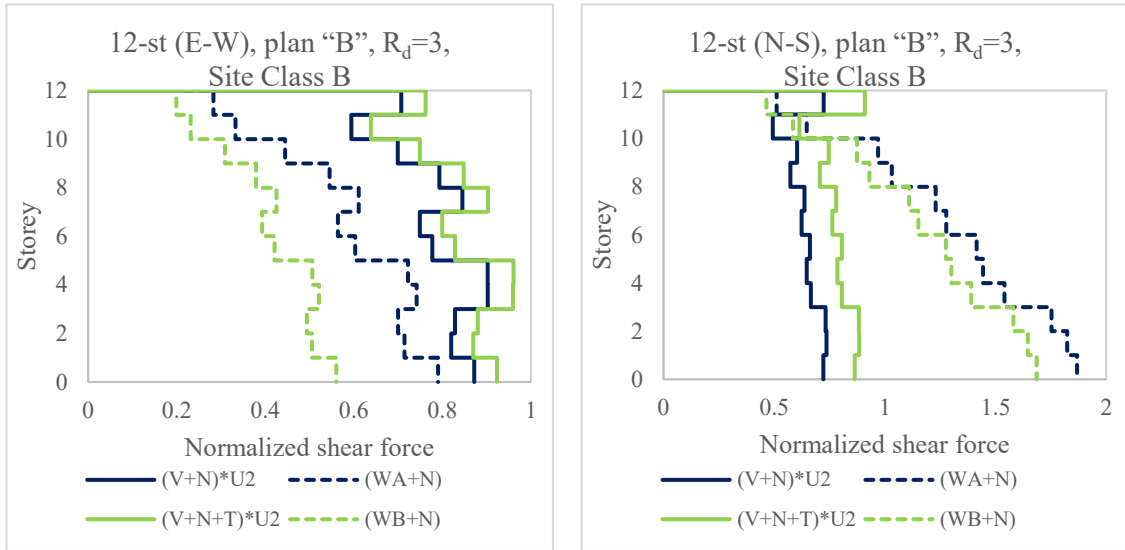
Figure 6.42: Normalized shear force distribution of the 12-storey building with plan "B", R_d=3, Site Class B.
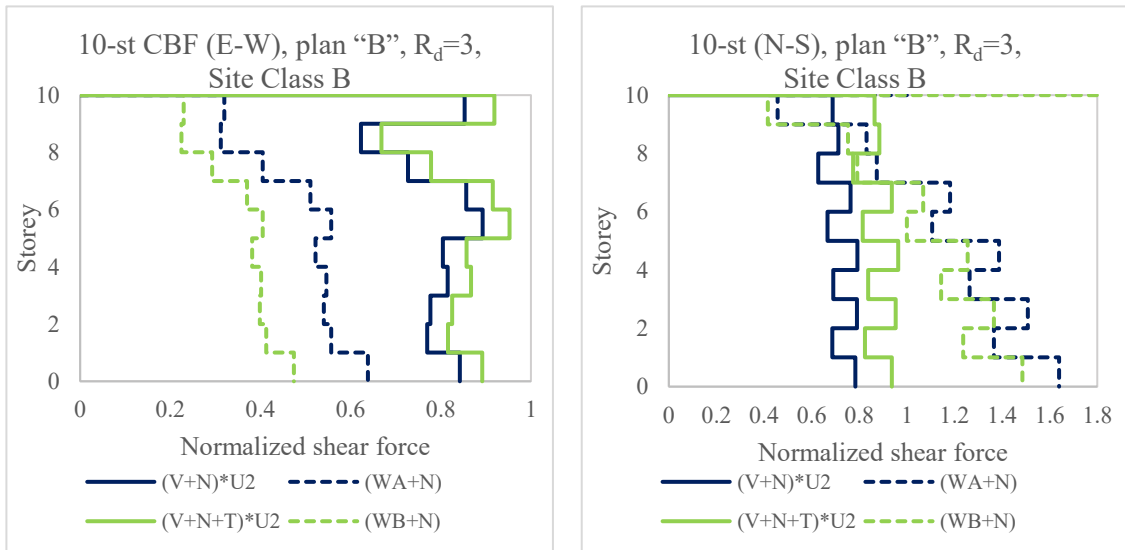
Figure 6.43: Normalized shear force distribution of the 10-storey building with plan "B", R_d=3, Site Class B.

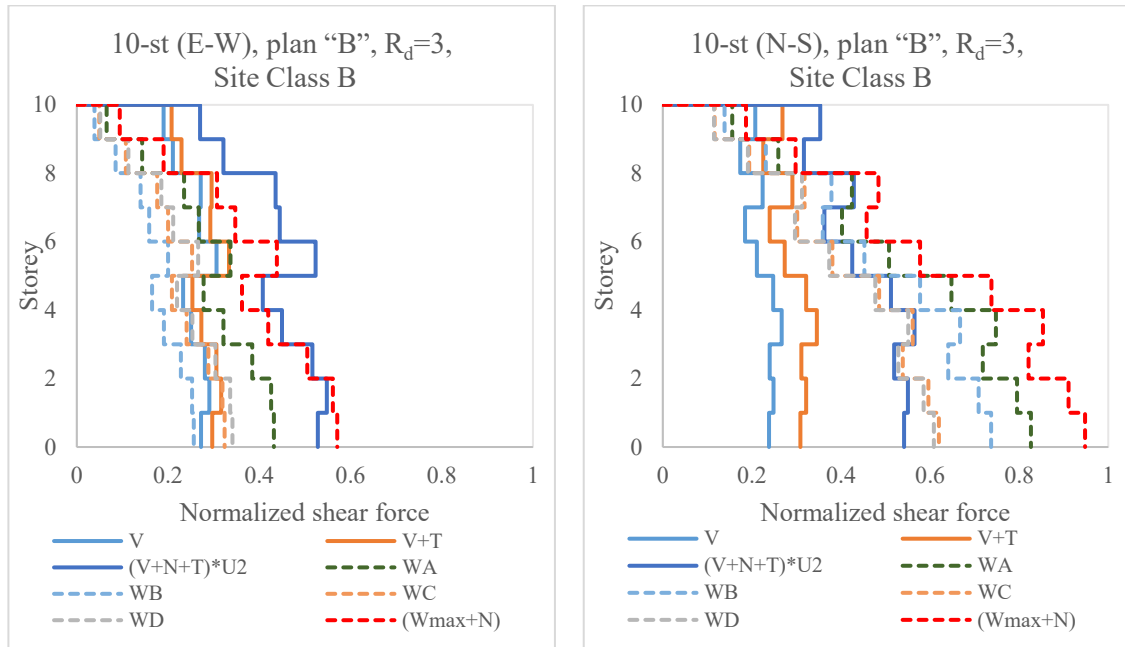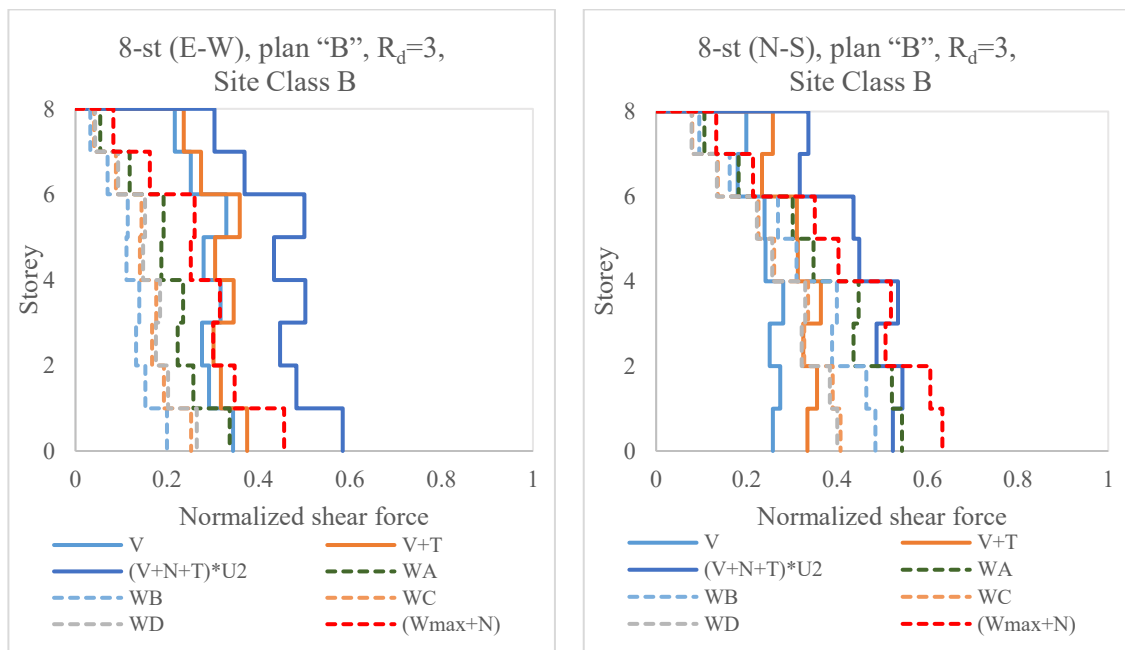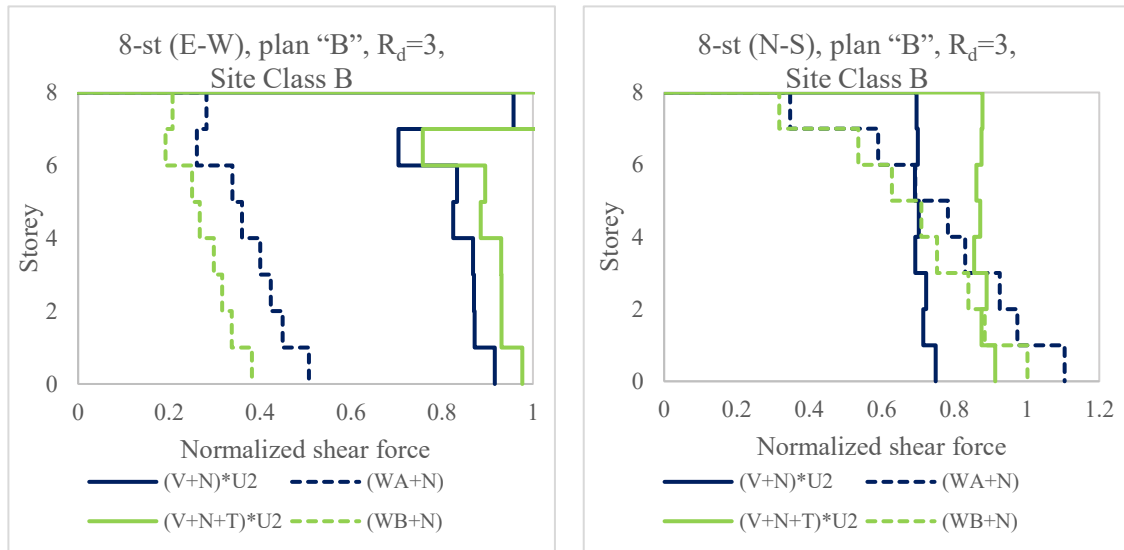**Figure 6.44:** Normalized shear force distribution of the 8-storey building with plan "B", R_d=3, Site Class B.

In these figures (**Figure 6.39** to **Figure 6.44**), there is no brace modifications needed in E-W direction. In N-S direction, in the case of 12- and 10-storey buildings, the bottom floor braces require larger size to behave elastically under wind load. The braces of the 8-storey building (N-S) respond adequately for both earthquake and wind loads. The trend observed for these buildings is more pronounced when they are located on Site Class B. Modifications of brace sizes at bottom floors are only required for 12-storey and 10-storey CBFs placed in N-S direction. The most critical case are the braces of the 1st floor where the wind-induced demand requires brace sizes double than brace's compression resistance resulted from earthquake design.

6.3. DEFLECTION VERIFICATION UNDER EARTHQUAKE AND WIND LOADS

After the strength criterion was verified, the verification of serviceability limit state, expressed in terms of interstorey drift, is discussed herein. According to NBCC 2015, buildings with ordinary occupancy type are restricted to interstorey drift less than $2.5\%h_s$, where h_s is the storey height, when subjected to earthquake load. Meanwhile, the interstorey drift deflection under wind load is limited to $h_s/500$. However, depending on the facade's material, this limit can decrease to $h_s/400$ or $0.25\%h_s$. As a result, the acceptable lateral deflection is 10 times lower in the case of wind action than earthquake action. It is noted that the importance factor for wind load, I_W, for serviceability limit state is 0.75. All interstorey drift values resulted from ETABS output for earthquake design were multiplied by $R_d R_o/I_E$ to take into account the inelastic action.

In the following figures (**Figure 6.45** to **Figure 6.48**), the identification of studied buildings is abbreviated as follow: the type of load considered (e.g. wind or earthquake), storey number, plan type, Site Class, type of CBF's ductility level (e.g. R_d = 2 or R_d = 3) and the direction of loading. For example, the notation provided in the legend of **Figure 6.45** (e.g. W,12-A-C-2,W-E) means the wind-induced interstorey drifts on the 12-storey building with plan "A" located on Site Class C, which has LD-CBF (R_d = 2) as lateral load resisting system and the direction of loading is W-E.

The interstorey drift along the building height resulted under wind and earthquake loads for the 12-storey buildings in both E-W and N-S directions is illustrated in **Figure 6.45**. As shown in the figure, the peak interstorey drifts under earthquake load is about $1.6\%h_s$ (N-

S direction) and $1.0\%h_s$ (E-W direction). These interstorey drift values resulted for the 12-storey MD-CBF building with plan "A", located on Site Class B. Under wind loads, all 12-storey buildings yield the interstorey drifts that exceed the code limit in N-S direction by 20% to 40%. In the E-W direction, in all cases, the interstorey drift under wind load is within the code limit of $0.25\%h_s$.

The interstorey drift for the 10-storey buildings is depicted in **Figure 6.46**, for the 8-storey buildings in **Figure 6.47** and for the 6- and 4-storey buildings in **Figure 6.48**. Except for two 10-storey MD-CBF buildings with plan "B" on Site Class B and Site Class C, where wind-induced interstorey drift exceeds the code limit in the middle floors, for all other buildings, the interstorey drift under both wind and earthquake load is within the code limit. As expected, the interstorey drift is larger in the N-S direction than in the E-W direction.

To summarize, buildings that are taller than 10 storeys, have smaller width-to-length ratio and possess higher ductility tend to exhibit higher interstorey drifts. Taller steel buildings are more flexible than low-rise buildings and undergo higher interstorey drift. Further, wind-induced interstorey drift is very critical for the 12-storey buildings, especially in the N-S direction, where the deflection criterion under wind load is not satisfied. For example, as shown in **Figure 6.23**, the CBF braces of 12-storey LD-CBF building with plan "A", on Site Class C, pass the strength criterion. However, the drift criterion under wind load is not satisfied and the stiffness of brace members has to increase at almost all floors. Designers should be aware of verifying both strength and serviceability criteria when designing steel braced frames in seismic areas and verifying them against wind load.
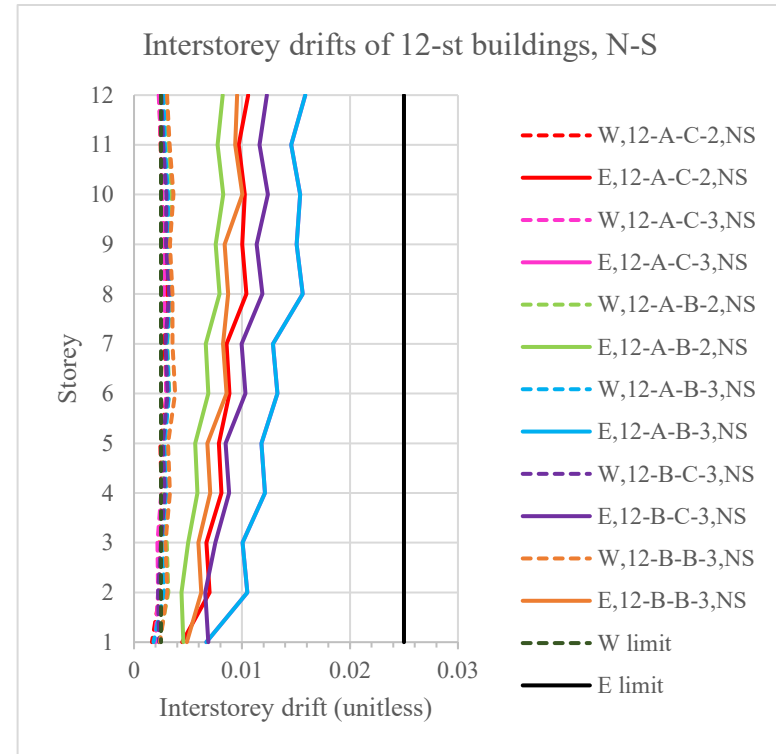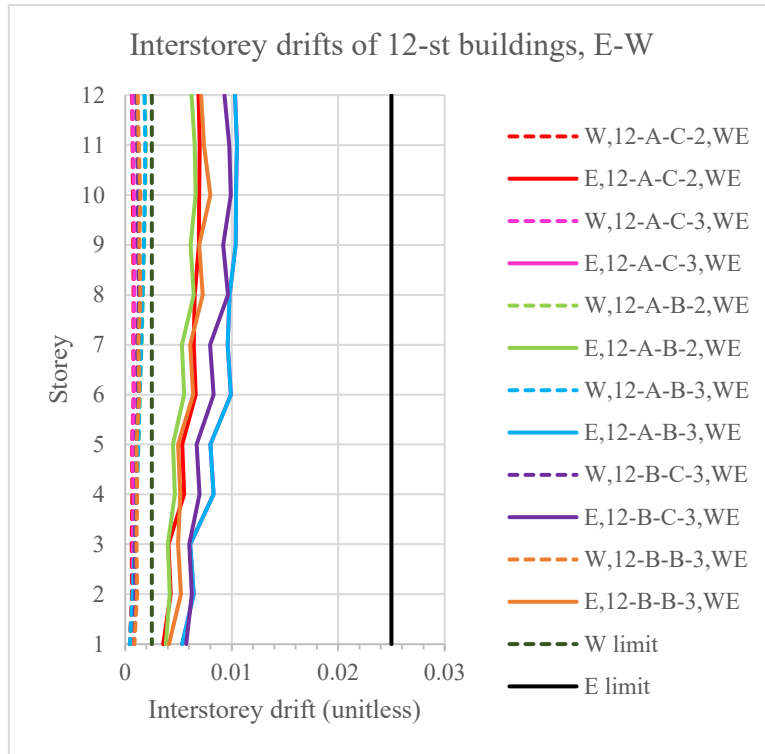
Figure 6.45: Wind- and earthquake-induced interstorey drifts of 12-storey buildings.
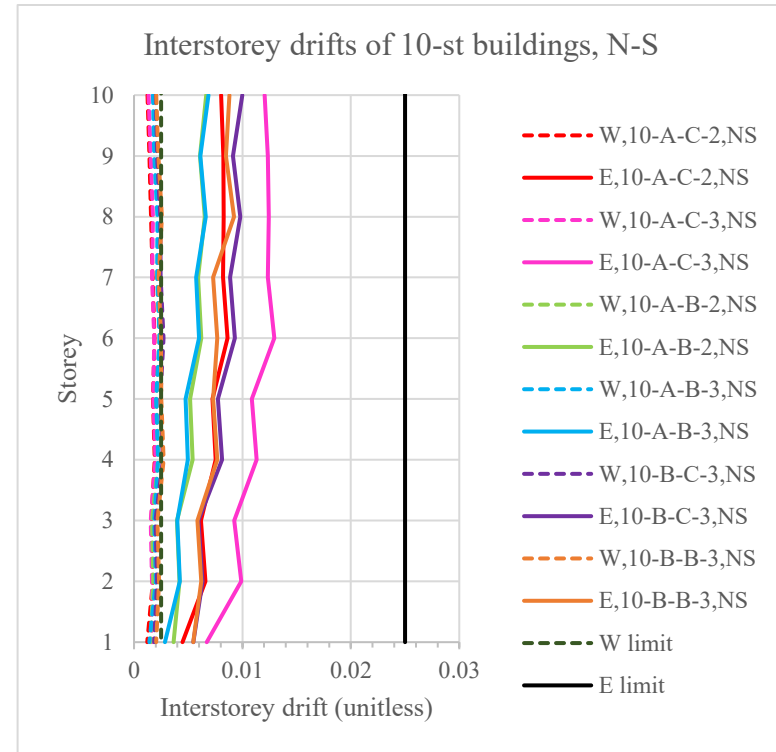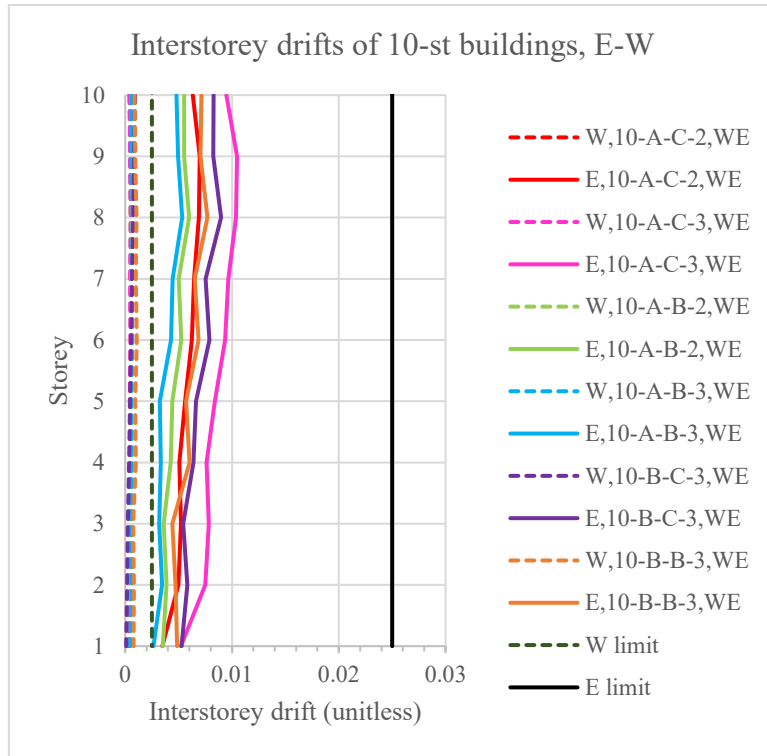
Figure 6.46: Wind- and earthquake-induced interstorey drifts of 10-storey buildings.
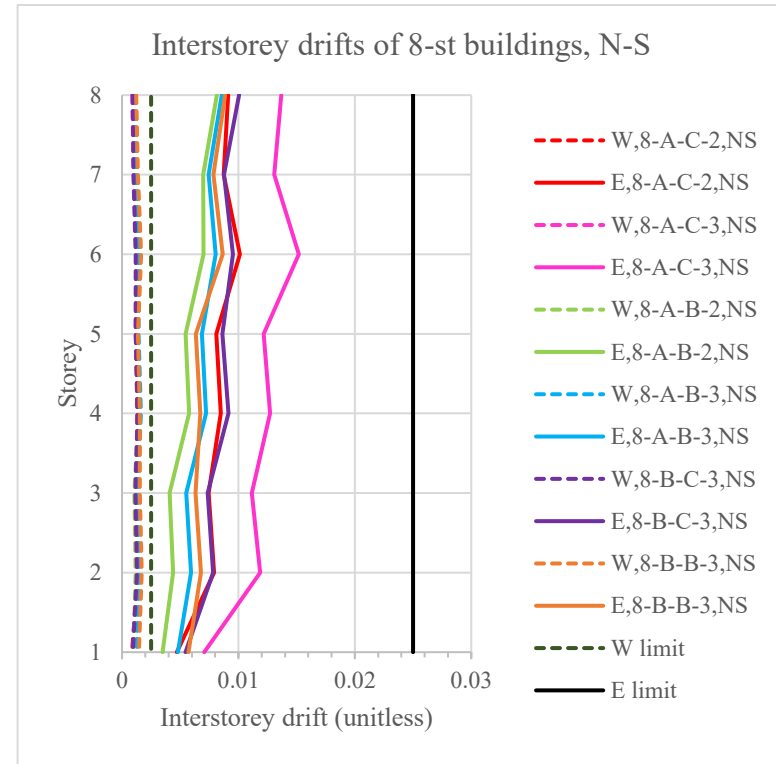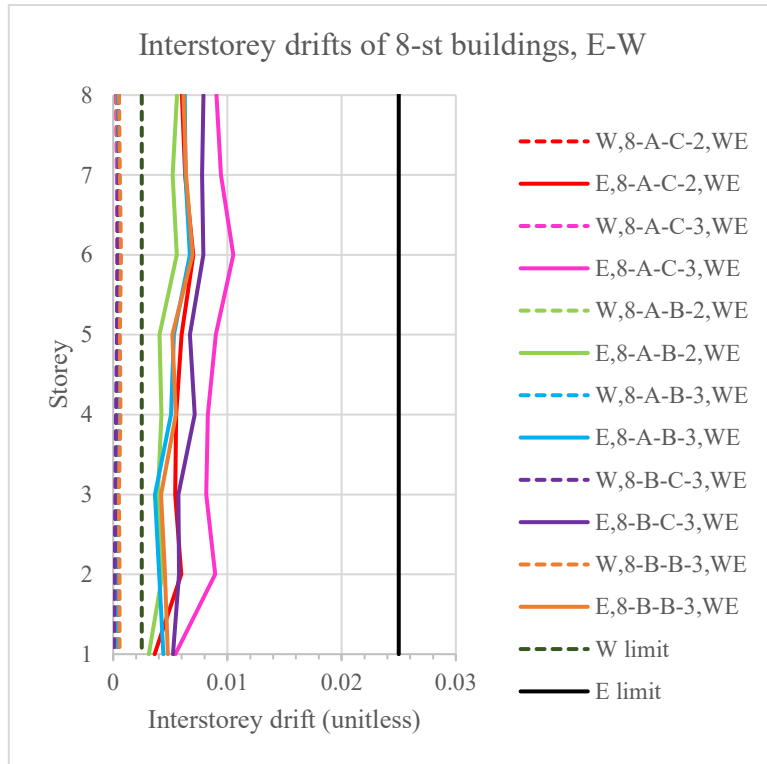
Figure 6.47: Wind- and earthquake-induced interstorey drifts of 8-storey buildings.
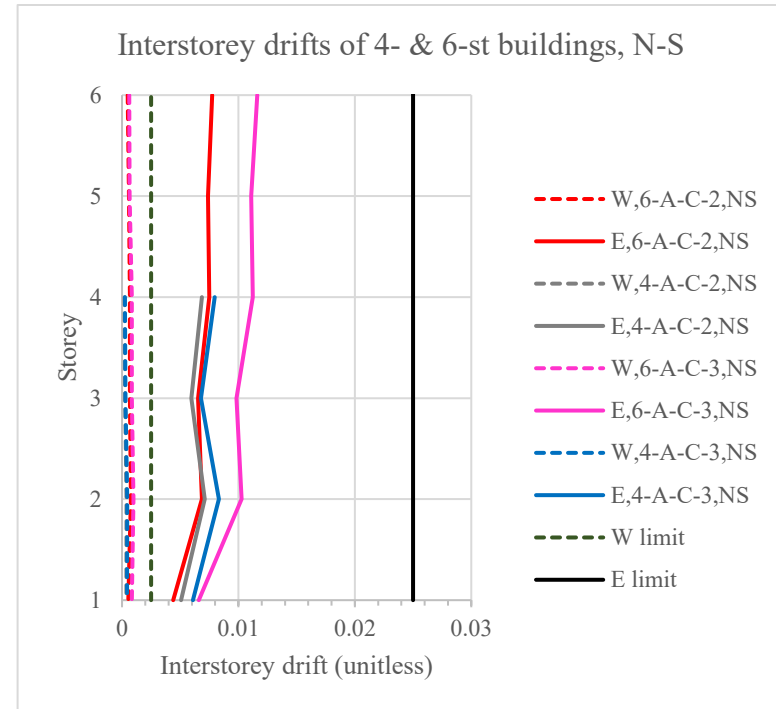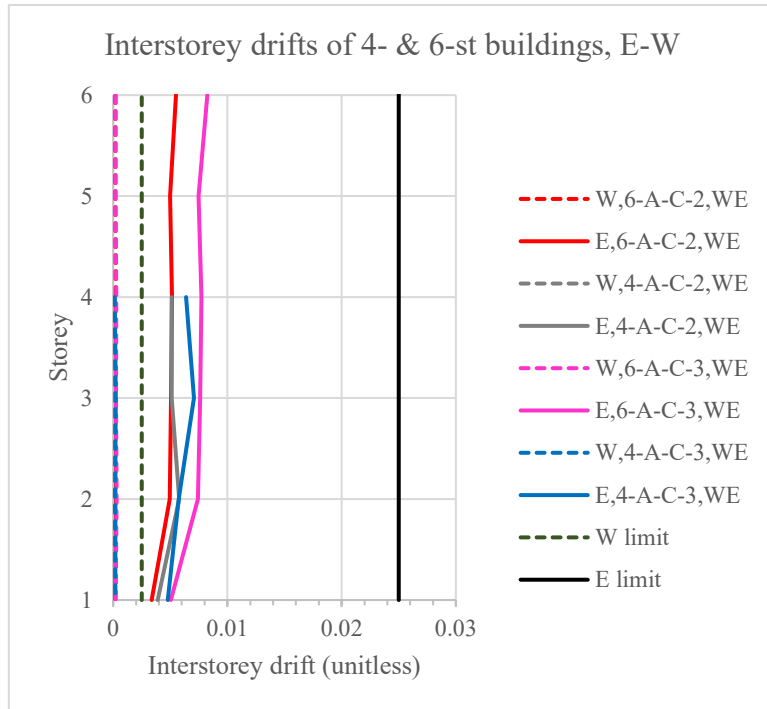
Figure 6.48: Wind- and earthquake-induced interstorey drifts of 4- and 6-storey buildings.

Chapter 7

CONCLUSIONS AND FUTURE WORK

7.1. CONCLUSIONS

The current thesis has examined the differences between wind- and earthquake-induced shear and torsion in low-rise and medium-rise buildings.

In this study, there were 22 steel buildings selected with heights ranging from 14.8 m (4-storey low-rise building) to 43.6 m (12-storey medium-rise building). The impact from building configurations was investigated by considering two width-to-length ratios: 1:4 (labelled plan "A") and 1:2 (labelled plan "B"). Thus, the first set of buildings with plan "A" comprises five buildings: 4-storey, 6-storey, 8-storey, 10-storey and 12-storey. The second set of buildings with plan "B" comprises only medium-rise buildings with 8, 10, and 12 storeys. In addition, two types of ductility levels were selected for concentrically braced frames: $R_d = 2$ and $R_d = 3$ together with two types of geotechnical profiles: Site Class C (firm soil) and Site Class B (rock).

Firstly, all buildings studied herein are designed to resist earthquake loads. The notional lateral loads, the torsion caused by accidental eccentricity and P-Δ effects are also considered in design. According to the NBCC provisions, all buildings are analyzed using the Equivalent Static Force Procedure and the Dynamic Analysis Procedure. The capacity

design method is applied for earthquake design. The structural irregularities were verified and all buildings are regular.

Accidental torsion, lateral notional load and P-Δ effects increase significantly the lateral load demand in braced frames. As an example, in the case of 12-storey LD-CBF building with plan "A" corresponding to length-to-width ratio 4:1 and located on Site Class C, the shear due to accidental torsion increases about 150% and that including notional lateral load, torsional and P-Δ effects increases about 210%. Shear caused by these effects is reduced when the building's length-to-width ratio decreases to 2:1.

Secondly, all low-rise and medium-rise steel buildings designed to resist earthquake loads were verified against wind load.

Regarding the wind loading provisions given in NBCC 2015, some ambiguities were found. It is concluded that, when partial wind loading Cases B and D are considered, the maximum torsion can be obtained on medium-rise buildings when deducting the wind pressures on half the building faces. When the same method is applied to low-rise buildings, wind-induced torsion, which are underestimated significantly in the current NBCC provisions, has been improved. However, the adequacy of wind-induced calculation for low-rise buildings can be improved further by implementing the provisions of ASCE/SEI 7-10.

The appropriate wind computing procedure plays an important role on determining wind loads. For example, comparing between the dynamic procedure versus the static procedure when computing the wind load on the larger facade of the 12-storey LD-CBF building with plan "A" on Site Class C, the former increases the wind force demand by 140%.

The comparison between shear provided by wind loads and earthquake loads has shown that building's configuration, ductility, location, geotechnical profile and loading direction have strong impacts on the design of braced frames proportioned to respond in the elastic range under wind load and in the inelastic range under earthquake load. Following are the conclusions yielded:

- The wind demand may become dominant when applied on the larger facade of steel braced frame buildings taller than 10 storeys, which possess larger ductility and are located on stiff soil or rock. In the case that wind load governs the design, earthquake loads may control the design of upper floor braces.

- The design of low-rise and some medium-rise buildings such as the 4-storey and 6-storey is governed by the earthquake load. Also, the earthquake load controls the design of braced frames parallel to the longer building dimension (e.g. the E-W direction).

- For an economic design of medium-rise steel braced frame buildings in Montreal area, it is suggested that LD-CBF is a better solution in comparison with MD-CBF. When LD-CBFs are selected to resist lateral loads, brace cross-sections designed for earthquake loads are able to respond in elastic range to wind load.

- In general, taller buildings with larger ductility level and larger length-to-width ratio tend to exhibit higher interstorey drifts under wind and earthquake loads. In all cases, the interstorey drifts under earthquake load are within the code limit. When wind applies perpendicular to the larger facade of the 12-storey MD-CBF building, it generates larger interstorey drifts, which exceed the code limit of 1/400 storey height. The exceedance found is approximately 30% to 40%. Therefore, in some cases, even

when the braces strength is adequate under wind and earthquake load, their stiffness need to be increased in order to satisfy the deflection criterion for wind loading.

- Therefore, special attention should be given to wind design when verifying both strength and serviceability criteria. Significant increases of braces cross-sections may be required when these braces were designed to respond in inelastic range under earthquake load.

7.2. FUTURE WORK

The current study only focuses on buildings with two different length-to-width ratios and two ductility levels of selected braced frame. It is believed that selecting other building sets with a variety of plan configurations, taller heights and different LFRSs, more valuable results can be witnessed. Also, it is recommended that more locations in Canada to be selected in order to study the effects of wind versus earthquake load and to conclude which one of the two lateral loads governs the members design.

In terms of wind loads, although this thesis has recommended and applied the methodology to tackle the issues existed in NBCC 2015, it is strongly believed that if the wind tunnel test results are applied, more reliable comparisons can be obtained.

REFERENCES

ASCE/SEI 7-10. 2010. Minimum design loads for buildings and other structures. Structural Engineering Institute of ASCE, Reston, VA.

AS-NZS 1170-2. 2011 – Structural design actions – Part 2: Wind actions (By Authority of New Zealand Structure Verification Method B1/VM1).

Computer and Structure, Inc., USA. 2016), CSI Analysis Reference Manual for ETABS, www.csiamerica.com.

CSA (Canadian Standard Association). 2014. Design of Steel Structures, CSA S16-14. Mississauga, Ontario.

Durst, C.S. .1960. Wind speeds over short periods of time. Meteor. Mag. 89, 181-187.

EN 1991-1-1 .2005: Eurocode 1: Actions on structures – Part 1-4: General actions – Wind actions.

EN 1998-1: Eurocode 8: Design of structures for earthquake resistance. Part 1: General rules, earthquake actions and rules for buildings.

Filiatrault, A., Tremblay, R., Christopoulos, C., Folz, B., Pettinga, D. 2013. Elements of earthquake engineering and Structural Dynamics. Third edition.

Isyumov, N., Case, P. C. 2000. Wind-induced torsional loads and responses of buildings, Proceedings of Structures Congress, Philadelphia, Pennsylvania, USA, Sponsored by ASCE/SEI, May 8-10.

Keast, D.C., Barbagallo, A., Wood, G.S. 2012. Correlation of wind load combinations including torsion on medium-rise buildings. Wind and Structures, An International Journal, 15(5), 423-439.

Mitchell, D., Tremblay, R., Karacabeyli, E., Paultre, P., Saatcioglu, M. and Anderson, D.L. 2003. Seismic Force Modification Factors for the Proposed 2005 NBCC. Canadian Journal of Civil Engineering.

NBCC 2010. User's Guide – NBCC 2010, Structural Commentaries (part 4). Issued by the Canadian Commission on Building and Fire Codes, National Research Council of Canada.

National building code of Canada 2015. Canadian Commission on building and fire codes, National research Council Canada. Associate Committee on the National Building Code, NRCC, Ottawa, ON.

Nguyen, S., Stathopoulos, T., Tirca, L. Wind-induced Shear and Torsion in Low- and Medium-rise Buildings: Provisions of National Building Code of Canada 2015 (NBCC 2015). Canadian Journal of Civil Engineering, 2017 (under review).

Stathopoulos, T., Elsharawy, M., Galal, K. 2013. Wind load combinations including torsion for rectangular medium-rise buildings. International journal of high-rise buildings. September 2013, Vol 2, no 3, 245-255.

Tamura, Y., Kikuchi, H., Hibi, K. 2003. Quasi-static wind load combinations for low- and middle-rise buildings. Journal of Wind Engineering and Industrial Aerodynamics, 91, 1613-1625.

Taranath, B. 2004. Wind and earthquake resistant buildings structural and analysis design.

New York: Marcel Dekker.

APPENDIX A

SUMMARY OF CBF DESIGNS OF STUDIED BUILDINGS

---

1. MEMBER CROSS-SECTIONS OF CBF OF STUDIED BUILDINGS

Table A.1: LD-CBF member cross-sections of the 10-st building, plan A, Site Class C.

Storey	E-W direction			N-S direction		
	Braces	Beams	Columns	Braces	Beams	Columns
10	HSS114.3X114.3X6.4	W460X74	W310X60	HSS114.3X114.3X7.9	W460X106	W310X60
9	HSS114.3X114.3X9.5	W460X128	W310X60	HSS139.7X139.7X7.9	W460X144	W310X60
8	HSS114.3X114.3X9.5	W460X144	W310X97	HSS139.7X139.7X9.5	W460X144	W310X117
7	HSS139.7X139.7X7.9	W460X82	W310X97	HSS152.4X152.4X9.5	W460X144	W310X117
6	HSS139.7X139.7X9.5	W460X128	W310X179	HSS152.4X152.4X9.5	W530X150	W310X226
5	HSS152.4X152.4X9.5	W460X82	W310X179	HSS177.8X177.8X9.5	W460X128	W310X226
4	HSS152.4X152.4X9.5	W460X128	W310X283	HSS177.8X177.8X9.5	W530X165	W360X347
3	HSS152.4X152.4X9.5	W460X82	W310X283	HSS177.8X177.8X9.5	W460X82	W360X347
2	HSS152.4X152.4X9.5	W460X144	W310X415	HSS177.8X177.8X9.5	W530X165	W360X509
1	HSS152.4X152.4X12.7	W460X82	W310X415	HSS177.8X177.8X12.7	W460X144	W360X509

Table A.2: LD-CBF member cross-sections of the 8-st building, plan A, Site Class C.

Storey	E-W direction			N-S direction		
	Braces	Beams	Columns	Braces	Beams	Columns
8	HSS114.3X114.3X6.4	W460X74	W310X60	HSS114.3X114.3X7.9	W460X106	W310X60
7	HSS139.7X139.7X6.4	W460X128	W310X60	HSS139.7X139.7X9.5	W460X144	W310X60
6	HSS139.7X139.7X7.9	W460X128	W310X107	HSS152.4X152.4X7.9	W460X144	W310X129
5	HSS139.7X139.7X9.5	W460X82	W310X107	HSS152.4X152.4X12.7	W460X128	W310X129
4	HSS152.4X152.4X9.5	W460X128	W310X226	HSS152.4X152.4X12.7	W530X150	W310X253
3	HSS152.4X152.4X9.5	W460X82	W310X226	HSS177.8X177.8X9.5	W460X128	W310X253
2	HSS152.4X152.4X9.5	W460X128	W310X313	HSS177.8X177.8X9.5	W530X165	W310X415
1	HSS152.4X152.4X12.7	W460X82	W310X313	HSS177.8X177.8X12.7	W460X89	W310X415

Table A.3: LD-CBF member cross-sections of the 6-st building, plan A, Site Class C.

Storey	E-W direction			N-S direction		
	Braces	Beams	Columns	Braces	Beams	Columns
6	HSS114.3X114.3X6.4	W460X74	W310X60	HSS114.3X114.3X9.5	W460X128	W310X60
5	HSS114.3X114.3X12.7	W460X128	W310X60	HSS152.4X152.4X9.5	W530X150	W310X60
4	HSS139.7X139.7X7.9	W460X128	W310X117	HSS152.4X152.4X9.5	W460X144	W310X143
3	HSS152.4X152.4X7.9	W460X128	W310X117	HSS177.8X177.8X9.5	W460X128	W310X143
2	HSS152.4X152.4X7.9	W460X128	W310X226	HSS177.8X177.8X9.5	W530X150	W310X283
1	HSS177.8X177.8X7.9	W460X82	W310X226	HSS177.8X177.8X12.7	W460X128	W310X283

Table A.4: LD-CBF member cross-sections of the 4-st building, plan A, Site Class C.

Storey	E-W direction			N-S direction		
	Braces	Beams	Columns	Braces	Beams	Columns
4	HSS114.3X114.3X9.5	W460X106	W310X60	HSS139.7X139.7X7.9	W460X128	W310X67
3	HSS152.4X152.4X7.9	W460X128	W310X60	HSS177.8X177.8X9.5	W530X165	W310X67
2	HSS152.4X152.4X9.5	W460X128	W310X143	HSS177.8X177.8X9.5	W530X150	W310X179
1	HSS177.8X177.8X9.5	W460X128	W310X143	HSS203.2X203.2X9.5	W460X128	W310X179

Table A.5: MD-CBF member cross-sections of the 12-st building, plan A, Site Class C.

Storey	E-W direction			N-S direction		
	Braces	Beams	Columns	Braces	Beams	Columns
12	HSS88.9X88.9X7.9	W460X74	W310X60	HSS114.3X114.3X6.4	W460X106	W310X60
11	HSS114.3X114.3X6.4	W460X82	W310X60	HSS114.3X114.3X9.5	W460X144	W310X60
10	HSS114.3X114.3X6.4	W460X128	W310X97	HSS114.3X114.3X9.5	W460X144	W310X117
9	HSS114.3X114.3X9.5	W460X106	W310X97	HSS139.7X139.7X9.5	W460X106	W310X117
8	HSS114.3X114.3X9.5	W460X128	W310X179	HSS139.7X139.7X9.5	W460X144	W310X226
7	HSS114.3X114.3X12.7	W460X74	W310X179	HSS152.4X152.4X9.5	W460X82	W310X226
6	HSS139.7X139.7X7.9	W460X128	W310X283	HSS152.4X152.4X9.5	W460X144	W360X347
5	HSS139.7X139.7X9.5	W460X74	W310X283	HSS152.4X152.4X12.7	W460X106	W360X347
4	HSS139.7X139.7X9.5	W460X128	W360X382	HSS152.4X152.4X12.7	W460X158	W360X509
3	HSS139.7X139.7X9.5	W460X74	W360X382	HSS152.4X152.4X12.7	W460X82	W360X509
2	HSS139.7X139.7X9.5	W460X128	W360X509	HSS152.4X152.4X12.7	W460X158	W360X592
1	HSS152.4X152.4X9.5	W460X82	W360X509	HSS177.8X177.8X9.5	W460X128	W360X592

Table A.6: MD-CBF member cross-sections of the 10-st building, plan A, Site Class C.

Storey	E-W direction			N-S direction		
	Braces	Beams	Columns	Braces	Beams	Columns
10	HSS88.9X88.9X7.9	W460X74	W310X60	HSS114.3X114.3X6.4	W460X106	W310X60
9	HSS114.3X114.3X6.4	W460X106	W310X60	HSS114.3X114.3X12.7	W460X144	W310X60
8	HSS114.3X114.3X7.9	W460X128	W310X107	HSS114.3X114.3X12.7	W460X144	W310X129
7	HSS114.3X114.3X9.5	W460X106	W310X107	HSS139.7X139.7X9.5	W460X106	W310X129
6	HSS114.3X114.3X12.7	W460X128	W310X202	HSS152.4X152.4X7.9	W460X144	W310X253
5	HSS139.7X139.7X7.9	W460X74	W310X202	HSS152.4X152.4X9.5	W460X106	W310X253
4	HSS139.7X139.7X7.9	W460X128	W310X283	HSS152.4X152.4X9.5	W460X144	W360X347
3	HSS139.7X139.7X9.5	W460X74	W310X283	HSS152.4X152.4X12.7	W460X82	W360X347
2	HSS139.7X139.7X9.5	W460X128	W310X415	HSS152.4X152.4X12.7	W460X158	W360X509
1	HSS152.4X152.4X9.5	W460X74	W310X415	HSS152.4X152.4X12.7	W460X106	W360X509

Table A.7: MD-CBF member cross-sections of the 8-st building, plan A, Site Class C.

Storey	E-W direction			N-S direction		
	Braces	Beams	Columns	Braces	Beams	Columns
8	HSS88.9X88.9X7.9	W460X74	W310X60	HSS114.3X114.3X6.4	W460X106	W310X60
7	HSS114.3X114.3X7.9	W460X106	W310X60	HSS139.7X139.7X7.9	W460X144	W310X60
6	HSS114.3X114.3X9.5	W460X128	W310X107	HSS139.7X139.7X7.9	W460X144	W310X143
5	HSS114.3X114.3X12.7	W460X74	W310X107	HSS152.4X152.4X9.5	W460X128	W310X143
4	HSS139.7X139.7X7.9	W460X128	W310X226	HSS152.4X152.4X9.5	W460X144	W310X253
3	HSS139.7X139.7X9.5	W460X74	W310X226	HSS177.8X177.8X7.9	W460X89	W310X253
2	HSS139.7X139.7X9.5	W460X128	W310X342	HSS177.8X177.8X7.9	W460X144	W310X415
1	HSS152.4X152.4X9.5	W460X74	W310X342	HSS177.8X177.8X9.5	W460X89	W310X415

Table A.8: MD-CBF member cross-sections of the 6-st building, plan A, Site Class C.

Storey	E-W direction			N-S direction		
	Braces	Beams	Columns	Braces	Beams	Columns
6	HSS114.3X114.3X6.4	W460X74	W310X60	HSS114.3X114.3X6.4	W460X106	W310X60
5	HSS114.3X114.3X9.5	W460X128	W310X60	HSS139.7X139.7X7.9	W460X144	W310X60
4	HSS114.3X114.3X9.5	W460X128	W310X117	HSS139.7X139.7X7.9	W460X128	W310X143
3	HSS139.7X139.7X7.9	W460X74	W310X117	HSS152.4X152.4X9.5	W460X128	W310X143
2	HSS139.7X139.7X7.9	W460X128	W310X226	HSS152.4X152.4X9.5	W460X144	W310X283
1	HSS152.4X152.4X7.9	W460X74	W310X226	HSS152.4X152.4X12.7	W460X106	W310X283

Table A.9: MD-CBF member cross-sections of the 4-st building, plan A, Site Class C.

Storey	E-W direction			N-S direction		
	Braces	Beams	Columns	Braces	Beams	Columns
4	HSS114.3X114.3X6.4	W460X82	W310X60	HSS114.3X114.3X7.9	W460X106	W310X67
3	HSS114.3X114.3X9.5	W460X128	W310X60	HSS139.7X139.7X9.5	W530X165	W310X67
2	HSS114.3X114.3X12.7	W460X128	W310X143	HSS152.4X152.4X7.9	W530X150	W310X179
1	HSS139.7X139.7X9.5	W460X128	W310X143	HSS177.8X177.8X7.9	W460X128	W310X179

Table A.10: LD-CBF member cross-sections of the 12-st building, plan A, Site Class B.

Storey	E-W direction			N-S direction		
	Braces	Beams	Columns	Braces	Beams	Columns
12	HSS88.9X88.9X7.9	W460X74	W200X46.1	HSS114.3X114.3X6.4	W460X97	W310X60
11	HSS114.3X114.3X6.4	W460X74	W200X46.1	HSS114.3X114.3X12.7	W460X144	W310X60
10	HSS114.3X114.3X6.4	W460X128	W310X86	HSS114.3X114.3X12.7	W460X128	W310X97
9	HSS114.3X114.3X9.5	W460X128	W310X86	HSS139.7X139.7X9.5	W460X144	W310X97
8	HSS114.3X114.3X12.7	W460X128	W310X158	HSS139.7X139.7X9.5	W460X144	W310X179
7	HSS114.3X114.3X12.7	W460X74	W310X158	HSS152.4X152.4X9.5	W460X82	W310X179
6	HSS114.3X114.3X12.7	W460X128	W310X226	HSS152.4X152.4X9.5	W460X158	W310X283
5	HSS139.7X139.7X7.9	W460X74	W310X226	HSS152.4X152.4X9.5	W460X128	W310X283
4	HSS139.7X139.7X7.9	W460X128	W310X283	HSS152.4X152.4X9.5	W530X150	W310X375
3	HSS152.4X152.4X7.9	W460X74	W310X283	HSS152.4X152.4X12.7	W460X82	W310X375
2	HSS152.4X152.4X7.9	W460X128	W310X415	HSS152.4X152.4X12.7	W460X144	W360X463
1	HSS152.4X152.4X9.5	W460X82	W310X415	HSS177.8X177.8X9.5	W460X97	W360X463

Table A.11: LD-CBF member cross-sections of the 10-st building, plan A, Site Class B.

Storey	E-W direction			N-S direction		
	Braces	Beams	Columns	Braces	Beams	Columns
10	HSS88.9X88.9X7.9	W460X74	W200X46.1	HSS114.3X114.3X4.8	W460X89	W200X46.1
9	HSS114.3X114.3X6.4	W460X82	W200X46.1	HSS139.7X139.7X6.4	W460X144	W200X46.1
8	HSS114.3X114.3X6.4	W460X128	W310X86	HSS139.7X139.7X6.4	W460X128	W310X107
7	HSS114.3X114.3X9.5	W460X128	W310X86	HSS139.7X139.7X9.5	W460X144	W310X107
6	HSS114.3X114.3X9.5	W460X128	W310X158	HSS139.7X139.7X9.5	W460X144	W310X179
5	HSS139.7X139.7X7.9	W460X82	W310X158	HSS152.4X152.4X9.5	W460X89	W310X179
4	HSS139.7X139.7X7.9	W460X128	W310X226	HSS152.4X152.4X7.9	W460X158	W310X283
3	HSS139.7X139.7X7.9	W460X82	W310X226	HSS152.4X152.4X9.5	W460X128	W310X283
2	HSS139.7X139.7X7.9	W460X128	W310X342	HSS152.4X152.4X9.5	W530X165	W310X375
1	HSS152.4X152.4X7.9	W460X82	W310X342	HSS152.4X152.4X12.7	W460X89	W310X375

Table A.12: LD-CBF member cross-sections of the 8-st building, plan A, Site Class B.

Storey	E-W direction			N-S direction		
	Braces	Beams	Columns	Braces	Beams	Columns
8	HSS88.9X88.9X7.9	W460X74	W200X46.1	HSS114.3X114.3X6.4	W460X106	W200X46.1
7	HSS114.3X114.3X7.9	W460X106	W200X46.1	HSS114.3X114.3X12.7	W460X144	W200X46.1
6	HSS114.3X114.3X7.9	W460X128	W310X97	HSS114.3X114.3X12.7	W460X144	W310X107
5	HSS114.3X114.3X12.7	W460X97	W310X97	HSS152.4X152.4X7.9	W460X128	W310X107
4	HSS114.3X114.3X12.7	W460X128	W310X158	HSS152.4X152.4X7.9	W530X150	W310X202
3	HSS139.7X139.7X7.9	W460X82	W310X158	HSS152.4X152.4X9.5	W460X128	W310X202
2	HSS139.7X139.7X7.9	W460X128	W310X253	HSS152.4X152.4X9.5	W530X165	W310X313
1	HSS139.7X139.7X9.5	W460X97	W310X253	HSS152.4X152.4X12.7	W460X89	W310X313

Table A.13: MD-CBF member cross-sections of the 12-st building, plan A, Site Class B.

Storey	E-W direction			N-S direction		
	Braces	Beams	Columns	Braces	Beams	Columns
12	HSS76.2X76.2X9.5	W460X74	W310X60	HSS88.9X88.9X7.9	W460X106	W310X60
11	HSS88.9X88.9X9.5	W460X74	W310X60	HSS114.3X114.3X7.9	W460X144	W310X60
10	HSS114.3X114.3X6.4	W460X128	W310X97	HSS114.3X114.3X7.9	W460X144	W310X107
9	HSS114.3X114.3X6.4	W460X82	W310X97	HSS114.3X114.3X12.7	W460X82	W310X107
8	HSS114.3X114.3X7.9	W460X128	W310X158	HSS114.3X114.3X12.7	W460X144	W310X202
7	HSS114.3X114.3X9.5	W460X82	W310X158	HSS139.7X139.7X9.5	W460X89	W310X202
6	HSS114.3X114.3X9.5	W460X128	W310X253	HSS139.7X139.7X9.5	W460X144	W310X313
5	HSS114.3X114.3X12.7	W460X74	W310X253	HSS152.4X152.4X7.9	W460X82	W310X313
4	HSS114.3X114.3X12.7	W460X128	W310X342	HSS152.4X152.4X7.9	W460X158	W310X454
3	HSS139.7X139.7X7.9	W460X74	W310X342	HSS152.4X152.4X9.5	W460X82	W310X454
2	HSS139.7X139.7X7.9	W460X128	W310X454	HSS152.4X152.4X9.5	W460X158	W360X509
1	HSS139.7X139.7X9.5	W460X89	W310X454	HSS152.4X152.4X9.5	W460X128	W360X509

Table A.14: MD-CBF member cross-sections of the 10-st building, plan A, Site Class B.

Storey	E-W direction			N-S direction		
	Braces	Beams	Columns	Braces	Beams	Columns
10	HSS76.2X76.2X7.9	W460X74	W200X46.1	HSS88.9X88.9X7.9	W460X106	W200X46.1
9	HSS88.9X88.9X9.5	W460X82	W200X46.1	HSS114.3X114.3X7.9	W460X144	W200X46.1
8	HSS114.3X114.3X6.4	W460X128	W310X97	HSS114.3X114.3X7.9	W460X144	W310X107
7	HSS114.3X114.3X6.4	W460X82	W310X97	HSS114.3X114.3X12.7	W460X82	W310X107
6	HSS114.3X114.3X7.9	W460X128	W310X158	HSS114.3X114.3X12.7	W460X144	W310X202
5	HSS114.3X114.3X9.5	W460X82	W310X158	HSS139.7X139.7X7.9	W460X106	W310X202
4	HSS114.3X114.3X9.5	W460X128	W310X253	HSS139.7X139.7X7.9	W460X144	W310X313
3	HSS114.3X114.3X12.7	W460X74	W310X253	HSS139.7X139.7X9.5	W460X82	W310X313
2	HSS114.3X114.3X12.7	W460X128	W310X342	HSS139.7X139.7X9.5	W460X144	W310X415
1	HSS139.7X139.7X7.9	W460X74	W310X342	HSS152.4X152.4X9.5	W460X82	W310X415

Table A.15: MD-CBF member cross-sections of the 8-st building, plan A, Site Class B.

Storey	E-W direction			N-S direction		
	Braces	Beams	Columns	Braces	Beams	Columns
8	HSS76.2X76.2X9.5	W460X74	W200X46.1	HSS88.9X88.9X7.9	W460X106	W200X46.1
7	HSS114.3X114.3X6.4	W460X82	W200X46.1	HSS114.3X114.3X9.5	W460X144	W200X46.1
6	HSS114.3X114.3X6.4	W460X128	W310X97	HSS114.3X114.3X9.5	W460X144	W310X107
5	HSS114.3X114.3X9.5	W460X128	W310X97	HSS139.7X139.7X7.9	W460X82	W310X107
4	HSS114.3X114.3X9.5	W460X128	W310X179	HSS139.7X139.7X7.9	W460X144	W310X202
3	HSS114.3X114.3X12.7	W460X82	W310X179	HSS139.7X139.7X9.5	W460X89	W310X202
2	HSS114.3X114.3X12.7	W460X128	W310X253	HSS139.7X139.7X9.5	W460X144	W310X342
1	HSS139.7X139.7X7.9	W460X74	W310X253	HSS152.4X152.4X9.5	W460X82	W310X342

Table A.16: MD-CBF member cross-sections of the 12-st building, plan B, Site Class C.

Storey	E-W direction			N-S direction		
	Braces	Beams	Columns	Braces	Beams	Columns
12	HSS88.9X88.9X7.9	W460X74	W310X60	HSS88.9X88.9X9.5	W460X106	W310X60
11	HSS114.3X114.3X6.4	W460X82	W310X60	HSS114.3X114.3X9.5	W460X144	W310X60
10	HSS114.3X114.3X7.9	W460X128	W310X97	HSS114.3X114.3X9.5	W460X144	W360X122
9	HSS139.7X139.7X6.4	W460X106	W310X97	HSS139.7X139.7X7.9	W460X106	W360X122
8	HSS139.7X139.7X6.4	W460X128	W310X179	HSS139.7X139.7X7.9	W460X144	W360X196
7	HSS139.7X139.7X7.9	W460X74	W310X179	HSS152.4X152.4X9.5	W460X89	W360X196
6	HSS139.7X139.7X7.9	W460X128	W310X283	HSS152.4X152.4X9.5	W460X144	W360X314
5	HSS139.7X139.7X9.5	W460X74	W310X283	HSS152.4X152.4X9.5	W460X106	W360X314
4	HSS139.7X139.7X9.5	W460X128	W360X382	HSS152.4X152.4X9.5	W460X158	W360X421
3	HSS152.4X152.4X9.5	W460X74	W360X382	HSS152.4X152.4X12.7	W460X82	W360X421
2	HSS152.4X152.4X9.5	W460X128	W360X509	HSS152.4X152.4X12.7	W460X158	W360X551
1	HSS152.4X152.4X9.5	W460X82	W360X509	HSS152.4X152.4X15.9	W460X106	W360X551

Table A.17: MD-CBF member cross-sections of the 10-st building, plan B, Site Class C.

Storey	E-W direction			N-S direction		
	Braces	Beams	Columns	Braces	Beams	Columns
10	HSS88.9X88.9X7.9	W460X74	W360X79	HSS88.9X88.9X9.5	W460X106	W360X79
9	HSS114.3X114.3X7.9	W460X106	W360X79	HSS114.3X114.3X12.7	W460X144	W360X79
8	HSS114.3X114.3X7.9	W460X128	W360X110	HSS114.3X114.3X12.7	W460X144	W360X122
7	HSS114.3X114.3X12.7	W460X106	W360X110	HSS139.7X139.7X9.5	W460X106	W360X122
6	HSS139.7X139.7X7.9	W460X128	W360X196	HSS139.7X139.7X9.5	W460X144	W360X216
5	HSS152.4X152.4X7.9	W460X74	W360X196	HSS152.4X152.4X9.5	W460X106	W360X216
4	HSS152.4X152.4X7.9	W460X128	W360X287	HSS152.4X152.4X9.5	W460X144	W360X347
3	HSS152.4X152.4X7.9	W460X74	W360X287	HSS152.4X152.4X9.5	W460X82	W360X347
2	HSS152.4X152.4X7.9	W460X128	W360X421	HSS152.4X152.4X9.5	W460X158	W360X509
1	HSS152.4X152.4X9.5	W460X74	W360X421	HSS152.4X152.4X12.7	W460X106	W360X509

Table A.18: MD-CBF member cross-sections of the 8-st building, plan B, Site Class C.

Storey	E-W direction			N-S direction		
	Braces	Beams	Columns	Braces	Beams	Columns
8	HSS114.3X114.3X6.4	W460X74	W310X60	HSS114.3X114.3X6.4	W460X106	W360X79
7	HSS114.3X114.3X7.9	W460X106	W310X60	HSS114.3X114.3X12.7	W460X144	W360X79
6	HSS114.3X114.3X9.5	W460X128	W310X107	HSS114.3X114.3X12.7	W460X144	W360X134
5	HSS139.7X139.7X7.9	W460X74	W310X107	HSS139.7X139.7X9.5	W460X128	W360X134
4	HSS139.7X139.7X7.9	W460X128	W310X226	HSS139.7X139.7X9.5	W460X144	W360X216
3	HSS139.7X139.7X9.5	W460X74	W310X226	HSS152.4X152.4X9.5	W460X89	W360X216
2	HSS152.4X152.4X7.9	W460X128	W310X342	HSS152.4X152.4X9.5	W460X144	W360X347
1	HSS152.4X152.4X9.5	W460X74	W310X342	HSS152.4X152.4X12.7	W460X89	W360X347

Table A.19: MD-CBF member cross-sections of the 12-st building, plan B, Site Class B.

Storey	E-W direction			N-S direction		
	Braces	Beams	Columns	Braces	Beams	Columns
12	HSS76.2X76.2X9.5	W460X74	W310X60	HSS76.2X76.2X9.5	W460X106	W310X60
11	HSS114.3X114.3X6.4	W460X74	W310X60	HSS114.3X114.3X7.9	W460X144	W310X60
10	HSS114.3X114.3X6.4	W460X128	W310X86	HSS114.3X114.3X7.9	W460X144	W360X101
9	HSS114.3X114.3X7.9	W460X82	W310X86	HSS114.3X114.3X12.7	W460X82	W360X101
8	HSS114.3X114.3X7.9	W460X128	W310X143	HSS114.3X114.3X12.7	W460X144	W360X162
7	HSS114.3X114.3X12.7	W460X82	W310X143	HSS139.7X139.7X7.9	W460X89	W360X162
6	HSS114.3X114.3X12.7	W460X128	W310X253	HSS139.7X139.7X7.9	W460X144	W360X237
5	HSS114.3X114.3X12.7	W460X74	W310X253	HSS139.7X139.7X9.5	W460X82	W360X237
4	HSS114.3X114.3X12.7	W460X128	W310X342	HSS139.7X139.7X9.5	W460X158	W360X347
3	HSS139.7X139.7X7.9	W460X74	W310X342	HSS139.7X139.7X9.5	W460X82	W360X347
2	HSS139.7X139.7X7.9	W460X128	W310X454	HSS139.7X139.7X9.5	W460X158	W360X463
1	HSS139.7X139.7X9.5	W460X89	W310X454	HSS152.4X152.4X9.5	W460X128	W360X463

Table A.20: MD-CBF member cross-sections of the 10-st building, plan B, Site Class B.

Storey	E-W direction			N-S direction		
	Braces	Beams	Columns	Braces	Beams	Columns
10	HSS76.2X76.2X9.5	W460X74	W200X46.1	HSS88.9X88.9X6.4	W460X106	W200X46.1
9	HSS114.3X114.3X6.4	W460X82	W200X46.1	HSS114.3X114.3X7.9	W460X144	W200X46.1
8	HSS114.3X114.3X6.4	W460X128	W310X86	HSS114.3X114.3X7.9	W460X144	W310X97
7	HSS114.3X114.3X7.9	W460X82	W310X86	HSS114.3X114.3X12.7	W460X82	W310X97
6	HSS114.3X114.3X7.9	W460X128	W310X158	HSS114.3X114.3X12.7	W460X144	W310X179
5	HSS114.3X114.3X12.7	W460X82	W310X158	HSS139.7X139.7X7.9	W460X106	W310X179
4	HSS114.3X114.3X12.7	W460X128	W310X226	HSS139.7X139.7X7.9	W460X144	W310X253
3	HSS139.7X139.7X7.9	W460X74	W310X226	HSS139.7X139.7X9.5	W460X82	W310X253
2	HSS139.7X139.7X7.9	W460X128	W310X342	HSS139.7X139.7X9.5	W460X144	W310X375
1	HSS139.7X139.7X9.5	W460X74	W310X342	HSS152.4X152.4X9.5	W460X82	W310X375

Table A.21: MD-CBF member cross-sections of the 8-st building, plan B, Site Class B.

Storey	E-W direction			N-S direction		
	Braces	Beams	Columns	Braces	Beams	Columns
8	HSS76.2X76.2X9.5	W460X74	W200X46.1	HSS88.9X88.9X6.4	W460X106	W200X46.1
7	HSS114.3X114.3X6.4	W460X82	W200X46.1	HSS114.3X114.3X7.9	W460X144	W200X46.1
6	HSS114.3X114.3X6.4	W460X128	W310X97	HSS114.3X114.3X7.9	W460X144	W310X97
5	HSS114.3X114.3X9.5	W460X128	W310X97	HSS114.3X114.3X12.7	W460X82	W310X97
4	HSS114.3X114.3X9.5	W460X128	W310X179	HSS114.3X114.3X12.7	W460X144	W310X179
3	HSS114.3X114.3X12.7	W460X82	W310X179	HSS139.7X139.7X9.5	W460X89	W310X179
2	HSS114.3X114.3X12.7	W460X128	W310X253	HSS139.7X139.7X9.5	W460X144	W310X283
1	HSS139.7X139.7X7.9	W460X74	W310X253	HSS152.4X152.4X7.9	W460X82	W310X283

2. EARTHQUAKE LOAD DISTRIBUTION AND FUNDAMENTAL PERIODS FROM DYNAMIC ANALYSIS OF STUDIED BUILDINGS

Dynamic procedure is only required for buildings taller than 60 m and for those with $T_1 > 2.0$ s. However, in this study, the dynamic analysis procedure was considered for all buildings for comparison purpose.

For the 10-storey LD-CBF building, with plan "A", on Site Class C, the periods in two main orthogonal directions are: $T_{E-W} = 2.04$ s and $T_{N-S} = 1.88$ s and the distribution of shear force from the Equivalent Static Force Procedure and the Dynamic Analysis Procedure is given in **Figure A.1**a. Similarly, for the 8-storey LD-CBF building, the periods are: $T_{E-W} = 1.65$ s and $T_{N-S} = 1.58$ s. The shear distribution is shown in **Figure A.1**b.

The periods of the 6-storey LD-CBF building, plan "A", on Site Class C are: $T_{E-W} = 1.27$ s and $T_{N-S} = 1.14$ s and those of the similar 4-storey building are: $T_{E-W} = 0.797$ s and $T_{N-S} = 0.723$ s. The shear distribution of these buildings is shown in **Figure A.2**a and **Figure A.2**b. For these buildings with $T_1 < 2.0$ s, dynamic analysis is not required.

The periods of the 12-storey MD-CBF building, plan "A", on Site Class C are: $T_{E-W} = 2.76$ s and $T_{N-S} = 2.51$ s. The shear distribution is presented in **Figure A.3**.
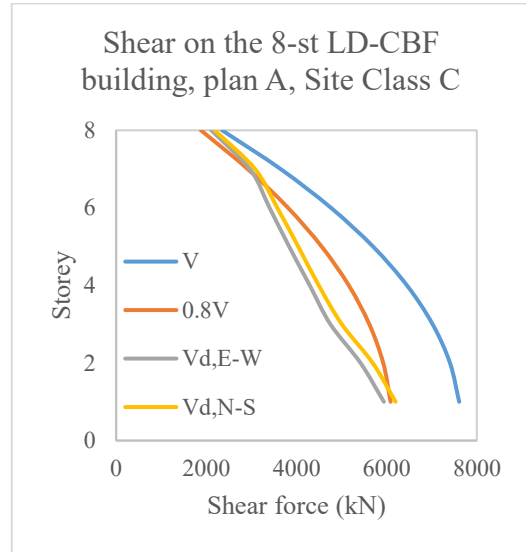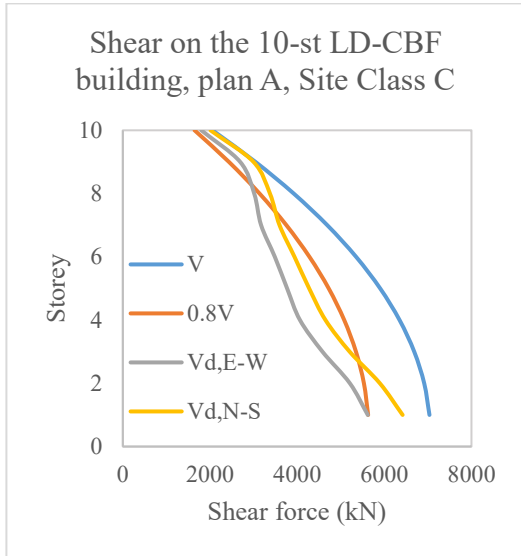
Figure A.1: Shear distribution over the building height: a) 10-storey LD-CBF building,

plan "A", Site Class C, b) 8-storey LD-CBF building, plan "A", Site Class C.

Figure A.2: Shear distribution over the building height: a) 6-storey LD-CBF building, plan

"A", Site Class C, b) 4-storey LD-CBF building, plan "A", Site Class C.

As resulted the shear in the E-W direction should be slightly increased to match $0.8V$. The periods of the 10-storey MD-CBF building, plan "A", on Site Class C are: $T_{E-W} = 2.09$ s and $T_{N-S} = 2.03$ s. Those for the 8-storey one are: $T_{E-W} = 1.75$ s and $T_{N-S} = 1.63$ s.

Shear force distribution of the plan A 12-storey MD-CBF building on Site Class C
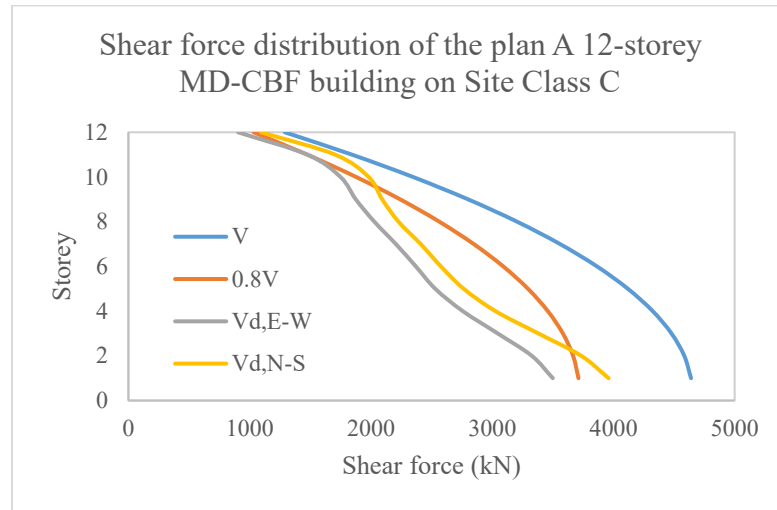
Figure A.3: Shear distribution over the building height: 12-st MD-CBF building, plan "A", Site Class C.

The periods of the 6- and 4-storey buildings are: $T_{E-W} = 1.27$ s; $T_{N-S} = 1.29$ s; $T_{E-W} = 0.86$ s and $T_{N-S} = 0.77$ s, respectively. The shear distribution for these buildings is shown in **Figure A.4**a; **Figure A.4**b; **Figure A.5**a and **Figure A.5**b.
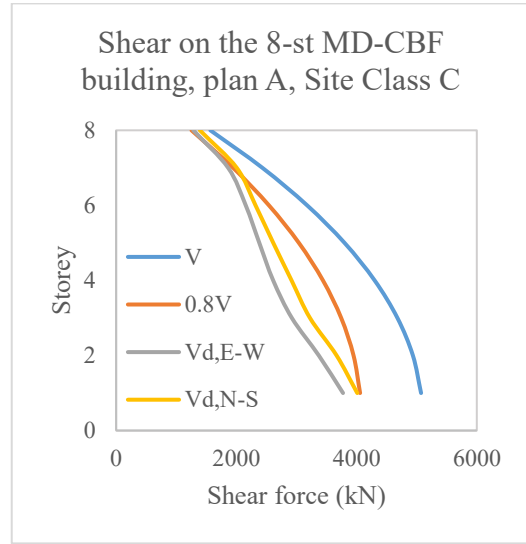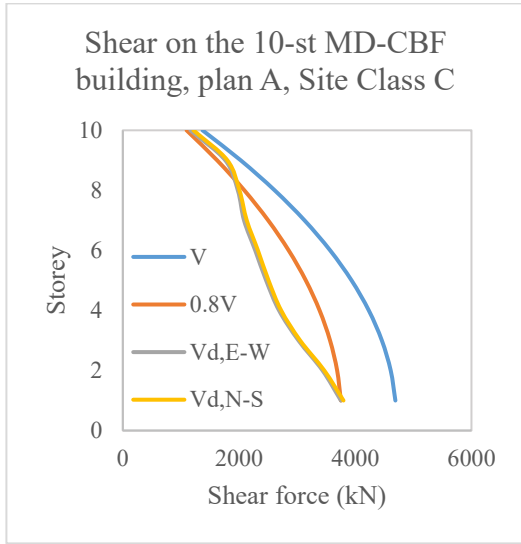
a)   b)

Figure A.4: Shear distribution over the building height: a) 10-storey MD-CBF building, plan "A", Site Class C, b) 8-storey MD-CBF building, plan "A", Site Class C.
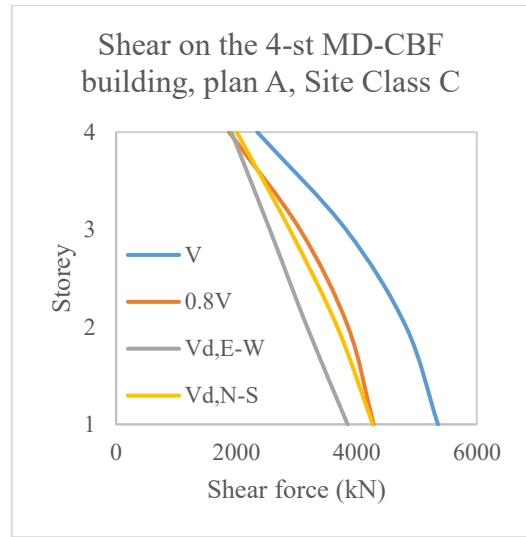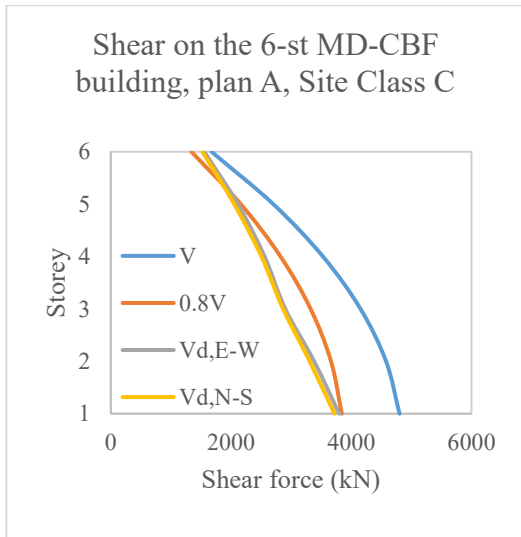
a)   b)

Figure A.5: Shear distribution over the building height: a) 6-storey MD-CBF building, plan "A", Site Class C, b) 4-storey MD-CBF building, plan "A", Site Class C.

The shear in the E-W direction of the 4-st MD-CBF building needs to be slightly increased.

The periods of the 12-storey LD-CBF building, plan "A", on Site Class B are: $T_{E-W} = 2.92$ s and $T_{N-S} = 2.68$ s. **Figure A.6** shows the shear distribution of this building.

Shear force distribution of the plan A 12-storey LD-CBF building on Site Class B
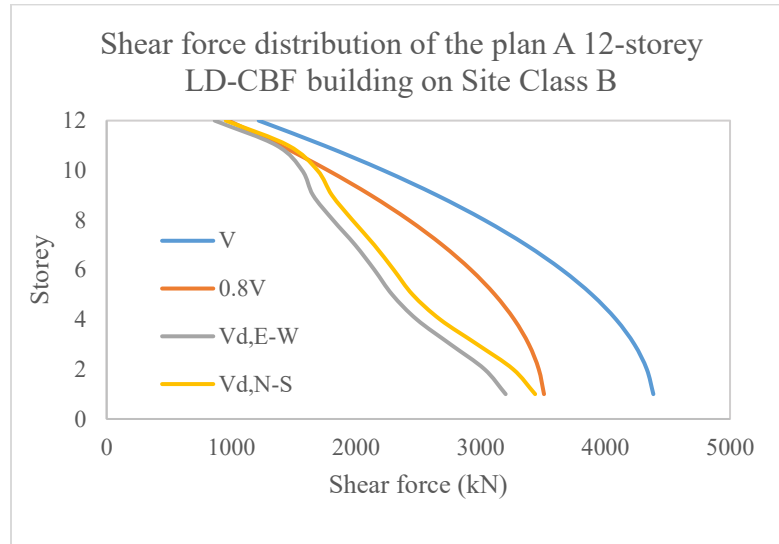
Figure A.6: Shear distribution over the building height: 12-st LD-CBF building, plan "A", Site Class B.

The periods of the 10-storey LD-CBF building, plan "A", on Site Class B are: $T_{E-W} = 2.37$ s and $T_{N-S} = 2.16$ s. Those for the 8-storey building are: $T_{E-W} = 1.84$ s and $T_{N-S} = 1.63$ s. The shear distribution of these buildings is shown in **Figure A.7**a and **Figure A.7**b.
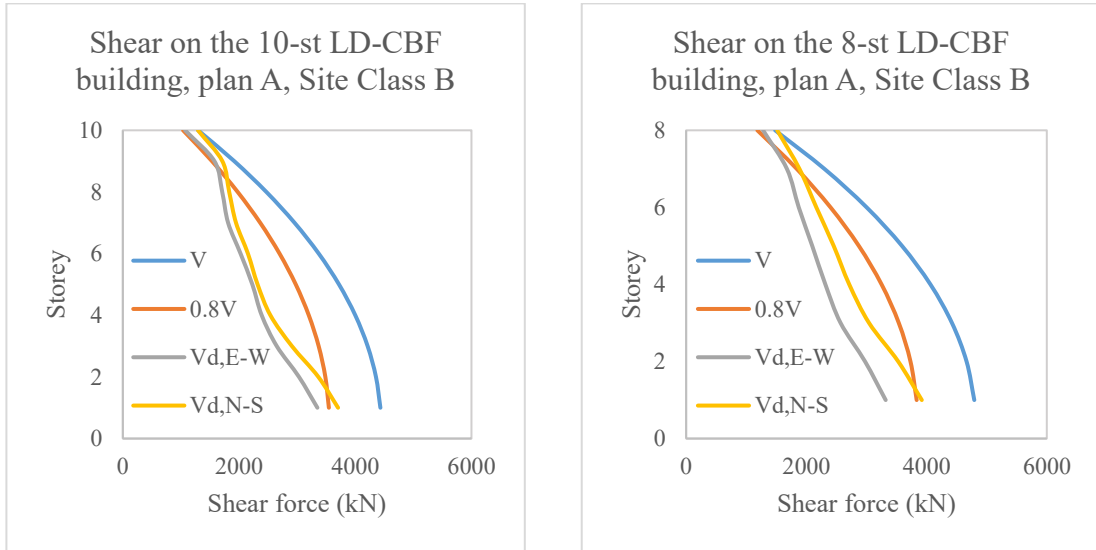
a)   b)

Figure A.7: Shear distribution over the building height: a) 10-storey LD-CBF building, plan "A", Site Class B, b) 8-storey LD-CBF building, plan "A", Site Class B.

The periods of the 12-storey MD-CBF building, plan "A", on Site Class B are: $T_{E-W} = 2.9$ s and $T_{N-S} = 2.62$ s. Shear distribution of this building is presented in **Figure A.8**.
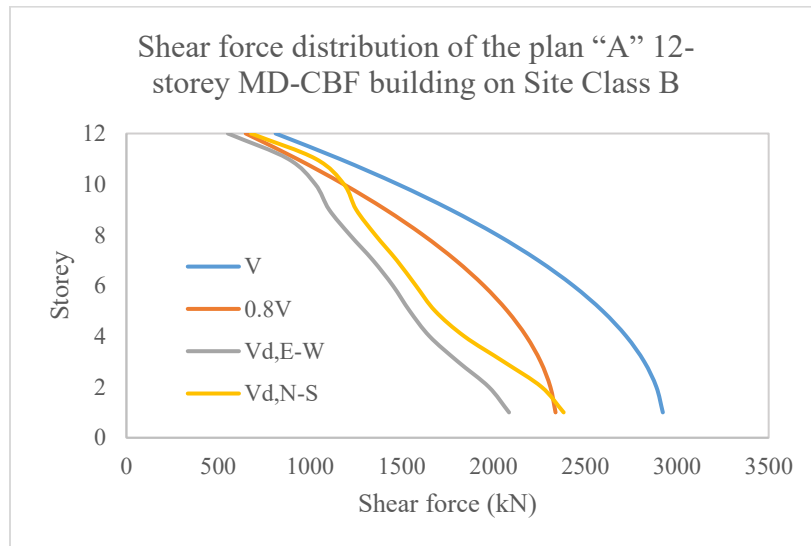
Figure A.8: Shear distribution over the building height: 12-storey MD-CBF building, plan "A", Site Class B.

The periods of the 10-storey LD-CBF building, plan "A", on Site Class B are: $T_{E-W} = 2.37$ s and $T_{N-S} = 2.16$ s. The results for the 8-storey building are: $T_{E-W} = 1.84$ s and $T_{N-S} = 1.63$ s. The shear distribution of these buildings is shown in **Figure A.9**a and **Figure A.9**b.

The periods of the plan "A", 10-storey MD-CBF building on Site Class B are $T_{E-W} = 2.38$ s and $T_{N-S} = 2.14$ s.
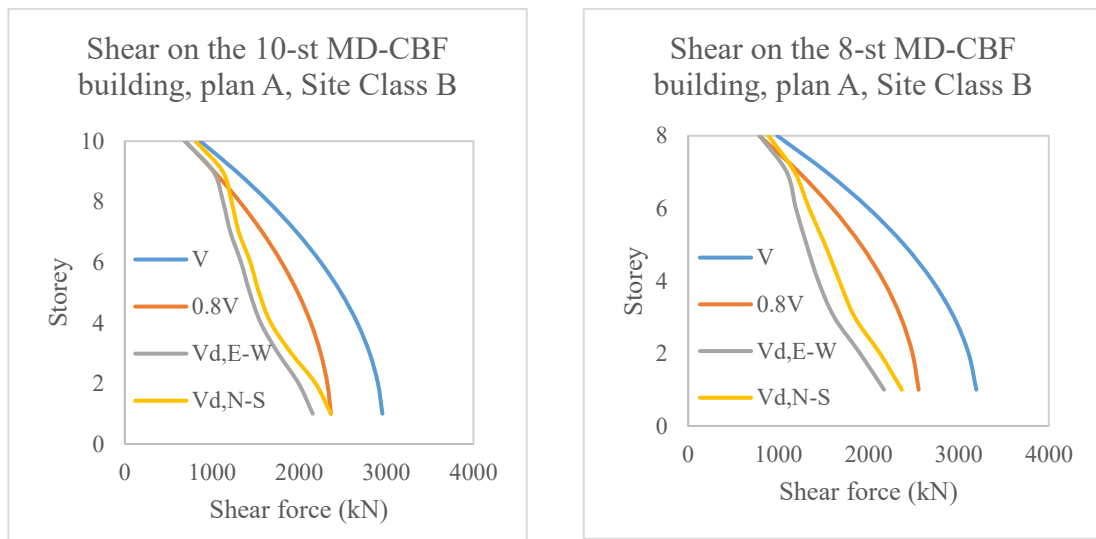
a)   b)

Figure A.9: Shear distribution over the building height: a) 10-storey MD-CBF building, plan "A", Site Class B, b) 8-storey MD-CBF building, plan "A", Site Class B.

The periods of the 12-storey MD-CBF building, plan "B", on Site Class C are: $T_{E-W} = 2.79$ s and $T_{N-S} = 2.63$ s. Shear distribution of this building is presented in **Figure A.10**.

The periods of the 10-storey are: $T_{E-W} = 2.2$ s and $T_{N-S} = 2.0$ s. The results for the 8-storey building are: $T_{E-W} = 1.72$ s and $T_{N-S} = 1.63$ s. The shear distribution of these buildings is shown in **Figure A.11**a and **Figure A.11**b.
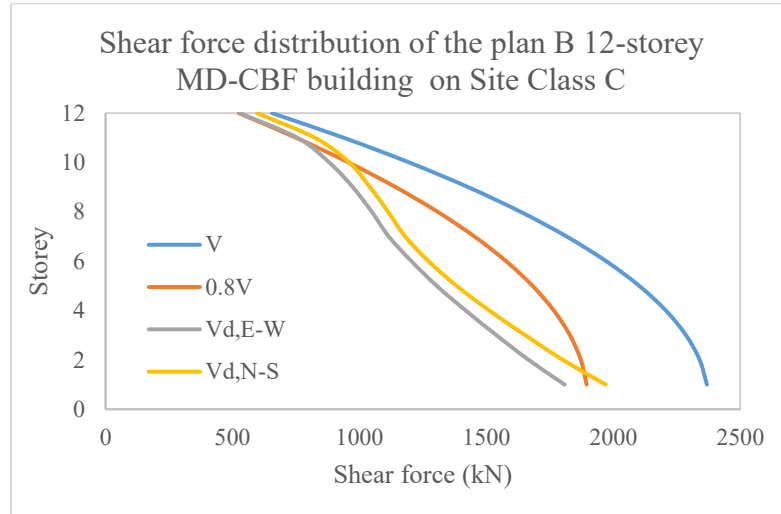
Figure A.10: Storey shear distribution over the building height: 12-st MD-CBF building, plan "B", Site Class C.
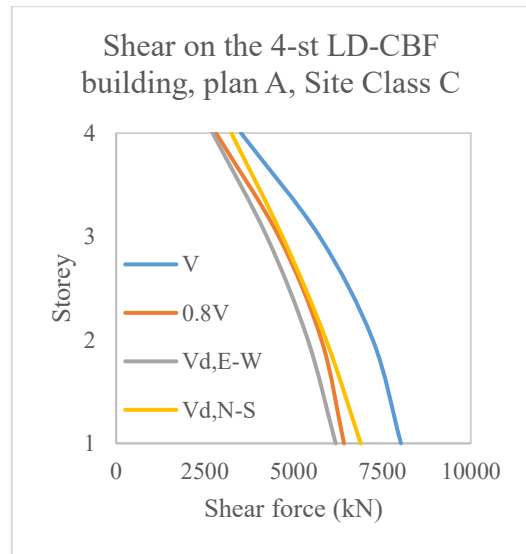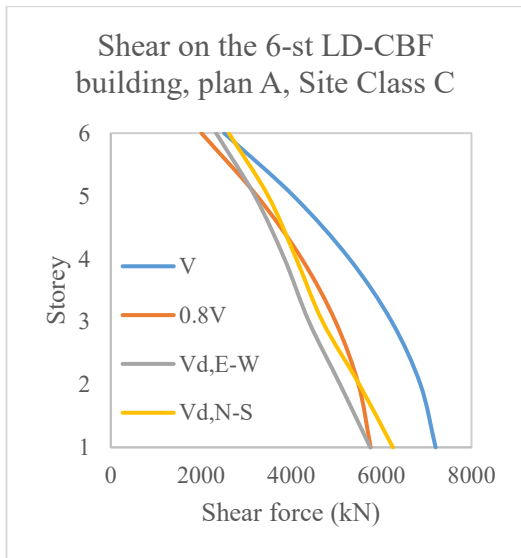
The periods of the 12-storey MD-CBF building, plan "B", on Site Class B are: $T_{E-W} = 2.92$ s and $T_{N-S} = 2.82$ s. The periods of the 10-storey are: $T_{E-W} = 2.45$ s and $T_{N-S} = 2.30$ s. The results for the 8-storey building are: $T_{E-W} = 1.88$ s and $T_{N-S} = 1.83$ s. The shear distribution of these buildings is shown in **Figure A.12**, **Figure A.13**a and **Figure A.13**b.
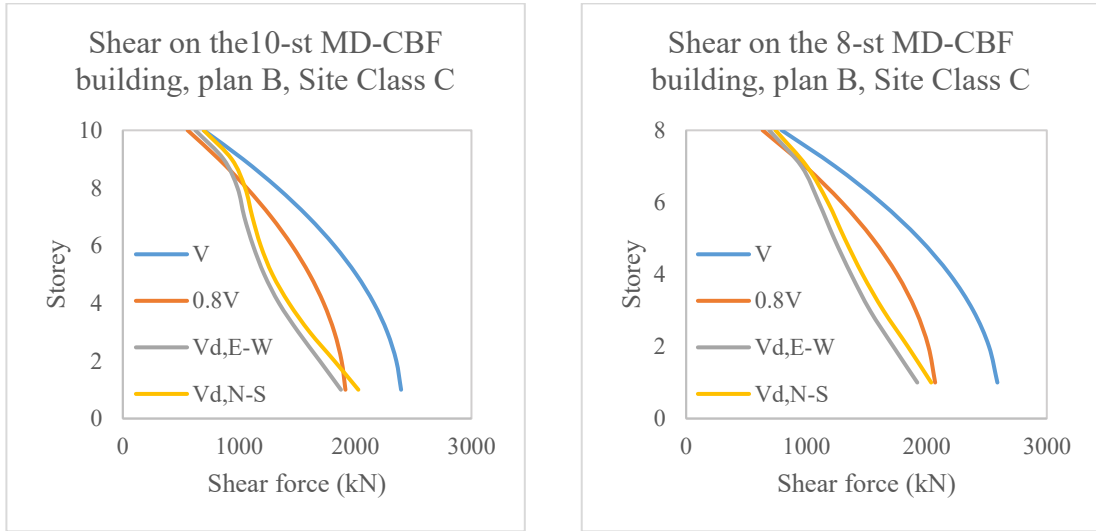
a)   b)

Figure A.11: Shear distribution over the building height: a) 10-storey MD-CBF building, plan "B", Site Class C, b) 8-storey MD-CBF building, plan "B", Site Class C.

The periods of the plan "B", 12-storey MD-CBF building on Site Class B are $T_{E-W} = 2.92$ s and $T_{N-S} = 2.82$ s.
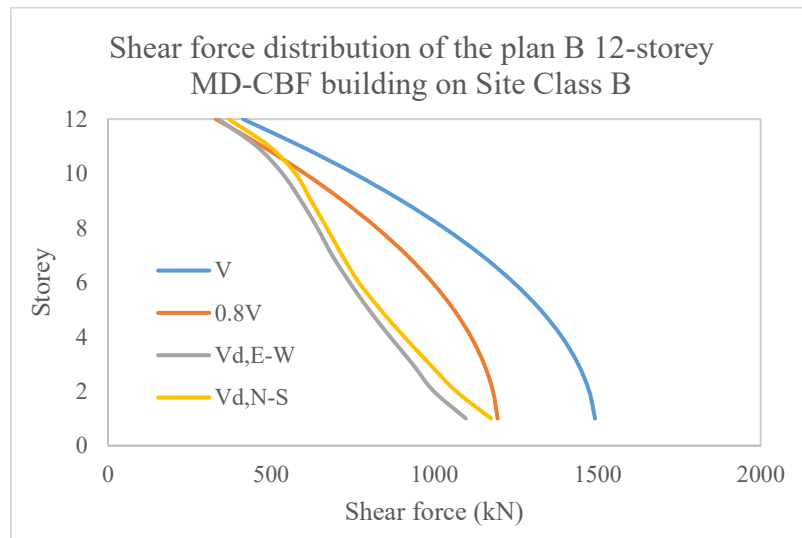
Figure A.12: Shear distribution over the building height: 12-storey MD-CBF building, plan "B", Site Class B.
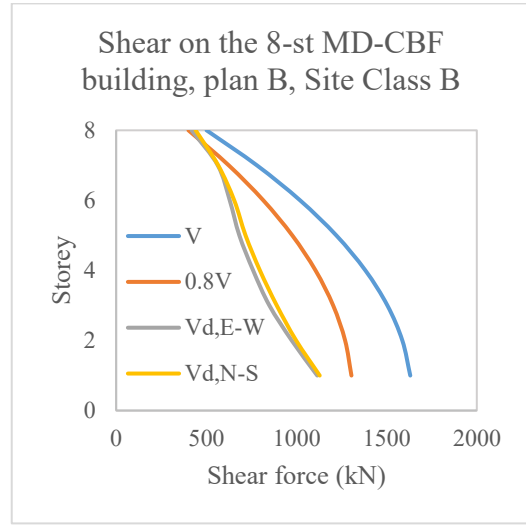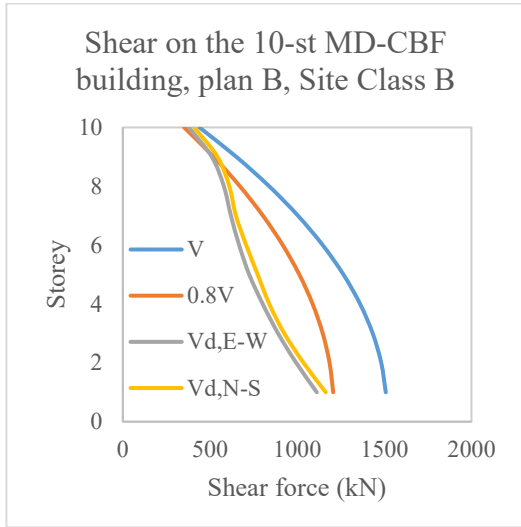
a)   b)

Figure A.13: Shear distribution over the building height: a) 10-storey MD-CBF building, plan "B", Site Class B, b) 8-storey MD-CBF building, plan "B", Site Class B.

APPENDIX B

DETAILED WIND DESIGNS

Appendix B shows the detailed wind calculation as an example of two buildings in the study of Tamura et al. (2003).

1. THE BUILDINGS OF TAMURA ET AL. (2003)

The dimension of the chosen buildings in the study of Tamura et al. (2003) is $B \times L \times H = 30\ m \times 42.5\ m \times 12.5\ m$ and $B \times L \times H = 20m \times 50\ m \times 50\ m$. The former building is lower than 20 m and has the ratio $H/B = 12.5/30 < 1$; therefore, it is categorized as low-rise building. The latter is classified as a medium-rise building because: $H > 20\ m$ and $H/B = 50/20 < 1$.

The low-rise building is assumed to have 4 storeys: the height of the first storey is 3.5 m and the typical storey height is 3 m. 2 CBFs are located in each major direction. The medium-rise building is assumed to be a 12-story building with typical storey height of 3.6 m. The plans of the two buildings are shown in **Figure B.1** and **Figure B.5**.

All beam to beam, beam to column, brace to beam and to column connections are pinned. All beams and columns are made of CSA G.40.21-350W steel with $F_u = 450\ MPa$ and $F_y = 345\ MPa$.

1.1. THE 50 M-HIGH BUILDING

This building is classified as a medium-rise office building. The typical floor plan and CBF elevation are shown in **Figure B.1**. For gravity design, dead load, live load and snow load remain the same as given in **Table 3.2**. The building is designed under gravity and earthquake loads as shown in Chapter 3. The natural frequency of this building is: $f_n = 0.29\ Hz$.
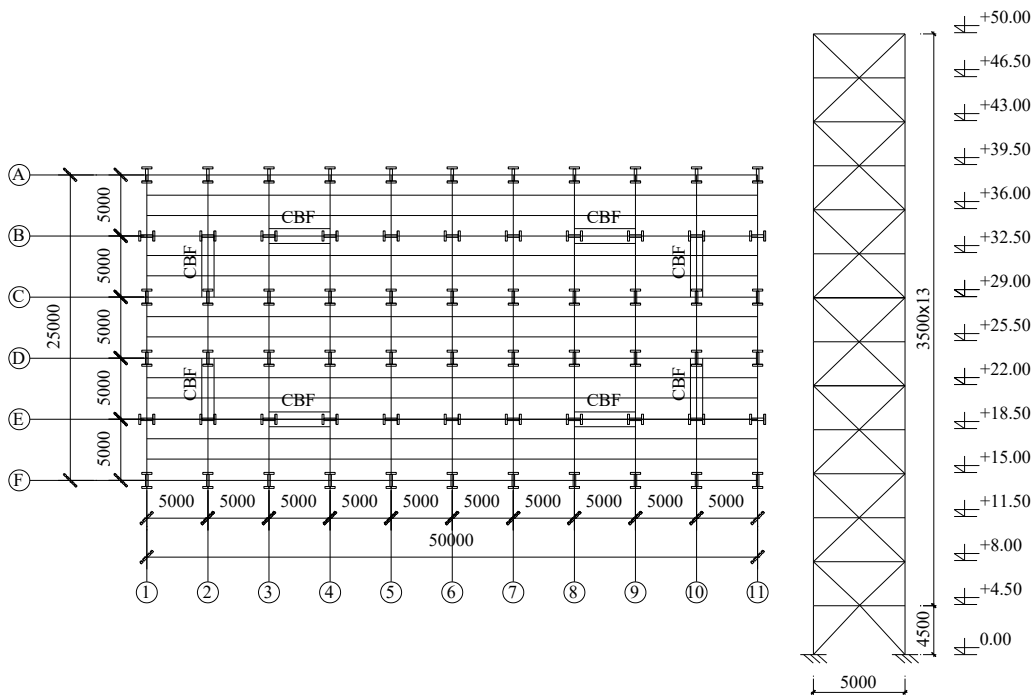
Figure B.1: Typical horizontal plan and CBF elevation of the 50 m high building.

1.1.1. NBCC 2015

By knowing the building configurations and its natural frequency, the appropriate wind computing procedure can be determined following the flow chart in **Figure 2.1**. The current building has:

$$\begin{cases} H = 50\,m < 60\,m \\ \dfrac{H}{w} = \dfrac{50}{25} = 2 < 4 \\ f_n = 0.29\,Hz < 1\,Hz \end{cases}$$

Based on these conditions, the dynamic procedure is chosen. Equation (2-14) is used to calculate the wind pressure. As given in the study, the building is located in the urban terrain area. Therefore, the exposure factor, C_e, is computed corresponding to Exposure B as following:

$$C_e = 0.5 \left(\frac{h}{12.7}\right)^{0.5} \quad for \; 0.5 \le C_e \le 2.5 \tag{B-1}$$

The gust factor, C_g, is given as:

$$C_g = 1 + g_p(\sigma/\mu) \tag{B-2}$$

The value of σ/μ, can be computed by the following formulas:

$$\frac{\sigma}{\mu} = \sqrt{\frac{K}{C_{eH}}\left(B + \frac{sF}{\beta}\right)} \tag{B-3}$$

$$s = \frac{\pi}{3}\left[\frac{1}{1 + \dfrac{8f_n H}{3V_H}}\right]\left[\frac{1}{1 + \dfrac{10f_n w}{V_H}}\right] \tag{B-4}$$

$$F = \frac{(1220f_n/V_H)^2}{[1 + (1220f_n/V_H)^2]^{4/3}} \tag{B-5}$$

$$V_H = \bar{V}\sqrt{C_{eH}} \tag{B-6}$$

$$\bar{V} = \sqrt{\frac{2I_w q}{\rho}C_{eH}} \tag{B-7}$$

where g_p is the peak factor; K is a factor related to the surface roughness coefficient of the terrain and is 0.1 for rough terrain; C_{eH} is the exposure factor evaluated at the top of the

building, which is $C_e = 0.5(50/12.7)^{0.5} = 0.99$; B is the background turbulence factor, which is found in Figure 4.1.7.8, NBCC 2015, to be 0.85 in E-W direction and 0.475 in N-S direction; f_n is the fundamental frequency, which is 0.28 Hz in E-W direction and 0.29 Hz in N-S direction; s is the size reduction factor, which is 0.85 in E-W direction and 0.475 in N-S direction; F is the gust energy ratio at the natural frequency of the structure, which is 0.172 in E-W direction and 0.169 in N-S direction; β is the critical damping ratio in the along-wind direction, which is 0.01 for steel structure; H is the height of the building; $\bar{V}$ is the reference wind speed at a height of 10 m in m/s, which is 25.39 m/s; V_H is the mean wind the speed at the top of the structure, which is 25.28 m/s; w is the effective width of windward face of the building. Consequently, the gust factor, C_g is found:

$$C_{g,W-E} = 1 + 3.71 \times 0.525 = 2.95 \; in \; E-W \; direction$$

$$C_{g,N-S} = 1 + 3.72 \times 0.387 = 2.44 \; in \; N-S \; direction$$

Topographic factor, C_t, is taken as 1 as the building is not located on hills or escarpments or there is no slope.

The external pressure, C_p, is determined by following Figures A-4.1.7.5.(2) and (3), NBCC 2015. In windward walls, C_p is expressed by:

$$\begin{cases} C_p = 0.6 \; for \; H/D < 0.25 \\ C_p = 0.27(H/D + 2) \; for \; 0.25 \le H/D < 1 \\ C_p = 0.8 \; for \; H/D \ge 1 \end{cases}$$

In leeward walls, it is:

$$\begin{cases} C_p = -0.3 \; for \; H/D < 0.25 \\ C_p = -0.27(H/D + 0.88) \; for \; 0.25 \le H/D < 1 \\ C_p = -0.5 \; for \; H/D \ge 1 \end{cases}$$

Therefore, the fraction of building height over the along-wind dimension, H/D, is required

to determine C_p. In windward walls:

$$\begin{cases} \dfrac{H}{D} = \dfrac{50}{50} = 1 \ (E - W \ direction) \rightarrow C_p = 0.8 \\ \dfrac{H}{D} = \dfrac{50}{25} = 2 \ (N - S \ direction) \rightarrow C_p = 0.8 \end{cases}$$

In leeward walls:

$$\begin{cases} C_p = -0.5 \ (E - W \ direction) \\ C_p = -0.5 \ (N - S \ direction) \end{cases}$$

The value of reference velocity pressure, q, is determined for Montreal, which is 0.42 kPa.

Topographic factor, C_t, is taken as 1. The importance factor, I_w, is 1 because the building

is grouped in normal importance category and ultimate limit state is used.

Table B.1 and **Table B.2** summarize the calculations of parameters and the wind pressures

yielded in both orthogonal directions of the studied building.

Table B.1: Parameters and wind pressure in E-W direction for the 50 m high building of

Tamura et al. (2003) according to Dynamic procedure (NBCC 2015).

Story	$\dfrac{h}{m}$	C_p-windward	C_p-leeward	C_e	C_g	C_t	I_w	$\dfrac{q}{kPa}$	$\dfrac{p}{kPa}$
14	50	0.80	-0.50	0.99	2.44	1	1	0.42	1.14
13	46.5	0.80	-0.50	0.96	2.44	1	1	0.42	1.10
12	43	0.80	-0.50	0.92	2.44	1	1	0.42	1.06
11	39.5	0.80	-0.50	0.88	2.44	1	1	0.42	1.01
10	36	0.80	-0.50	0.84	2.44	1	1	0.42	0.97
9	32.5	0.80	-0.50	0.80	2.44	1	1	0.42	0.92
8	29	0.80	-0.50	0.76	2.44	1	1	0.42	0.87
7	25.5	0.80	-0.50	0.71	2.44	1	1	0.42	0.82
6	22	0.80	-0.50	0.66	2.44	1	1	0.42	0.76
5	18.5	0.80	-0.50	0.60	2.44	1	1	0.42	0.69
4	15	0.80	-0.50	0.54	2.44	1	1	0.42	0.63
3	11.5	0.80	-0.50	0.50	2.44	1	1	0.42	0.58
2	8	0.80	-0.50	0.50	2.44	1	1	0.42	0.58
1	4.5	0.80	-0.50	0.50	2.44	1	1	0.42	0.58

Table B.2: Parameters and wind pressure in N-S direction for the 50 m high building of

Tamura et al. (2003) according to Dynamic procedure (NBCC 2015).

Story	$\dfrac{h}{m}$	C_p windward	C_p leeward	C_e	C_g	C_t	I_w	$\dfrac{q}{kPa}$	$\dfrac{p}{kPa}$
14	50	0.80	-0.50	0.99	2.95	1	1	0.42	1.28
13	46.5	0.80	-0.50	0.96	2.95	1	1	0.42	1.23
12	43	0.80	-0.50	0.92	2.95	1	1	0.42	1.19
11	39.5	0.80	-0.50	0.88	2.95	1	1	0.42	1.14
10	36	0.80	-0.50	0.84	2.95	1	1	0.42	1.09
9	32.5	0.80	-0.50	0.80	2.95	1	1	0.42	1.03
8	29	0.80	-0.50	0.76	2.95	1	1	0.42	0.97
7	25.5	0.80	-0.50	0.71	2.95	1	1	0.42	0.91
6	22	0.80	-0.50	0.66	2.95	1	1	0.42	0.85
5	18.5	0.80	-0.50	0.60	2.95	1	1	0.42	0.78
4	15	0.80	-0.50	0.54	2.95	1	1	0.42	0.70
3	11.5	0.80	-0.50	0.50	2.95	1	1	0.42	0.65
2	8	0.80	-0.50	0.50	2.95	1	1	0.42	0.65
1	4.5	0.80	-0.50	0.50	2.95	1	1	0.42	0.65

As permitted in NBCC 2015 for medium-rise buildings, the most critical wind-induced effects are determined by examining 4 partial loading cases. The wind pressure and the corresponding tributary area of each load case are illustrated as following.

In Case A, the wind pressure is applied fully on all wall faces separately in each major direction. To determine the tributary area, the tributary height and width are needed. The former is equal to 100% the horizontal dimension perpendicular to the wind direction. The tributary height is determined as shown in **Figure B.2**. In particular, the tributary areas of the top story, the typical story and the first story in E-W direction are shown in the following equations:

$$A_{top,E-W} = \frac{3.5}{2} \times 25 = 43.75 \; m^2; A_{top,N-S} = \frac{3.5}{2} \times 50 = 87.5 \; m^2$$

$$A_{typ,E-W} = \frac{3.5 + 3.5}{2} \times 25 = 87.5 \; m^2; A_{typ,N-S} = \frac{3.5 + 3.5}{2} \times 50 = 175 \; m^2$$

$$A_{first,E-W} = \frac{3.5 + 4.5}{2} \times 25 = 100 \; m^2; A_{first,N-S} = \frac{3.5 + 4.5}{2} \times 50 = 200 \; m^2$$
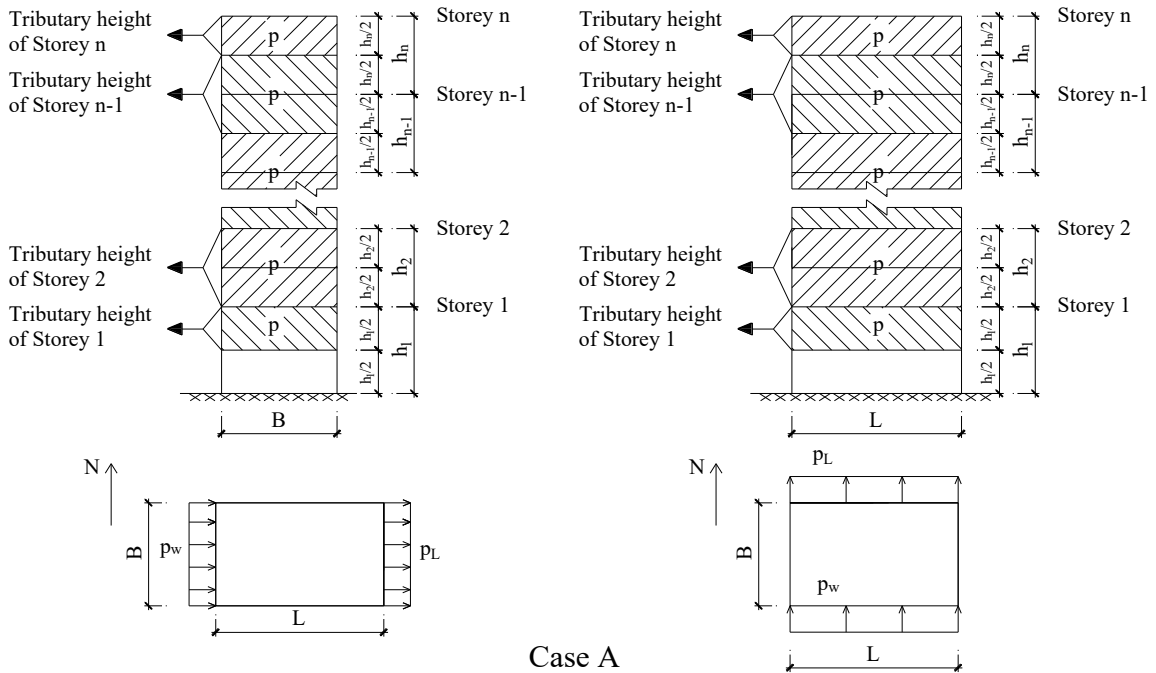
Figure B.2: Tributary area for partial loading Case A – NBCC 2015.

The same procedure is applied for the N-S direction. After having determined the tributary area, the wind load results from the product of wind pressure and the corresponding tributary area. The wind pressure in Case A is equal to 100% of the values given in **Table B.2**. For instance, the wind force applied on the 10th storey (a typical storey) is: $W_{10,E-W} = 1.36\ kPa \times 87.5\ m^2 = 118.79\ kN$.

Because the building is symmetrical, no torsion is created in Case A. The resulted wind pressure, tributary area and the wind loads in both E-W and N-S directions for load Case A are shown on **Table B.3**.

Table B.3: Tributary areas and wind-induced storey shears for the 50 m high building of Tamura et al. (2003) – Case A – according to Dynamic procedure (NBCC 2015).

Story	p	Tributary area		Wind load		Wind base shear	
		E-W	N-S	E-W	N-S	E-W	N-S
	kPa	m²	m²	kN	kN	kN	kN
14	1.28	43.75	87.5	70.00	115.85	56	100
13	1.23	87.5	175	135.01	223.43	164	292
12	1.19	87.5	175	129.83	214.86	268	478
11	1.14	87.5	175	124.43	205.93	367	655
10	1.09	87.5	175	118.79	196.60	462	825
9	1.03	87.5	175	112.87	186.80	553	986
8	0.97	87.5	175	106.62	176.45	638	1138
7	0.91	87.5	175	99.98	165.46	718	1280
6	0.85	87.5	175	92.86	153.69	792	1413
5	0.78	87.5	175	85.16	140.93	860	1534
4	0.70	87.5	175	76.68	126.90	922	1644
3	0.65	87.5	175	70.56	116.77	978	1745
2	0.65	87.5	175	70.56	116.77	1035	1845
1	0.65	100	200	80.64	133.45	1099	1960

The maximum shear in each direction is considered in shear coefficient computation.

$$C_{V,E-W} = \frac{V}{q_H BL} = \frac{V}{qC_e BL} = \frac{1099}{0.42 \times 0.99 \times 25 \times 50} = 2.11$$

$$C_{V,N-S} = \frac{V}{q_H BL} = \frac{V}{qC_e BL} = \frac{1960}{0.42 \times 0.99 \times 25 \times 50} = 3.76$$

According to the recommendation in Chapter 4, the maximum torsions can be obtained in Case B when the wind pressure is applied on half of the wall faces. Therefore, the tributary area in E-W direction for Case B is taken as half of Case A. The tributary area in Case B is described in **Figure B.3**.

$$A_{top,E-W} = \frac{3.5}{2} \times \frac{25}{2} = 21.88 \ m^2; A_{top,N-S} = \frac{3.5}{2} \times \frac{50}{2} = 43.75 \ m^2$$

$$A_{typ,E-W} = \frac{3.5 + 3.5}{2} \times \frac{25}{2} = 43.75 \; m^2; A_{typ,N-S} = \frac{3.5 + 3.5}{2} \times \frac{50}{2} = 87.5 \; m^2$$

$$A_{first,E-W} = \frac{3.5 + 4.5}{2} \times \frac{25}{2} = 50 \; m^2; A_{first,N-S} = \frac{3.5 + 4.5}{2} \times \frac{50}{2} = 100 \; m^2$$
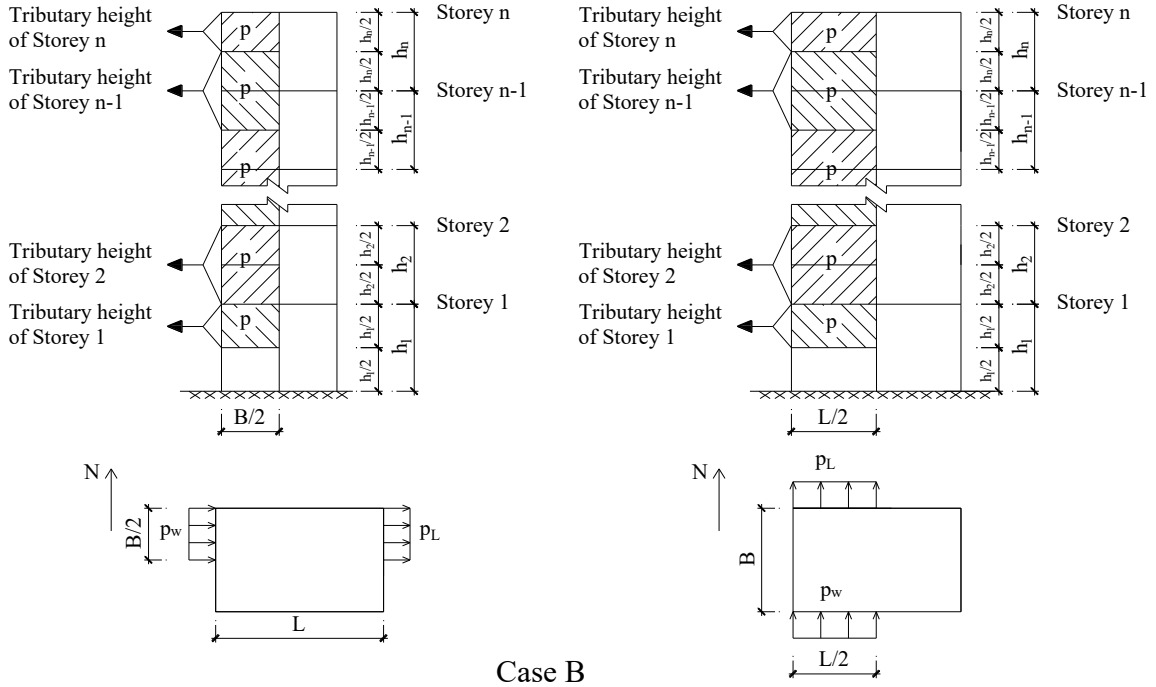
Case B

Figure B.3: Tributary area for partial loading Case B.

Torsional effects are created from the unbalance of wind pressure:

$$T = W \times e$$

where W is the wind load and e is the eccentricity of wind load, which is equal to $B/4 = 25/4 = 6.25 \; m$ in E-W direction and $L/4 = 50/4 = 12.5 \; m$ in N-S direction. Torsions are computed separately in each direction according to the definition of this load case. For example, the wind force applied on the 10th storey (a typical storey) is: $W_{10,E-W} = 0.97 \; kPa \times 43.75 \; m^2 = 42 \; kN$. The torsion in the same storey is: $T_{10,E-W} = 42 \; kN \times 6.25 \; m = 263 \; kNm$. The maximum wind-induced base shears and torsional moments

found in this case are: $W_{E-W} = 550\ kN$; $W_{N-S} = 980\ kN$ and $T = 12734\ kNm$. The

corresponding shear and torsional coefficients are: $C_{V,E-W} = 1.32$; $C_{V,N-S} = 2.18$ and

$$C_T = \frac{T}{q_H B^2 L} = \frac{T}{q C_e B^2 L} = \frac{12734}{0.42 \times 0.99 \times 25^2 \times 50} = 0.98$$

75% of the wind pressure is applied fully simultaneously on wall faces in Case C.

Therefore, the tributary area in this case is the same to Case A in both direction. No torsion

is created in this case. The maximum shear coefficients resulted from Case C is therefore

equal to 75% those of Case A: $C_{V,E-W} = 1.58$; $C_{V,N-S} = 2.82$.

Half of the wind pressure from Case C is reduced from part of the projected area in Case

D (**Figure B.4**). The tributary areas of the deducted wind pressure is equal to Case B, which

are:

$$A_{top,E-W,0.38p} = A_{top,E-W,0.75p} = \frac{3.5}{2} \times \frac{25}{2} = 21.88\ m^2;$$

$$A_{top,N-S,0.38p} = A_{top,N-S,0.75p} = \frac{3.5}{2} \times \frac{50}{2} = 43.75\ m^2$$

$$A_{typ,E-W,0.38p} = A_{typ,E-W,0.75p} = \frac{3.5 + 3.5}{2} \times \frac{25}{2} = 43.75\ m^2;$$

$$A_{typ,N-S,0.38p} = A_{typ,N-S,0.75p} = \frac{3.5 + 3.5}{2} \times \frac{50}{2} = 87.5\ m^2$$

$$A_{first,E-W,0.38p} = A_{first,E-W,0.75p} = \frac{3.5 + 4.5}{2} \times \frac{25}{2} = 50\ m^2;$$

$$A_{first,N-S,0.38p} = A_{first,N-S,0.75p} = \frac{3.5 + 4.5}{2} \times \frac{50}{2} = 100\ m^2$$
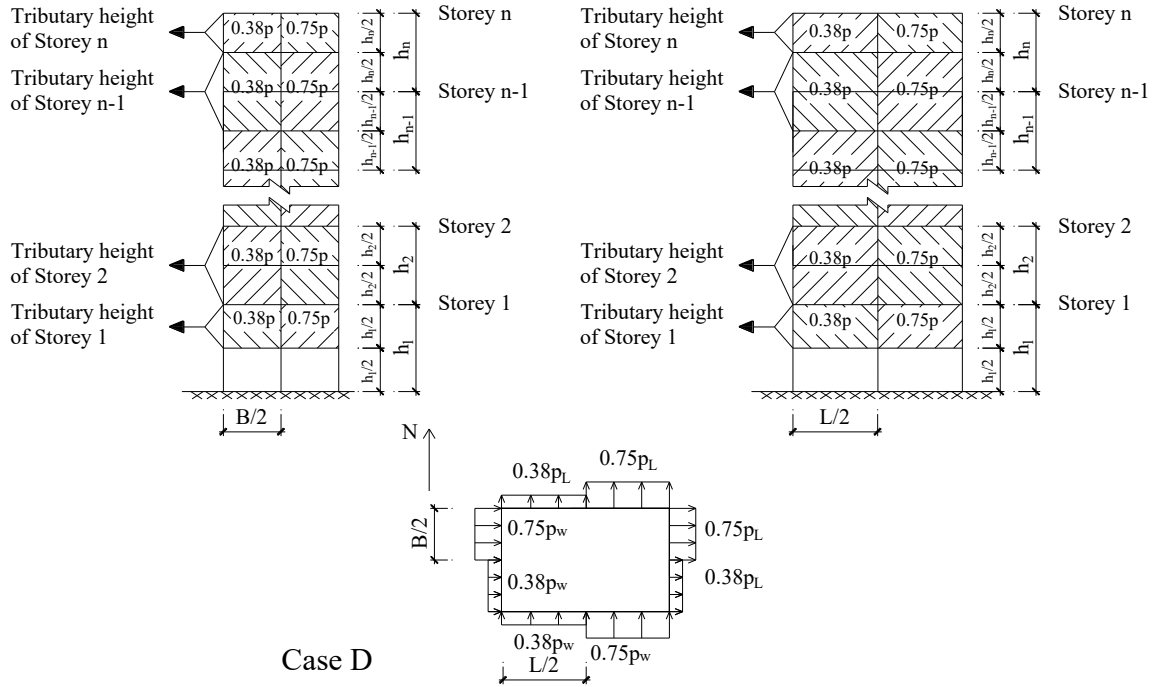
Figure B.4: Tributary area for partial loading Case D.

The torsional moments are computed as:

$$T = W_{E-W} \times e_{E-W} + W_{N-S} \times e_{N-S}$$

where W_{E-W} and W_{N-S} are the wind loads in E-W and N-S directions, respectively; e_{E-W} and e_{N-S} are the corresponding eccentricities of the wind loads and equal to $B/4 = 6.25\ m$ in E-W direction and $L/4 = 12.5\ m$ in N-S direction. Torsions from both orthogonal directions are added together in this load case. For example, the shears and torsion due to wind load on the 10th storey are:

$$W_{10,E-W} = (0.75 \times 1.36\ kPa + 0.38 \times 1.36\ kPa) \times 43.75\ m^2 = 66.82\ kN$$

$$W_{10,N-S} = (0.75 \times 1.12\ kPa + 0.38 \times 1.12\ kPa) \times 87.5\ m^2 = 110.59\ kN$$

$$T_{10} = 0.75{\times}1.36\ kPa{\times}43.75\ m^2{\times}6.25\ m + 0.75{\times}1.12\ kPa{\times}87.5\ m^2{\times}12.5\ m$$

$$- 0.38{\times}1.36\ kPa{\times}43.75\ m^2{\times}6.25\ m$$

$$- 0.38{\times}1.12\ kPa{\times}87.5\ m^2{\times}12.5\ m = 599.98\ kNm$$

The normalized shear and torsional coefficients in Case D are: $C_{V,E-W} = 1.48$; $C_{V,N-S} = 2.46$; $C_T = 0.53$.

The shear and torsional coefficients are compared within all 4 partial loading cases and only two highest base shears and the maximum base torsion are selected for the comparisons shown in Chapter 4. **Table B.4** summarizes the results from all cases and the maximum results are bolded.

Table B.4: Maximum shear and torsions regarding the dynamic procedure NBCC 2015 in E-W and N-S directions – 50 m high building of Tamura et al. (2003).

	Base shear		Base torsion			C_V		C_T		
	E-W	N-S	E-W	N-S	Combined	E-W	N-S	E-W	N-S	Combined
	kN	kN	kNm	kNm	kNm					
Case A	**1099**	**1960**				**2.11**	**3.76**			
Case B	687	1137	3847	**12735**		1.32	2.18	0.30	**0.98**	
Case C	824	1470				1.58	2.82			
Case D	773	1279			6940	1.48	2.46			0.53

1.1.2. ASCE/SEI 7-10

As permitted by ASCE/SEI 7-10, the Directional Procedure can be used for building of all heights. At the same time, the Envelope Procedure is limited only for low-rise buildings. Therefore, the Directional Procedure, is chosen to compute wind loads of the current building.

To start, Equation (2-19) is used to compute the wind pressure. According to the assumptions made previously, the current building is enclosed. As a result, the peak internal pressure coefficient, (GC_{pi}), is equal to 0. The gust factor, G, is determined differently between flexible and rigid structures. The ASCE/SEI 7-10 stipulates that buildings that have natural frequency greater than $1\ Hz$ are considered flexible, while those that are lesser than $1\ Hz$ are rigid buildings. The natural frequency of this building is found to be $0.285\ Hz < 1\ Hz$. Consequently, the current structure is classified as flexible. For flexible structures, the gust factor, G, is given, accordingly:

$$G_f = 0.925 \left(\frac{1 + 1.7 I_{\bar{z}} \sqrt{g_Q^2 Q^2 + g_R^2 R^2}}{1 + 1.7 g_v I_{\bar{z}}} \right) \tag{B-8}$$

g_Q and g_v are taken as 3.4 and g_R is calculated by

$$g_R = \sqrt{2 \ln(3600 n_1)} + \frac{0.577}{\sqrt{2 \ln(3600 n_1)}} \tag{B-9}$$

R is the resonant response factor and is given by:

$$R = \sqrt{\frac{1}{\beta} R_n R_h R_B (0.53 + 0.47 R_L)} \tag{B-10}$$

$$R_n = \frac{7.47 N_1}{(1 + 10.3 N_1)^{5/3}} \tag{B-11}$$

$$N_1 = \frac{n_1 L_{\bar{z}}}{\bar{V}_{\bar{z}}} \tag{B-12}$$

$$R_\ell = \frac{1}{\eta} - \frac{1}{2\eta^2} (1 - e^{-2\eta}) \ for\ \eta > 0 \tag{B-13}$$

$$R_\ell = 1 \; for \; \eta = 0 \qquad\qquad (B\text{-}14)$$

where the subscript ℓ can be taken as h, B and L, respectively.

n_1 is the fundamental natural frequencies of the building, which are 0.294 Hz and 0.285 Hz in E-W and N-S direction, respectively.

$R_\ell = R_h$ setting $\eta = 4.6n_1h/\overline{V}_{\bar{z}}$

$R_\ell = R_B$ setting $\eta = 4.6n_1B/\overline{V}_{\bar{z}}$

$R_\ell = R_L$ setting $\eta = 15.4n_1L/\overline{V}_{\bar{z}}$

$\overline{V}_{\bar{z}}$ is the mean hourly wind speed at height $\bar{z}$ and is determined as

$$\overline{V}_{\bar{z}} = \bar{b}\left(\frac{\bar{z}}{10}\right)^{\bar{\alpha}} V \qquad\qquad (B\text{-}15)$$

where $\bar{b}$ and $\bar{\alpha}$ are constant listed in **Table B.5**. All values are taken for exposure B, which corresponds to suburban terrain. V is basic wind speed in m/s.

Table B.5: Parameters for open-terrain and urban-terrain exposures – ASCE/SEI 7-10.

Exposure	α	z_g	$\hat{a}$	$\hat{b}$	$\bar{\alpha}$	$\bar{b}$	c	ℓ (m)	$\bar{\epsilon}$	z_{min} (m)
B	7	365.76	1/7	0.84	1/4	0.45	0.3	97.54	1/3	9.14
C	9.5	274.32	1/9.5	1	1/6.5	0.65	0.2	152.4	1/5	4.57

All ASCE/SEI 7-10 values are multiplied by 1.53^2 due to the difference between the 3-second and 1-hour wind speed used in ASCE/SEI 7-10 and NBCC 2015, respectively. The reference wind velocity pressure in Montreal is determined to be $0.42 \, kPa$ or $0.42 \times 10^{-3} \, Pa$. This pressure is equal to a wind speed of:

$$v = \sqrt{\frac{2q}{r_{h0}}} = \sqrt{\frac{2 \times 0.42 \times 10^{-3} Pa}{1.2929 kg/m^3}} = 25.48 m/s$$

This wind speed is calculated over 1 hour and needs to be multiplied by 1.53 to obtain the speed computed for 3 seconds as prescribed in ASCE/SEI 7-10.

$$V = v \times 1.53 = 25.48 \times 1.53 = 39.1 m/s$$

Therefore, the wind velocity is considered 39.1 m/s for Montreal.

The gust factors were found to be 1.09 and 1.23 for E-W and N-S direction, respectively.

The velocity pressure, q, is evaluated at height z above the ground for windward walls, and at height h for leeward walls. They are given as:

$$q = q_w = q_z = 0.613 K_z K_{zt} K_d V^2 \tag{B-16}$$

$$q = q_l = q_h = 0.613 K_z K_{zt} K_d V^2 \tag{B-17}$$

According to Figure 27.4-1 (ASCE/SEI 7-10), the external pressure coefficient, C_p, is 0.8 for flat roof buildings in windward walls and -0.5 for leeward walls in E-W direction and -0.3 in N-S direction. The topographic factor and the directionality factor are taken as 1 and 0.85, respectively. The velocity pressure exposure coefficient, K_d, is determined differently with different exposure terrains:

$$9.7m < z < z_g : K_z = 2.01 \left(\frac{z}{z_g}\right)^{2/\alpha} \tag{B-18}$$

Equation (B-18) is specified for buildings that are higher than $9.7\ m$. Urban and suburban areas, wooded areas, or areas with closely spaced obstructions are defined as Exposure B in ASCE/SEI 7-10. At the same time, open terrain with scattered obstructions with height

smaller than approximately 9.14 m is classified as Exposure C. The values of z_g and α are different for each category and are presented in **Table B.5**.

The summary of wind pressure computations following the Directional Procedure in ASCE/SEI 7-10 is given in **Table B.6** and **Table B.7**.

.**Table B.6:** Wind pressure E-W direction - 50 m high building of Tamura et al. (2003) – according to Directional Procedure (ASCE/SEI 7-10).

Story	K_d	K_z windward	K_z leeward	K_{zt}	G	V m/s	C_p windward	C_p leeward	p kPa
14	0.85	1.14	1.14	1	1.09	39.1	0.8	-0.3	0.92
13	0.85	1.11	1.14	1	1.09	39.1	0.8	-0.3	0.91
12	0.85	1.09	1.14	1	1.09	39.1	0.8	-0.3	0.89
11	0.85	1.06	1.14	1	1.09	39.1	0.8	-0.3	0.88
10	0.85	1.04	1.14	1	1.09	39.1	0.8	-0.3	0.86
9	0.85	1.01	1.14	1	1.09	39.1	0.8	-0.3	0.84
8	0.85	0.97	1.14	1	1.09	39.1	0.8	-0.3	0.82
7	0.85	0.94	1.14	1	1.09	39.1	0.8	-0.3	0.80
6	0.85	0.90	1.14	1	1.09	39.1	0.8	-0.3	0.78
5	0.85	0.86	1.14	1	1.09	39.1	0.8	-0.3	0.76
4	0.85	0.81	1.14	1	1.09	39.1	0.8	-0.3	0.73
3	0.85	0.75	1.14	1	1.09	39.1	0.8	-0.3	0.69
2	0.85	0.67	1.14	1	1.09	39.1	0.8	-0.3	0.65
1	0.85	0.58	1.14	1	1.09	39.1	0.8	-0.3	0.59

Table B.7: Wind pressure N-S direction- 50 m high building of Tamura et al. (2003) – according to Directional Procedure (ASCE/SEI 7-10).

Story	K_d	K_z windward	K_z leeward	K_{zt}	G	$\frac{V}{m/s}$	C_p windward	C_p leeward	$\frac{p}{kPa}$
14	0.85	1.14	1.14	1	1.01	39.1	0.8	-0.5	1.05
13	0.85	1.11	1.14	1	1.01	39.1	0.8	-0.5	1.04
12	0.85	1.09	1.14	1	1.01	39.1	0.8	-0.5	1.03
11	0.85	1.06	1.14	1	1.01	39.1	0.8	-0.5	1.01
10	0.85	1.04	1.14	1	1.01	39.1	0.8	-0.5	1.00
9	0.85	1.01	1.14	1	1.01	39.1	0.8	-0.5	0.98
8	0.85	0.97	1.14	1	1.01	39.1	0.8	-0.5	0.96
7	0.85	0.94	1.14	1	1.01	39.1	0.8	-0.5	0.94
6	0.85	0.90	1.14	1	1.01	39.1	0.8	-0.5	0.92
5	0.85	0.86	1.14	1	1.01	39.1	0.8	-0.5	0.89
4	0.85	0.81	1.14	1	1.01	39.1	0.8	-0.5	0.87
3	0.85	0.75	1.14	1	1.01	39.1	0.8	-0.5	0.83
2	0.85	0.67	1.14	1	1.01	39.1	0.8	-0.5	0.79
1	0.85	0.58	1.14	1	1.01	39.1	0.8	-0.5	0.73

4 wind loading cases are considered following the Directional procedure. For Case 1, for example, the wind-induced shears in both directions of the 10th storey are:

$$W_{10,E-W} = 0.86 \; kPa{\times}87.5 \; m^2 = 75 \; kN$$

$$W_{10,N-S} = 1 \; kPa{\times}175 \; m^2 = 175 \; kN$$

The shears are summed by adding the values of all 14 storeys at the base level. The maximum shears are $W_{E-W} = 1108.46 \; kN$ and $W_{N-S} = 2503.66 \; kN$. These two shear values are then normalized as following:

$$C_{V,E-W} = \frac{V}{q_H BL} = \frac{W_{E-W}}{qK_h BL} = \frac{940}{0.42{\times}1.14{\times}25{\times}50} = 1.57$$

$$C_{V,N-S} = \frac{V}{q_H BL} = \frac{W_{N-S}}{qK_h BL} = \frac{2208}{0.42{\times}1.14{\times}25{\times}50} = 3.69$$

Here, the exposure factor is defined as K_z instead of C_e as in the case of NBCC 2015.

In Case 2, the wind pressures are separately applied on wall faces in E-W and N-S directions. According to **Figure 2.4**, the shear values in this case are 75% of the wind loads given in Case 1. Therefore, the shear coefficients are $C_{V,E-W} = 1.39$ and $C_{V,N-S} = 3.14$.

There are two torsion values and they are computed as follows:

$$\begin{cases} M_{E-W} = 0.75(P_{w,E-W} + P_{l,E-W})B_{E-W}e_{E-W} \\ M_{N-S} = 0.75(P_{w,N-S} + P_{l,N-S})B_{N-S}e_{N-S} \end{cases}$$

where

$$\begin{cases} e_{E-W} = \pm0.15B_{E-W} = \pm0.15\times25 = \pm3.75 \ m \\ e_{N-S} = \pm0.15B_{N-S} = \pm0.15\times50 = \pm7.5 \ m \end{cases}$$

Torsions of the 10th storey is computed as an example:

$$\begin{cases} M_{10,E-W} = 0.75\times0.86\times3.5 \ m\times25 \ m\times\pm3.75 \ m = \pm212 \ kNm \\ M_{10,N-S} = 0.75\times1\times3.5 \ m\times50 \ m\times\pm7.5 \ m = \pm984 \ kNm \end{cases}$$

The maximum accumulated torsions at the base level are: $M_{E-W} = 2645 \ kNm$ and $M_{N-S} = 10025 \ kNm$. The torsion created in N-S direction is the maximum base torsion of Case 2 and it is chosen to determine the torsional coefficient:

$$C_T = \frac{T}{q_H B^2 L} = \frac{T}{q K_h B^2 L} = \frac{10025}{0.42\times1.14\times25^2\times50} = 0.67$$

The shears in Case 3 are 75% of Case 1 that apply simultaneously in both directions. Therefore, the shear coefficients are: $C_{V,E-W} = 1.39$ and $C_{V,N-S} = 3.14$.

In Case 4, shears are taken as 56.3% of Case 1 at the same time in both directions. The shear coefficients are taken accordingly as $C_{V,E-W} = 0.563\times1.57 = 0.89$ and $C_{V,N-S} =$

$0.563{\times}3.69 = 2.08$. The torsional moments and eccentricities are defined explicitly by ASCE/SEI 7-10:

$$M = 0.563\left(P_{w,E-W} + P_{l,E-W}\right)B_{E-W}E - W0.563(P_{w,N-S} + P_{l,N-S})B_{N-S}e_{N-S}$$

where

$$\begin{cases} e_{E-W} = \pm0.15B_{E-W} = \pm0.15{\times}25 = \pm3.75\ m \\ \ e_{N-S} = \pm0.15B_{N-S} = \pm0.15{\times}50 = \pm7.5\ m \end{cases}$$

Again, torsion in the 10$^{\text{th}}$ storey is computed as an example:

$$M_{10,E-W} = 0.563{\times}0.86{\times}3.5\ m{\times}25\ m{\times}\pm3.75\ m + 0.563{\times}1{\times}3.5\ m{\times}50\ m{\times}\pm7.5\ m$$

$$= \pm898\ kNm$$

Table B.8: Maximum shear and torsions regarding the Directional Procedure ASCE/SEI 7-10 in E-W and N-S directions – 50 m high building of Tamura et al. (2003).

	Base shear		Base torsion			C_V		C_T		
	E-W	N-S	E-W	N-S	Combined	E-W	N-S	E-W	N-S	Combined
	kN	kN	kNm	kNm	kNm					
Case 1	**940**	**2208**				**1.57**	**3.69**			
Case 2	831	1878	2645	**10025**		1.39	3.14	0.18	**0.67**	
Case 3	831	1878				1.39	3.19			
Case 4	529	1243			9223	0.89	2.08			0.62

Table B.8 summarize the results of all 4 cases regarding the Directional Procedure. Only the maximum values (bolded) are selected for the comparisons in Chapter 4.

1.2. THE 12.5 M-HIGH BUILDING

The 12.5 m building in the study of Tamura et al. (2003) is classified as a low-rise office building. For gravity design, dead load, live load and snow load are remained the same as

given in **Table 3.2**. The building is designed similar as described in Chapter 3. The natural frequency of the building is 1.38 Hz.
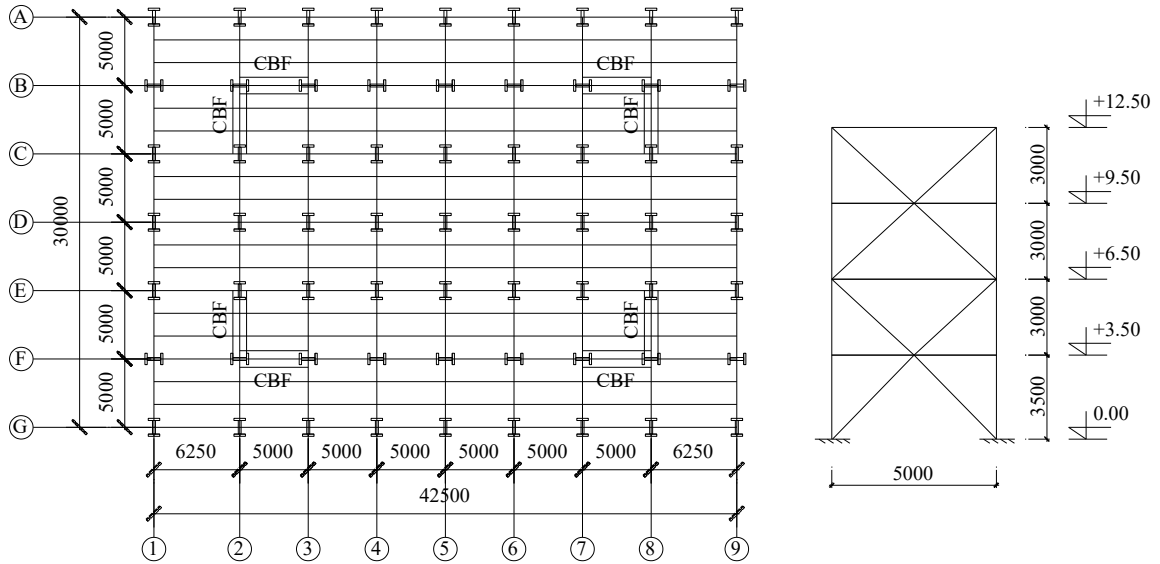
Figure B.5: Typical horizontal plan and CBF elevation of the 12.5 m high building.

1.2.1. NBCC 2015

Firstly, the appropriate procedure is determined so that the wind load computations can be carried out by considering the following conditions:

$$\begin{cases} H = 12.5\, m < 60\, m \\ \dfrac{H}{w} = \dfrac{12.5}{30} = 0.42 < 4 \\ f_n = 1.38\, Hz > 1\, Hz \end{cases}$$

Therefore, the static procedure is chosen. Furthermore, the building under consideration is classified as a low-rise building as building height is lower than 20 m and $H/D_s < 1$. Consequently, the procedure stipulated for low-rise buildings is applied.

The wind pressure is computed following Equation (2-14). As explained in Chapter 2, two load cases given in NBCC 2015 for low-rise buildings can be merged into one single load

case. According to the study of Tamura et al. (2003), the building is tested under different exposure conditions: open and urban-terrain. Therefore, the wind loads in the current study will be calculated for both conditions. The exposure factor, C_e, is computed as Equation (B-19) for the open-terrain and as Equation (B-20) for the case of urban-terrain.

$$C_e = max \begin{cases} (h/10)^{0.2} \\ 0.9 \end{cases} \tag{B-19}$$

$$C_e = max \begin{cases} 0.7(h/12)^{0.3} \\ 0.7 \end{cases} \tag{B-20}$$

The external peak values of $C_p C_g$ on low-rise building surfaces are determined regarding Figure 4.1.7.6.-A NBCC 2015. The values of the current building are for the case of flat-roof building ($0°$ roof slope). The value of reference velocity pressure, q, is determined for Montreal, where the building is assumed to locate in, which is 0.42 kPa. Topographic factor, C_t, is taken as 1 as the building is not located on hills or escarpments or there is no slope. The importance factor, I_w, is 1 for a building of normal importance category under ultimate limit state design. Wind pressures for each area are determined as following:

$$p_c = I_w q C_e C_t (C_{p1E} C_{g1E} - C_{p4E} C_{g4E}) \tag{B-21}$$

$$p_r = I_w q C_e C_t (C_{p1} C_{g1} - C_{p4} C_{g4}) \tag{B-22}$$

Torsion is created by the unbalance between wind loads on corner and the rest of the building wall. Equation (4-5) is used to compute wind-induced torsion in each floor in both orthogonal directions. The maximum base shear in each direction and the maximum torsion are selected to compute the shear and torsional coefficients.

The computed wind base shear and torsion is summarized in **Table B.9** and **Table B.10**.

Table B.9: Maximum shear and torsions in E-W and N-S directions – Urban-terrain – 12.5 m-high building of Tamura et al. (2003) – according to NBCC 2015.

Story	W_{E-W}	T_{E-W}	W_{N-S}	T_{N-S}	$C_{V,E-W}$	$C_{V,N-S}$	C_T
	kN	kNm	kN	kNm			
4	19.15	12.98	26.41	31.77			
3	56.99	25.65	78.58	94.55			
2	94.83	25.65	130.75	157.33			
1	135.82	27.78	187.26	225.34	0.33	0.47	0.019

Table B.10: Maximum shear and torsions in E-W and N-S directions – Open-terrain – 12.5 m-high building of Tamura et al. (2013) – according to NBCC 2015.

Story	W_{E-W}	T_{E-W}	W_{N-S}	T_{N-S}	$C_{V,E-W}$	$C_{V,N-S}$	C_T
	kN	kNm	kN	kNm			
4	28.26	19.16	38.97	46.89			
3	81.76	36.27	112.73	135.65			
2	131.35	33.61	181.11	217.93			
1	184.06	35.72	253.78	305.37	0.31	0.45	0.018

1.2.2. ASCE/SEI 7-10

For low-rise buildings, ASCE/SEI 7-10 stipulates that the wind loads can be computed with the appliance of either the Envelope Procedure or the Directional Procedure. Therefore, both procedures are used to determine wind loads. The results will be compared and only the maximum values are selected for the comparisons in Chapter 4.

1.2.2.1. Envelope Procedure

Due to the assumption that the building is enclosed, the wind-induced internal pressure is eliminated and Equation (2-20) becomes:

$$p = q_h \left(G C_{pf} \right) \tag{B-23}$$

q_h is the velocity pressure evaluated at mean roof height h, and is computed as following for SI:

$$q = q_w = q_z = 0.613 K_z K_{zt} K_d V^2 \qquad \text{(B-24)}$$

The natural frequency of the building is required to determine its rigidity. Based on the analysis ran on ETABS, the natural frequency of the building is $1.38\,Hz > 1\,Hz$. Therefore, the current building is classified as a rigid. The directionally factor for buildings is $K_d = 0.85$. The topographic factor for the building is taken as 1 and the wind velocity is considered to be $39.1\,m/s$, as illustrated previously for the 50 m-high building. The velocity pressure exposure coefficient, K_d, is determined by Equation (B-18).

The peak external pressure coefficient, (GC_{pf}), is determined from Figure 28.4-1 (ASCE/SEI 7-10). As similar to NBCC 2015, these values vary with the locations on wall faces. They are reported in **Table B.11**.

After the wind pressure is known, it will be multiplied by the corresponding tributary area to get the wind force. Wind force on each story is the summation of loads determined on the wall corner and the other part of the wall face.

Table B.11: (GC_{pf}) values for buildings in open-terrain exposure – ASCE/SEI 7-10.

GC_{pf1}	GC_{pf1E}	GC_{pf4}	GC_{pf4E}
0.4	0.61	-0.29	-0.43

Two additional torsional load cases are added in ASCE/SEI 7-10 comparing to NBCC 2015 to take into account the effects of torsion in low-rise buildings (**Figure 2.5**). In these cases, only 25% of wind pressure is placed on half of the building wall, which in turns create

greater torsions comparing to the Canadian provisions. The computed maximum wind base shear and torsion according to ASCE/SEI 7-10 are selected to calculate the shear and torsional coefficients. Results are reported in **Table B.12** and **Table B.13**.

Table B.12: Maximum shear and torsions - E-W and N-S directions – Urban-terrain – 12.5 m-high building of Tamura et al. (2003) – according to Envelope Procedure (ASCE/SEI 7-10).

Story	W_{E-W}	T_{E-W}	W_{N-S}	T_{N-S}	$C_{V,E-W}$	$C_{V,N-S}$	C_T
	kN	kNm	kN	kNm			
4	19.91	66.26	28.76	142.03			
3	59.73	198.79	86.29	426.09			
2	99.54	331.32	143.82	710.15			
1	142.68	474.90	206.15	1017.88	0.35	0.52	0.091

Table B.13: Maximum shear and torsions - E-W and N-S directions – Open-terrain – 12.5 m-high building of Tamura et al. (2003) – according to Envelope Procedure (ASCE/SEI 7-10).

Story	W_{E-W}	T_{E-W}	W_{N-S}	T_{N-S}	$C_{V,E-W}$	$C_{V,N-S}$	C_T
	kN	kNm	kN	kNm			
4	27.26	90.75	39.39	194.50			
3	81.79	272.24	118.18	583.51			
2	136.32	453.74	196.96	972.52			
1	195.39	650.35	282.31	1393.95	0.69	1.04	0.182

1.2.2.2. Directional Procedure

According to ASCE/SEI 7-10, the Directional Procedure can be applied to buildings of all heights. Therefore, this procedure is also carried out and the corresponding coefficients will be compared with those of the Envelope Procedure. Wind pressure computed

following the Directional Procedure is carried out as shown in Equation (2-19). As explained previously, because the building is enclosed, the effects from the peak internal pressure coefficient, (GC_{pi}), can be ignored. The velocity pressure, q, is evaluated at height z above the ground for windward walls, and at height h for leeward walls. They are given as following:

$$q = q_w = q_z = 0.613 K_z K_{zt} K_d V^2 \qquad \text{(B-25)}$$

$$q = q_l = q_h = 0.613 K_z K_{zt} K_d V^2 \qquad \text{(B-26)}$$

The velocity pressure exposure, K_z, is calculated differently in each equation. While in windward walls, K_z is constant in all floors as it is only computed with z equal to the height of the building, it is different in each floor in leeward walls with z equal to the height of the floor under consideration. According to Figure 27.4-1, the external pressure coefficient, $C_{p,}$ is 0.8 for flat roof buildings in windward walls and 0.416 for leeward walls. The value in leeward walls is computed by linearly interpolating regarding the ratio $L/B = 1.42$ of the current building in E-W direction. L and B are defined as the horizontal dimensions of the building parallel and normal to wind direction, respectively. This value is -1.42 in N-S direction. The gust factor, G, of this building is determined as 0.85 for rigid structures. All other parameters are taken as similar to what is described in the Envelope Procedure.

Partial load cases of the Directional Procedure are carried out following **Figure 2.4**. Only the maximum results from the Directional Procedure are reported in **Table B.14**, considering urban-terrain area, and **Table B.15** when the buildings are in open-terrain area.

Table B.14: Maximum shear and torsions - E-W and N-S directions – Urban-terrain – 12.5 m-high building of Tamura et al. (2003) – according to. Directional Procedure - ASCE/SEI 7-10.

Story	W_{E-W}	T_{E-W}	W_{N-S}	T_{N-S}	$C_{V,E-W}$	$C_{V,N-S}$	C_T
	kN	kNm	kN	kNm			
4	28.60	96.51	42.47	203.07			
3	82.95	279.97	123.47	590.35			
2	133.74	451.36	199.51	953.89			
1	185.57	626.31	277.46	1326.60	0.45	0.68	0.09

Table B.15: Maximum shear and torsions - E-W and N-S directions – Open-terrain – 12.5 m-high building of Tamura et al. (2003) – according to. Directional Procedure - ASCE/SEI 7-10.

Story	W_{E-W}	T_{E-W}	W_{N-S}	T_{N-S}	$C_{V,E-W}$	$C_{V,N-S}$	C_T
	kN	kNm	kN	kNm			
4	40.42	136.43	60.47	289.13			
3	118.29	399.23	177.24	847.41			
2	192.30	649.02	288.61	1379.91			
1	268.96	907.74	404.33	1933.19	0.71	1.07	0.17

The maximum coefficients resulted from this procedure are compared with those from the Envelope Procedure. Directional Procedure produces higher values and are considered.

Table B.16: Maximum shear and torsions coefficients -12.5 m-high building of Tamura et al. (2003) – according to Directional and Envelope Procedure.

	$C_{V,E-W}$	$C_{V,N-S}$	C_T
Urban-terrain	0.45	0.68	0.09
Open-terrain	**0.71**	**1.07**	**0.17**

2. THE RESULTS OF THE OTHER STUDIES

Similar processes are carried out for all other studies. Based on the building natural frequency, the wind computation procedures applied on these buildings according to NBCC 2015 can be determined. In terms of ASCE/SEI 7-10, the Directional Procedure is applied for all buildings, while the Envelope Procedure is used only for low-rise buildings. The procedures used for these buildings are shown in **Table B.17**.

Table B.17: Wind computation procedure of experimental buildings.

Study	f_n	H/w	H (m)	Procedure	
				NBCC 2015	ASCE/SEI 7-10
Isyumov & Case (2000)	4.1	0.5	4.88	Static	Envelope/Directional
Keast et al. (2012)	0.33	3	60	Dynamic	Directional
Stathopoulos et al. (2013)	1	0.51	20	Dynamic	Envelope/Directional
	0.67	0.77	30	Dynamic	Directional
	0.5	1.02	40	Dynamic	Directional

All wind partial loading cases are considered to study the most severe wind-induced effects acting on these buildings. On each building, one maximum shear in each major direction and the maximum torsion are selected to compute the shear and torsional coefficients. These code-computed coefficients are presented in **Table B.18**.

Table B.18: Shear and torsional coefficients from code computations and wind tunnel tests.

Study	Building dimension LxBxH (m)	Exposure terrain	$C_{V,E-W}$			$C_{V,N-S}$			C_T		
			WTT*	NBCC 2015	ASCE/SEI 7-10	WTT	NBCC 2015	ASCE/SEI 7-10	WTT	NBCC 2015	ASCE/SEI 7-10
Tamura et al. (2013)	42.5x30x12.5	Open	0.375	0.314	0.688	0.625	0.453	1.035	0.145	0.018	0.182
	42.5x30x12.5	Urban	0.417	0.327	0.347	0.521	0.473	0.519	0.181	0.019	0.091
	50x25x50	Urban	2.000	2.117	1.572	4.000	3.762	3.693	0.671	0.980	0.671
Stathopoulos et al. (2013)	61x39x20	Open	0.511	0.352	0.543	0.927	0.533	0.922	0.150	0.022	0.162
	61x39x30	Open	0.767	0.756	0.766	1.279	1.215	1.471	0.220	0.281	0.272
	61x39x40	Open	1.023	1.188	1.174	1.758	1.815	1.994	0.250	0.421	0.363
Keast et al. (2012)	40x20x60	Open	2.250	2.581	2.562	6.000	5.021	6.034	1.260	1.288	1.398
Isyumov & Case (2000)	29.25x9.75x4.88	Urban							0.395	0.071	0.384

*WTT: Wind tunnel test